AD-A082 663 NAVAL SURFACE WEAPONS CENTER DAHLGREN LAB VA F/G 8/2
TERRESTRIAL AND CELESTIAL CARTOGRAPHY,(U)
MAY 79 A V HERSHEY
UNCLASSIFIED NSWC/DL-TR-3789 NL

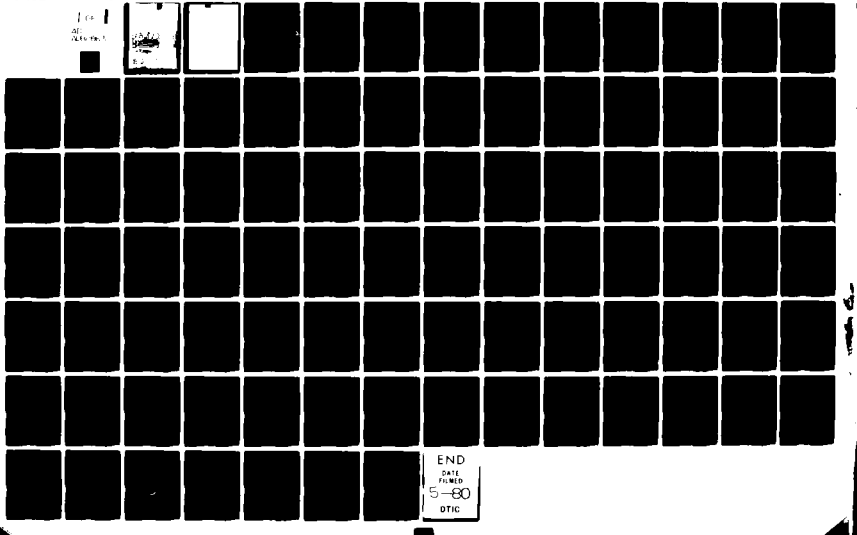

END
DATE FILMED
5-80
DTIC

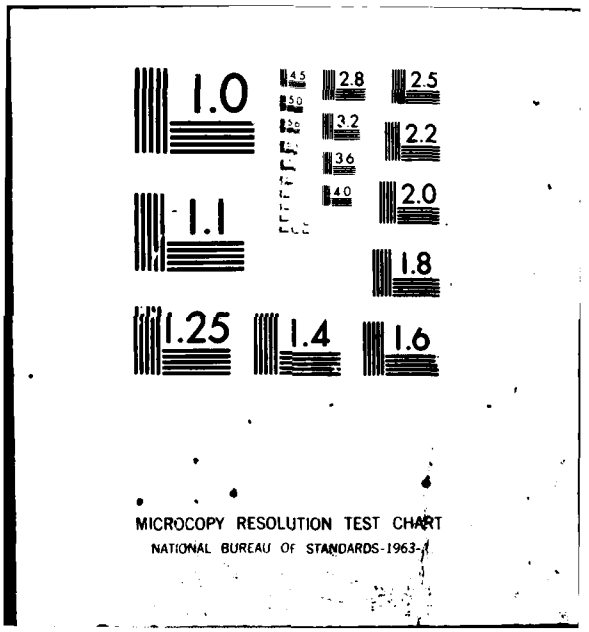
1.0
1.1
1.25
1.4
1.6
1.8
2.0
2.2
2.5
2.8
3.2
3.6
4.0
4.5
5.0
MICROCOPY RESOLUTION TEST CHART
NATIONAL BUREAU OF STANDARDS-1963-A

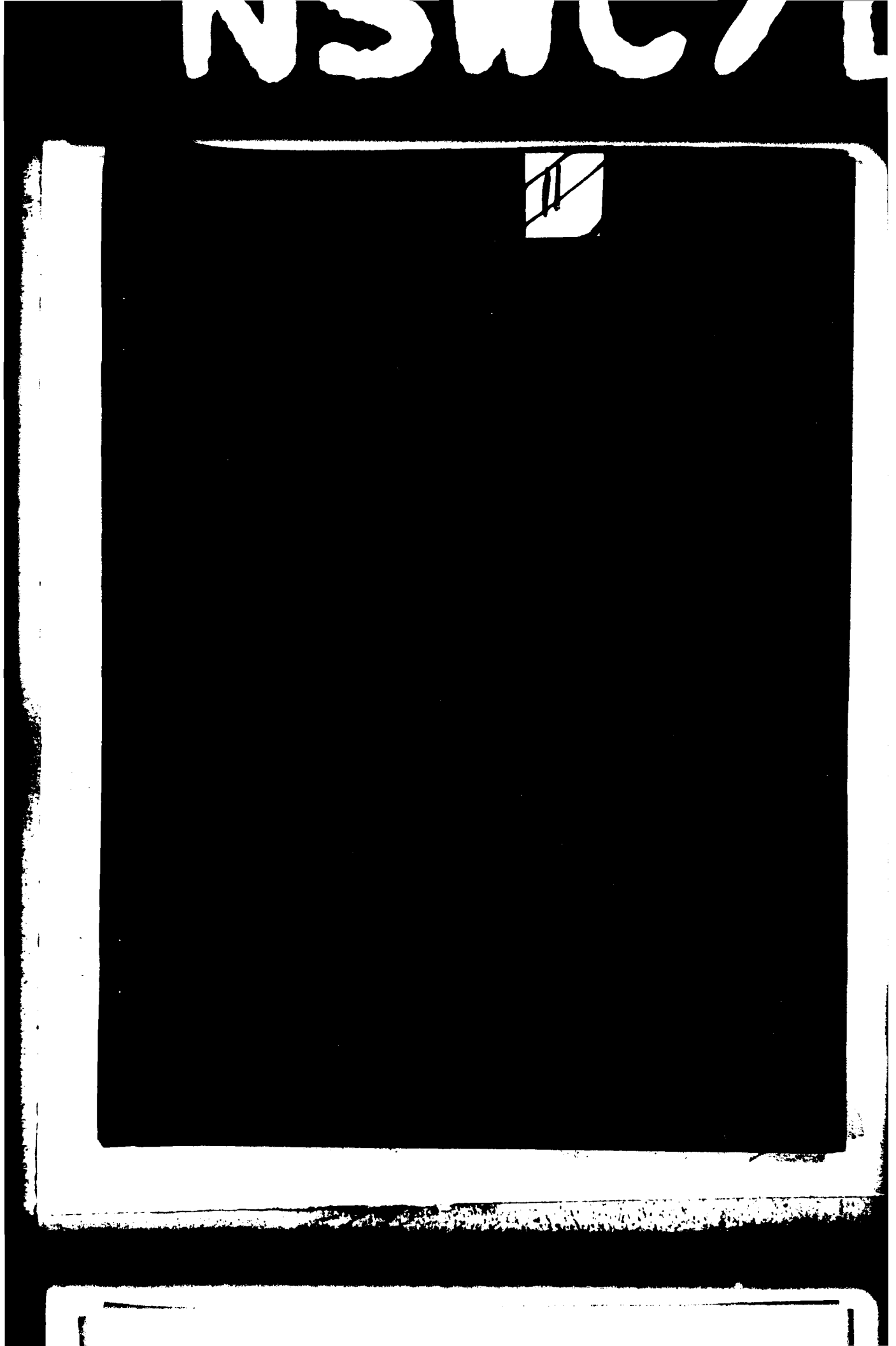

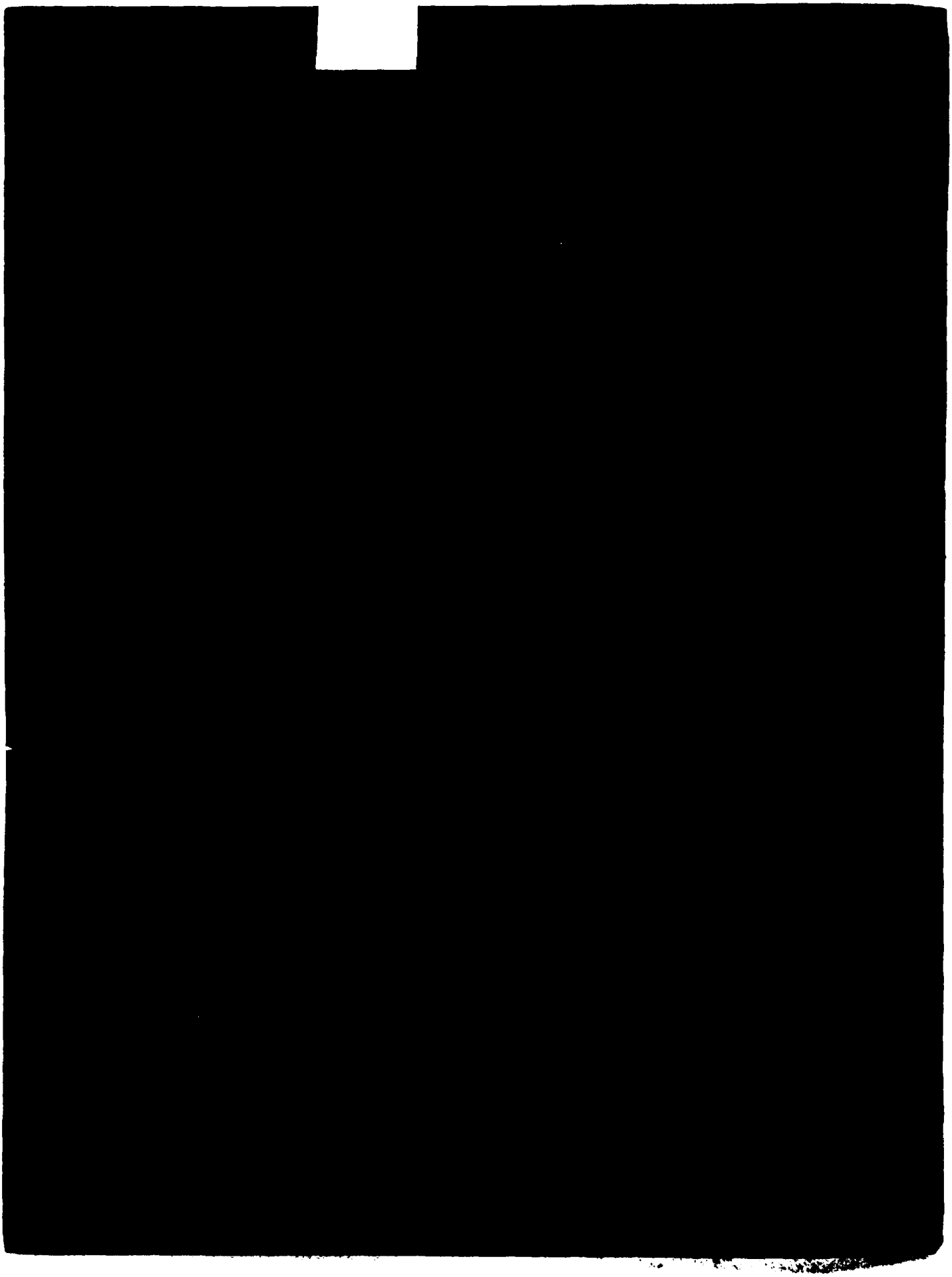

# TERRESTRIAL AND CELESTIAL CARTOGRAPHY



By

A. V. HERSHEY

Science and Mathematics Research Group

## TABLE OF CONTENTS



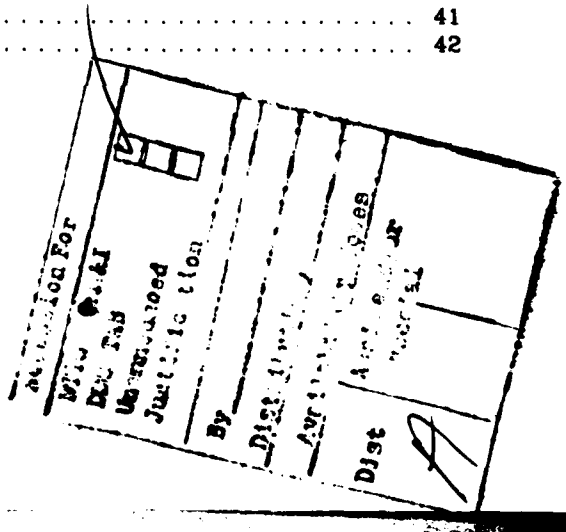

## FOREWORD

A reordering of terrestrial data has applications to the determination of whether a satellite is over sea or over land. A catalog of celestial data has applications to navigation by stellar observation. It is the purpose of this report to present a survey of data which are useful for computer cartography. The manuscript was completed by 21 May 1979.

Released by:

Ralph A. Niemann
Head, Strategic Systems Department

## ABSTRACT

World Data Bank I has been reordered in such a way that the latitudes where coastlines cross meridians are sorted in order of latitude for each minute of longitude. Whether a satellite position is over sea or over land is determined by the parity of the next lower crossing. Stellar data on distance and velocity as well as direction are given in a small catalog. Boundary data for moon maria, constellations, and the Milky Way are given in a set of files.

## INTRODUCTION

The time has come when all maps[1] can be printed with the aid of a computer and a cathode ray printer. It is possible to print in a few seconds a map which has taken days to trace by hand. With the data for the map stored on magnetic tape, it is possible to update the map with little additional effort.

Geographic map data have applications to any displays where there is a correlation of specific data with geographic boundaries. They are useful in earth sciences for maps of distributions of economic value or population density. They are useful in meteorology for weather maps and for satellite photographs of cloud cover. They are useful in nautical astronomy for maps of paths of eclipses and navigation satellites. They are useful to military commands for maps of the positions and the motions of military targets.

Not only are data banks useful as backgrounds for thematic displays, but they may also serve as repositories of definitions for official boundaries.

Previous reports from the Naval Surface Weapons Center[3-5] have given documentations of cartographic and calligraphic repertories for electronic digital computers. The cartographic repertories contain data for the coast lines and boundaries of the World, the United States, and the Potomac River. The calligraphic repertories contain complete alphabets of occidental origin and many characters of oriental origin.

A natural extension of the terrestrial cartography is to celestial cartography. The astronomical and the astrophysical literature have been searched for representative reference material. Limitations of scope preclude the listing of more than a few of the most general references[9-42]. The present report gives documentation of analysis and programming which went into the preparation of a celestial catalog.

The digitization of each repertory was accomplished in two stages. In the first stage, each configuration was approximated by polygonal lines which were sketched on tracing paper or on graph paper. In the second stage, the coordinates of the corners in the polygonal lines were scaled and were recorded in digital form on coding paper. The digitizations are available in the form of punched cards and magnetic tape. Inasmuch as the digitizations were limited to a discrete raster, no map or alphabet could quite be used as an exact basis for the design of the digitizations.

Available in terrestrial cartography are maps which present merely the outline of an area such as the coastlines of oceans and maps which present the topography of the land in the form of contours of constant elevation. Available in lunar cartography are color maps which indicate the boundaries of maria and contour maps which indicate the topography of the moon. Available in celestial cartography are charts which indicate the outlines of celestial objects and charts which indicate the brightness of the objects in the form of isophotes of constant brightness or charts which indicate the rate of recession in the form of isokines of constant radial velocity.

The scope of the present project in cartography is limited to the digitization of maps of the first kind where only outlines are displayed. Problems arise in connection with the choice of contour to be used in the digitization. For coastlines, a choice must be made between the outermost navigable land and the innermost navigable sea. For the maria, the boundaries are not well defined, because the mountains rise gradually from the edges of the maria.

The format of the map data is the same as the format for tapes on the obsolete Naval Ordnance Research Calculator. The same format continues to be used because

it is convenient for the digitization of new data and because it is compatible with the many copies of data which have been distributed already to outside agencies. A subroutine converts the format of any data from a conventional FORTRAN format to the special NORC format for cartography.

A FORTRAN cartographic subroutine controls the preparation of maps. It refers to an external subroutine for the transformation of geographic coordinates into map coordinates. Any mapping projection can be used in the transformation subroutine. The cartographic subroutine controls the masking of data in areas extraneous to the map, and provides unlimited variations of dots and dashes for line formats.

The FORTRAN typographic system controls the preparation of both cartography and typography. There are three versions of the system. All use the same input and prepare the same output. They differ as to word length in the arithmetic unit and as to interface between arithmetic unit and tape units. The IBM 360 computer has a word length of 32 bits and requires assembler language subroutines in order to control the bit configuration on tape. The UNIVAC 1108 computer has a word length of 36 bits and requires the subroutine NTRAN in order to control the bit configuration on tape. The CDC 6600 computer has a word length of 60 bits and permits control over the bit configuration through the FORTRAN instructions BUFFER IN and BUFFER OUT. Documentation in the present report covers only the programming for the CDC 6600 computer.

The data banks which have been prepared for the present report are intended for use as backgrounds in thematic maps. The data banks are illustrated by a set of maps in Appendix C. At a size of 6″ × 8″ the maps are at too small a scale to indicate more than the scope of the data. Each data bank is illustrated by a separate map. Superposition of data banks in the same map would be too congested. Printing in different colors on the same map would alleviate congestion but would be against government regulations.

## TERRESTRIAL CARTOGRAPHY

### Resources

There are many maps and atlases of the world. The classical source of data for coastlines was the World Hydrographic Chart of the Navy Hydrographic Office. Especially noteworthy are the Atlas of the World of the National Geographic Society, and the World Aeronautical Charts of the Aeronautical Chart and Information Center. Many topographic quadrangles are available from the United States Geological Survey and the Coast and Geodetic Survey. The ultimate source of data is the Universal Automatic Map Compilation Equipment at the Army Engineer Topographic Laboratories. In the UNAMACE system the two views of a stereographic aerial camera are matched under computer control. The elevation of each feature is derived from the disparity between the two views of the stereographic camera. The elevations are interpolated to determine contour lines.

### Coordinates

A point on the oblate surface of the earth is defined geographically by its latitude and longitude. At Doppler radar stations satellites are tracked in orbit. Determinations of the positions of the stations relative to the center of mass of the earth have been described by Anderle[2]. Calibration of the geographic coordinates against the positions

of the Doppler stations makes it possible to convert geographic coordinates into geometric coordinates. For small scale maps the geographic coordinates can be equated to polar coordinates on a sphere. The Cartesian coordinates $x, y, z$ are related to polar coordinates $r, \theta, \phi$ by the equations

$$x = r \sin\theta \cos\phi \tag{1}$$

$$y = r \sin\theta \sin\phi \tag{2}$$

$$z = r \cos\theta \tag{3}$$

where $r$ is the radius of the sphere, $\theta$ is identified with the complement of the latitude, and $\phi$ is identified with the longitude. Although the spherical simulation is only approximate geometrically, it is true cartographically.

Many mapping transformations for the transfer of points on a sphere to points on a plane have been listed by Pearson[8]. Conformal transformations have the advantage that local details have true shapes, but the ranges of argument are infinite. Equidistant projections have the disadvantage that they are distorted near the poles, but the ranges of argument are finite. For numerical analysis the cylindrical or polar equidistant projections are most appropriate because their metrics are bounded.

## EQUATOR AND GRID

A useful data base consists of the latitudes and longitudes for meridians and parallels. Data are recorded at every degree along each line and for lines at every fifteen degrees between lines.

## THE WORLD

A digitization of the continental United States was made at the Naval Surface Weapons Center[3]. This digitization contains 10000 data.

The first major digitization of the coastlines of the world was made at the Naval Surface Weapons Center. The digitization has come to be known as World Data Bank Zero. It contains 8000 data for the coastlines.

The next digitization of the world was made at the Central Intelligence Agency. The digitization is known as World Data Bank I. It contains 64000 data for coastlines and 26000 data for international boundaries.

All three data banks are available in the same format. Each datum is expressed by

a 16-character word with the following format.

| Character Numbers | Interpretation |
|---|---|
| 1 | 0 for N, 1 for S |
| 2-4 | degrees of latitude |
| 5 | 0 for N, 1 for S |
| 6-8 | minutes of latitude |
| 9 | 0 for E, 1 for W |
| 10-12 | degrees of longitude |
| 13 | 0 for E, 1 for W |
| 14-16 | minutes of longitude |

A sequence of steps in a continuous line is terminated by a row of sevens.

The ultimate digitization of the world is World Data Bank II, which has been prepared at the Central Intelligence Agency[6,7]. It contains 2.8 million data for coasts, islands, and lakes, 2.5 million data for rivers, and 0.4 million data for political boundaries. A description has been presented by Anderson, Angel, and Gorny[7].

World Data Bank II covers five separate areas which are named for their principal continents. There are separate files in each area for coasts, islands, lakes (CIL), for rivers (RIV), and for boundaries (BDY).

The number of lines in each file is required in order to process the file, while the number of data in the file determines the length of the file. The number of data in each file is given in the following table.

| Principal Continent | File | Number of Lines | Number of Data |
|---|---|---|---|
| N. America | CIL | 5665 | 819765 |
| | RIV | 1333 | 332863 |
| | BDY (National) | 32 | 8469 |
| | BDY (Internal) | 223 | 61845 |
| S. America | CIL | 2202 | 390730 |
| | RIV | 1373 | 460626 |
| | BDY | 197 | 63269 |
| Europe | CIL | 2581 | 338064 |
| | RIV | 951 | 196280 |
| | BDY | 127 | 48451 |
| Africa | CIL | 1778 | 311938 |
| | RIV | 2340 | 598086 |
| | BDY | 371 | 114837 |
| Asia | CIL | 9342 | 924891 |
| | RIV | 3128 | 911608 |
| | BDY | 190 | 106164 |

The data in World Data Bank II are ranked in order of importance. A list of ranks

is given in the following table.

I Coasts, Islands, Lakes

- 01 Principal coasts, islands, lakes.
- 02 Major additional islands and lakes.
- 03 Intermediate additional islands and lakes.
- 04 Minor additional islands and lakes.
- 06 Major intermittent lakes.
- 07 Minor intermittent lakes.
- 08 Reefs.
- 09 Major salt pans.
- 10 Minor salt pans.
- 13 Major ice shelves.
- 14 Minor ice shelves.
- 15 Glaciers.

II Rivers

- 01 Principal rivers.
- 02 Major additional rivers.
- 03 Intermediate additional rivers.
- 04 Minor additional rivers.
- 05 Double-lined rivers.
- 06 Major intermittent rivers.
- 07 Intermediate intermittent rivers.
- 08 Minor intermittent rivers.
- 10 Major canals.
- 11 Minor canals.
- 12 Irrigation canals.

III Boundaries

- 01 Established boundaries.
- 02 Disputed boundaries.
- 03 Other boundaries.

The files are divided into physical records with 180 fields in each record. Each field contains 20 characters, and each character is an 8-bit byte in EBCDIC. Each line is preceded by a 20-character header field with the following format.

| Character Numbers | Interpretation |
|---|---|
| 1-7 | Identification number |
| 8-9 | Rank |
| 10-15 | Number of data |
| 16-20 | Serial number |

Each datum occupies a 20-character field with the following format.

| Character Numbers | Interpretation |
|---|---|
| 1-2 | degrees of latitude |
| 3-4 | minutes of latitude |
| 5-6 | seconds of latitude |
| 7 | N or S |
| 8-10 | degrees of longitude |
| 11-12 | minutes of longitude |
| 13-14 | seconds of longitude |
| 15 | E or W |
| 16-20 | serial number |

Each 20-character field can be decoded with the aid of a FORTRAN format statement. However, the speed of computation is more than three times as fast if the FORMAT instructions are replaced with extraction mills which use AND and SHIFT to convert BCD characters into integers and then decuple and sum the integers to form binary numbers. The volume of data is half as large and the speed of computation is fifty times as fast if the data are converted from BCD format to binary format. The data are biased in order to avoid one's complements, and are expressed in seconds in order to avoid loss of accuracy. Latitude is expressed as seconds north of the south pole and longitude is expressed as seconds east of the 180th meridian.

The fineness of representation with the format in World Data Bank Zero is limited to the expression of angles in degrees and minutes. If the interpretation of the same characters is modified to express angles in degrees and decimals, then the fineness of representation with the format is equivalent to the expression of angles in degrees, minutes, and seconds. A substitution of other arguments for latitude and longitude makes the cartographic subroutine capable of the graphic representation of any arguments. Insofar as the range of argument with the format is limited to 1000, an end-of-line is marked by the arguments 1000, 0 and an end-of-file is marked by the arguments 1000, 1000. Minor modifications in programming through UPDATE make the cartographic subroutine capable of plotting directly on CalComp plotters with full accuracy.

In the digitization of an irregular coastline, a compromise must be made between fidelity of representation and volume of data. Along each step of the polygonal simulation the true coastline wanders from side to side by an amount which is a fraction of the length of step. It is the amplitude of the deviation of the true line from the polygonal line which defines the accuracy of the digitization. A meaningful gauge of accuracy would be the root mean square deviation in angular measure. It is fashionable to quote the scale of a map as a measure of the accuracy, whereas the scale of the map may range from a microdot to a lobby globe with the same relative accuracy.

In order to gain insight into the magnitude of error the length of coastline has been computed for World Data Bank Zero. The length of the coast is twelve times the circumference of the earth and the average length of step is 33' of arc. Insofar as the deviation of the coastline is less than one third of the length of step the accuracy of this data bank is on the order of 11' of arc. The accuracy of World Data Bank I is

judged to be on the order of 2' of arc, while the accuracy of World Data Bank II is judged to be on the order of 3" of arc. In addition to a quantitative requirement for accuracy there is the subjective requirement that the digitization must look right to the eye.

The size of the data bank should be matched to the scale of the map. There is no merit in a digitization to an error which is less than the thickness of line or the spacing in the raster. A finer digitization would merely thicken the line. The average length of step should be seven times the width of line. The cartographic subroutine casts out data which are too closely spaced.

An area may be indicated by a contour line which follows the perimeter of the area, or the area may be indicated by a grid of parallel lines which fills the interior of the area. Let the area with its contour line and its grid of lines be defined to be a domain. In cartography, domains are indicated by coastlines, by contour lines, by areas of color, or by areas of hatching. In calligraphy, domains are the characters, which are generated either by strokes between raster points or by scans parallel to one side of the raster. There is a need for programming which can fill a contour line with a grid of lines, or can derive the contour line around a grid of lines.

The contour line is defined by a sequence of coordinate pairs which locate the vertices of a polygon. The sequence starts at an initial point and ends at a final point. For a closed contour the final point must coincide with the initial point. The common loci of the initial point and the final point are represented by two pairs in the sequence of coordinate pairs.

A grid of lines is defined by a sequence of coordinate pairs which locate where grid lines cross the contour lines. Wherever a grid line crosses a domain, the ends must be indicated by two pairs in the sequence of coordinate pairs. Wherever a vertex or extremum of the contour line osculates a grid line, it still must be represented by two coordinate pairs. In the conversion of a contour into a grid each vertex is tested to determine whether its adjacent sides lie on the same side or on opposite sides of the grid line which it intercepts. If they are on the same side, the coordinate pair of the vertex is duplicated in the sequence of crossing coordinates. When the contour closes on itself the initial and the final coordinate pairs remain in the sequence of coordinate pairs. It is necessary to search for duplicate coordinate pairs and eliminate one of them if they do not represent an extremum.

Difficulties arise when the contour line does not close on itself or when it overlaps itself. Such imperfections must be removed from the contour line before the contour line can be filled with grid lines. Even then there can be miscounts in the number of coordinate pairs. It is necessary to assume that any grid line which is adjacent to a domain has a length less than a tolerance if the grid line has a valid parity, but has a length more than the tolerance if there is a miscount of the crossings. Wherever a grid line fails the tolerance its parity is corrected by the duplication of a coordinate pair at the beginning of failure.

NASA has been flying satellites with altimeters to determine the height of the ocean along the path of the satellite. The altimetry of the ocean is upset whenever the satellite passes over land. A project was established to determine by computation from map data when the satellite would be over sea or over land. World Data Bank I was selected as the data base for the project. Unfortunately, there are a few errors of closure in this data base. The editing of the data base was reduced to a manageable level by use of a program which searched through every line beginning and printed each one which was not matched exactly by a line ending. Each line ending was adjusted by a small amount to make it match a line beginning.

The data were interpolated to provide the crossings of coastlines by meridians at every minute of longitude. Latitudes were counted positive northward from the south pole and longitudes were counted positive eastward from the 180th meridian. The interpolated data were sorted in order of latitude and longitude.

Inasmuch as there were too many data to sort in the core memory, the data were sorted in two stages. In the first stage, the data were distributed among 36 tape-files such that each file contained the data for a sector of 10° of longitude. The number of tape-files was determined by the number of buffers of nominal size which can be fitted into a memory of nominal size. The data in each tape-file then were transferred one tape-file at a time to a magnetic tape. During the transference a count was accumulated on the number of data on each of the 600 meridians in the tape-file. At the conclusion of the transference, the counts of data were written on a magnetic tape. In the second stage, the counts of data were read back into the core storage, and an index array was constructed from the counts of data. The coordinate data were read back into a data array at addresses which were specified by the index array. Thus the the data were sorted in serial order of increasing longitude. They were stored in an array which needed only be large enough to hold compactly the number of data in the largest tape-file. The data for each meridian were sorted by permutations which brought each datum into serial order of increasing latitude.

The presence of imperfections was revealed by a program which plotted a line wherever a meridian should span land, and a blank wherever the meridian should span sea. The 360° of longitude were spread out over 36 frames of cathode-ray printer output so that each meridian would be resolved distinctly. Wherever there was a miscount in the number of crossings, there were lines where there should be blanks. and there were blanks where there should be lines. Crossings were duplicated in the data until there were no longer any apparent discrepancies between lines and blanks.

In the final output the latitudes of crossings by meridians are arranged in serial order of latitude and longitude. The latitude is packed in the first sixteen bits and the longitude is packed in the second sixteen bits of each 32-bit word on magnetic tape. Whether the satellite is over land or over sea is determined simply by the parity of the number of crossings which are spanned by the latitude of the satellite.

In the shell-sort technique partitions of the data are partitioned progressively into halves until all of the data are sorted. An attempt to use shell-sorting ran out of time because it did not take advantage of the fact that the data are compact with respect to longitude but are sparse with respect to latitude.

## THE MOON

The most conspicuous feature of the full moon as viewed from the earth is the contrast in color between maria and mountains. Although the difference in color is clearly apparent in photographs of high contrast, the difference is not well defined in the maps of the moon. A boundary contour has been selected to outline the color. In the selection of the contour, the Photographic Lunar Atlas[15] was used as a guide to structure. The charts of the National Geographic Society[16] and the Aeronautical Chart and Information Center[17-19] were used as guides to location. Included with the boundary of color contrast are a few of the most prominent craters. The farside of the moon is covered with many small craters which are not included in the digitization.

## ROTATION

*Analysis*

In the preparation of maps of the sphere there often is a rotation of the sphere prior to map projection. Let **r** be the position of a point on the sphere before rotation and let **r'** be the position of the point after rotation. The position vectors are related by the equation

$$\mathbf{r}' = \mathbf{H} \cdot \mathbf{r} \tag{4}$$

where **H** is a rotation matrix. Let $x, y, z$ be the Cartesian coordinates of the point before rotation and let **i, j, k** be unit vectors in the directions of increasing $x, y, z$. Let the sphere be rotated successively through the Eulerian angles $\chi, \theta, \phi$ about the fixed axes **k, j, k**. Then the rotation matrix is given by the product of three matrices each of which performs a rotation through one of the three angles. The product is given by the equation

$$\mathbf{H} = \begin{Vmatrix} +\cos\chi\cos\theta\cos\phi - \sin\chi\sin\phi & -\sin\chi\cos\theta\cos\phi - \cos\chi\sin\phi & +\sin\theta\cos\phi \\ +\cos\chi\cos\theta\sin\phi + \sin\chi\cos\phi & -\sin\chi\cos\theta\sin\phi + \cos\chi\cos\phi & +\sin\theta\sin\phi \\ -\cos\chi\sin\theta & +\sin\chi\sin\theta & +\cos\theta \end{Vmatrix} \tag{5}$$

The elements of the matrix are computed by reference to a subroutine which stores them in an array in their natural order.

*Programming*

The elements of the rotation matrix are computed by reference to the following subroutine.

```
SUBROUTINE ROTATE (AC, AQ, AF, HM)
**********************************************************************************************
FORTRAN SUBROUTINE TO COMPUTE ROTATION MATRIX
**********************************************************************************************
```

Eulerian angles $\chi, \theta, \phi$ are given in the arguments AC, AQ, AF. The angles are expressed in degrees. The elements of the rotation matrix are stored in the 9-array HM.

## DATA CONVERSION

The conversion of map data into plot instructions is made with the aid of the following subroutines.

```
SUBROUTINE RDAMRC (NU, LC)
**********************************************************************************************
CDC 6600 SUBROUTINE TO READ ALPHAMERIC RECORD
**********************************************************************************************
```

An 80-column card record is read from an input file with unit number NU. The contents of the record are converted character by character into the corresponding FORTRAN integers and are stored in the array LC.

SUBROUTINE WRAMRC (NU, LC)

**********

**CDC 6600 SUBROUTINE TO WRITE ALPHAMERIC RECORD**

**********

**The contents of the array** LC **are converted number by number into the corresponding BCD characters and are written as an 80-column card record in an output file with unit number** NU.

SUBROUTINE CVMPDT (NI, NO)

**********

**FORTRAN CONVERSION OF MAP DATA FROM NORC FORMAT TO FORTRAN FORMAT**

**********

**Data are read one card at a time through subroutine** RDAMRC **from an input file with unit number** NI. **Four sixteen-digit words are stored in an array of 80 integers. The numbers in the array are decupled and summed to give real numbers for latitude and longitude. Whenever a 16-digit word is all sevens, the latitude is replaced by 1000 and the longitude is replaced by zero. The latitude and the longitude for each datum are written one card at a time on an output file with unit number** NO. **The processing of data continues until a NORC end-of-file is sensed in the input file, whereupon the latitude and the longitude both are replaced by 1000.**

SUBROUTINE CVDTMP (NI, NO)

**********

**FORTRAN CONVERSION OF MAP DATA FROM FORTRAN FORMAT TO NORC FORMAT**

**********

**Data are read one card at a time from an input file with unit number** NI. **Each card of input contains a latitude and a longitude in real number format. Each datum is converted to a 16-digit word in cartographic format. If the absolute value of either latitude or longitude is equal to or greater than 1000 the input card is interpreted as the end of a line of data, and the 16-digit word is replaced by sixteen sevens. Four sixteen-digit words are packed in an array of 80 integers. The array is written through subroutine** WRAMRC **as a card of output in the output file with unit number** NO. **The processing of data continues until the absolute values of both latitude and longitude are equal to or greater than 1000, whereupon a NORC end-of-file is written in the output file.**

SUBROUTINE CTGPHC (LW, KF, CF, CA, NI, NO, GNLTRN)

**********

**FORTRAN CARTOGRAPHIC SUBROUTINE**

**********

**Map data are read through subroutine** RDAMRC **one card at a time from an input file with unit number** NI. **The geographic coordinates in degrees and minutes are converted to floating point values in degrees. Reference to an external subroutine** GNLTRN **converts the geographic coorinates in array** AQ **into the map coordinates in array** FP **as follows.**

| | |
|---|---|
| AQ(1) = **latitude (degrees)** | FP(1) = **X-coordinate (map units)** |
| AQ(2) = **longitude (degrees)** | FP(2) = **Y-coordinate (map units)** |

**The data are bypassed if no value is placed in** FP **by subroutine** GNLTRN. **The map**

coordinates are scaled and masked to restrict the plotted line to the boundaries which are delimited by the array CF for the printer field and by the array CA for the mapped area as follows.

| | |
|---|---|
| CF(1) = left edge of printer field | CA(1) = left edge of mapped area |
| CF(2) = right edge of printer field | CA(2) = right edge of mapped area |
| CF(3) = upper edge of printer field | CA(3) = upper edge of mapped area |
| CF(4) = lower edge of printer field | CA(4) = lower edge of mapped area |

The line width is specified by argument LW and the line format is specified by the array KF as follows.

KF(1) = length of dash
KF(2) = length of space
KF(3) = length of dash
KF(4) = length of space
KF(5) = length of dash
KF(6) = length of space
KF(7) = length of dash
KF(8) = length of space

Plot instructions are written on the output file with unit number NO. The processing of data continues until a NORC end-of-file is sensed in the input file.

There have been several experimental versions of the cartographic subroutine. Input has been in NORC format, in FORTRAN format, and in both of the formats for World Data Bank II. Masking has been designed for rectangular maps and for circular maps. Output has been in the formats for the S-D4060 cathode-ray printer, for the CalComp 960 window shade, and for the CalComp 718 flatbed.

Subroutine CPWDII selects data from disk files and assembles the data in a single output file of data from World Data Bank II. The subroutine can be modified to give a set of subroutines with different criteria for the selection of data. The different subroutines in the set are linked together with COMMON statements which define the pointers and the buffer of the common output file.

Subroutine CTWDII is a modification of the cartographic subroutine which reads datum fields directly from a disk file and extracts latitude and longitude from each datum field with AND and SHIFT instructions.

## CELESTIAL CARTOGRAPHY

### Resources

Celestial objects include nebulae, satellites, planets, stars, clusters, and galaxies. The positions and the rates of change of the positions of the objects at a standard epoch are given in charts[12-14] and catalogs[32-39]. The positions as a function of time are given in almanacs[40-42]. The direction to each object and the radial velocity of the object are known accurately, but the distance to the object and the transverse velocity

are known only approximately. Other properties of the objects include dimensions, orientations, rotations, masses, and spectra.

**Measures of Time**

It is axiomatic that true time increases at a uniform rate in an isolated physical system. However, few physical systems are truly isolated. Time can be measured approximately by a mechanical device which oscillates, librates, or vibrates. In the conventional clock, an escapement mechanism drives a coiled spring and balanced wheel. The period of oscillation depends upon temperature, and orientation. In the pendulum clock, an escapement mechanism drives a pendulum. The period of libration depends upon amplitude and varies inversely with gravity. In a modern clock an electronic oscillator drives a tuning fork or a vibrating crystal. The period of vibration depends upon temperature and gravity. In the atomic clock a crystal oscillator is tuned continuously into resonance with the electromagnetic radiation from an atomic transition. Although the atomic clock is the most reliable clock, it still is affected slightly by interatomic perturbations and relativistic gravitation.

For the calibration of clocks there must be a time standard. In the beginning a second was defined to be $\frac{1}{86400}$ part of the solar day, which is the time interval from one crossing of the meridian by the sun to the next crossing of the meridian by the sun. The solar day is not uniform because of the eccentricity of the earth's orbit. It is necessary to distinguish between the apparent solar day and the mean solar day. The difference is called the equation of time, which does not exceed $16^m$.

Insofar as the earth's rotation is free of perturbation, a time standard may be based on the siderial day, which is the time interval between one crossing of the meridian by a distant star and the next crossing of the meridian by the star. The rotation of the earth on its axis is the basis for civil time and universal time. The rotation of the earth is affected by nutation and seasonal variations in the earth's moment of inertia. It is necessary to distinguish between the apparent siderial day and the mean siderial day. The difference is called the equation of the equinoxes, which does not exceed $1^s$.

Insofar as the entire solar system is free from perturbation by neighboring stellar systems, the solar system itself is the basis for an astronomical standard of time. The solar system is the basis for ephemeris time. The tropical year is the interval between one vernal equinox and the next vernal equinox, when the sun crosses the earth's equator. The tropical year is not constant. The Besselian year is a constant time interval which is equal to that tropical year which began in Greenwich at noon of the day before New Years of 1900. The tropical year grows longer than the Besselian year at the rate of $0^d.148$ per century. In 1950 ephemeris time was 29 seconds later than universal time.

In the modern definition of time, the second is defined astronomically as one part in 31556925.9747 of that tropical year which began in Greenwich on mean noon of the day before New Years of 1900, while the second is defined physically as the interval for 9192631770 cycles of the the hyperfine transition of the cesium atom in the ground state. The Besselian year is 365.2421988 ephemeris days. The Besselian year 1950.0 corresponds to 1950 January $0^d.923$ universal time.

**Systems of Coordinates**

A position on the celestial sphere is defined in terms of spherical polar coordinates. The poles of the celestial sphere are collinear with the poles of the earth, and the equator of the celestial sphere is coplanar with the equator of the earth. The vernal

equinox on the celestial sphere is the ascending node of the ecliptic on the equator. The right ascension $\alpha$ of a point is its azimuthal angle, and is measured positive toward the east from the vernal equinox. The declination $\delta$ is the copolar angle, and is measured positive toward the north from the equator.

Changes of coordinate axes are required for celestial cartography. Let $\theta_1, \phi_1$ be the polar coordinates of a point with respect to the polar axes $\mathbf{i}_1, \mathbf{j}_1, \mathbf{k}_1$, and let $\theta_2, \phi_2$ be the polar coordinates of the point with respect to the polar axes $\mathbf{i}_2, \mathbf{j}_2, \mathbf{k}_2$. The position vector $\mathbf{r}$ of the point on a sphere of radius $a$ is given by either of the equations

$$\frac{\mathbf{r}}{a} = \sin\theta_1 \cos\phi_1 \, \mathbf{i}_1 + \sin\theta_1 \sin\phi_1 \, \mathbf{j}_1 + \cos\theta_1 \, \mathbf{k}_1 \tag{6}$$

$$\frac{\mathbf{r}}{a} = \sin\theta_2 \cos\phi_2 \, \mathbf{i}_2 + \sin\theta_2 \sin\phi_2 \, \mathbf{j}_2 + \cos\theta_2 \, \mathbf{k}_2 \tag{7}$$

Let the pole $\mathbf{k}_2$ be oriented with coordinates $\theta_0, \phi_0$ with respect to axes $\mathbf{i}_1, \mathbf{j}_1, \mathbf{k}_1$. The azimuth of the ascending node of the equator of the pole $\mathbf{k}_2$ is the angle $\phi_0 + \frac{1}{2}\pi$. Let the azimuth of the axis $\mathbf{i}_2$ with respect to the ascending node be the angle $\chi_0$. The axes $\mathbf{i}_2, \mathbf{j}_2$ can be resolved in terms of the unit vectors

$$-\sin\phi_0 \, \mathbf{i}_1 + \cos\phi_0 \, \mathbf{j}_1 \tag{8}$$

$$-\cos\theta_0 (\cos\phi_0 \, \mathbf{i}_1 + \sin\phi_0 \, \mathbf{j}_1) + \sin\theta_0 \, \mathbf{k}_1 \tag{9}$$

The axes $\mathbf{i}_2, \mathbf{j}_2, \mathbf{k}_2$ are given in terms of the axes $\mathbf{i}_1, \mathbf{j}_1, \mathbf{k}_1$ by the equations

$$\begin{aligned} \mathbf{i}_2 = &-(\sin\phi_0 \cos\chi_0 + \cos\theta_0 \cos\phi_0 \sin\chi_0)\mathbf{i}_1 \\ &+ (\cos\phi_0 \cos\chi_0 - \cos\theta_0 \sin\phi_0 \sin\chi_0)\mathbf{j}_1 \\ &+ \sin\theta_0 \sin\chi_0 \, \mathbf{k}_1 \end{aligned} \tag{10}$$

$$\begin{aligned} \mathbf{j}_2 = &+ (\sin\phi_0 \sin\chi_0 - \cos\theta_0 \cos\phi_0 \cos\chi_0)\mathbf{i}_1 \\ &- (\cos\phi_0 \sin\chi_0 + \cos\theta_0 \sin\phi_0 \cos\chi_0)\mathbf{j}_1 \\ &+ \sin\theta_0 \cos\chi_0 \, \mathbf{k}_1 \end{aligned} \tag{11}$$

$$\begin{aligned} \mathbf{k}_2 = &+ \sin\theta_0 \cos\phi_0 \, \mathbf{i}_1 \\ &+ \sin\theta_0 \sin\phi_0 \, \mathbf{j}_1 \\ &+ \cos\theta_0 \, \mathbf{k}_1 \end{aligned} \tag{12}$$

Scalar multiplication of the position vector $\mathbf{r}$ by each of the axes $\mathbf{i}_2, \mathbf{j}_2, \mathbf{k}_2$ leads to the

equations

$$\sin\theta_2\cos\phi_2 = \sin\theta_0\sin\chi_0\cos\theta_1 + \cos\chi_0\sin\theta_1\sin(\phi_1-\phi_0) - \cos\theta_0\sin\chi_0\sin\theta_1\cos(\phi_1-\phi_0) \quad (13)$$

$$\sin\theta_2\sin\phi_2 = \sin\theta_0\cos\chi_0\cos\theta_1 - \sin\chi_0\sin\theta_1\sin(\phi_1-\phi_0) - \cos\theta_0\cos\chi_0\sin\theta_1\cos(\phi_1-\phi_0) \quad (14)$$

$$\cos\theta_2 = \cos\theta_0\cos\theta_1 + \sin\theta_0\sin\theta_1\cos(\phi_1-\phi_0) \quad (15)$$

The angle $\theta_2$ is the arctangent of the quotient between the square root of the sum of the squares of the first two expressions and the third expression. The angle $\phi_2$ is the arctangent of the quotient between the second expression and the first expression. The computation is accomplished by reference to a subroutine for the change of axes.

A change of coordinates from equatorial coordinates $\alpha, \delta$ to galactic coordinates $l^{II}, b^{II}$ is accomplished with the following interpretation.

$$\theta_1 = 90° - \delta \qquad \theta_0 = 62°\ 36' \qquad \theta_2 = 90° - b^{II} \quad (16)$$

$$\phi_1 = \alpha \qquad \phi_0 = 192°\ 15' \qquad \phi_2 = l^{II} \quad (17)$$

$$\chi_0 = -\ 33°\ 00' \quad (18)$$

The longitude in the galactic coordinates is measured from the direction of the center of the Galaxy. A change of coordinates from galactic coordinates $l^{II}, b^{II}$ to equatorial coordinates $\alpha, \delta$ is accomplished with the following interpretation.

$$\theta_1 = 90° - b^{II} \qquad \theta_0 = 62°\ 36' \qquad \theta_2 = 90° - \delta \quad (19)$$

$$\phi_1 = l^{II} \qquad \phi_0 = 123°\ 00' \qquad \phi_2 = \alpha \quad (20)$$

$$\chi_0 = -\ 102°\ 15' \quad (21)$$

The direction to the center of the Galaxy has the coordinates

$$\alpha = 265°\ 36' \qquad \delta = -\ 28°\ 55' \quad (22)$$

The direction to the center is recovered for $l^{II} = b^{II} = 0$.

The plane of a planetary orbit may be defined either by the right ascension $\alpha$ and the declination $\delta$ of the polar axis normal to the plane, or by the inclination $i$ of the plane with respect to the ecliptic, and the azimuth $\Omega$ of its ascending node as measured from the equinox. The longitude of the pole with respect to the equinox is $\Omega - \frac{1}{2}\pi$, and the latitude of the pole with respect to the plane of the ecliptic is $\frac{1}{2}\pi - i$. The ecliptic is inclined to the equator by the obliquity $\epsilon$.

A change of coordinates from equatorial coordinates $\alpha, \delta$ to ecliptic coordinates $i, \Omega$

is accomplished with the following interpretation.

$$\theta_1 = 90° - \delta \qquad \theta_0 = \epsilon \qquad \theta_2 = i \tag{23}$$

$$\phi_1 = \alpha \qquad \phi_0 = 270° \qquad \phi_2 = \Omega - 90° \tag{24}$$

$$\chi_0 = 0 \tag{25}$$

A change of coordinates from ecliptic coordinates $i, \Omega$ to equatorial coordinates $\alpha, \delta$ is accomplished with the following interpretation.

$$\theta_1 = i \qquad \theta_0 = \epsilon \qquad \theta_2 = 90° - \delta \tag{26}$$

$$\phi_1 = \Omega - 90° \qquad \phi_0 = 90° \qquad \phi_2 = \alpha \tag{27}$$

$$\chi_0 = 180° \tag{28}$$

The obliquity of the ecliptic for the equinox of 1950.0 is given by the equation

$$\epsilon = 23° \; 26' \; 44''.84 \tag{29}$$

in accordance with the Explanatory Supplement[41].

The ecliptic coordinates $i, \Omega$ are related to the equatorial coordinates $\alpha, \delta$ by the equations

$$+ \sin i \sin \Omega = \cos \delta \cos \alpha \tag{30}$$

$$- \sin i \cos \Omega = \sin \delta \sin \epsilon + \cos \delta \sin \alpha \cos \epsilon \tag{31}$$

$$\cos i = \sin \delta \cos \epsilon - \cos \delta \sin \alpha \sin \epsilon \tag{32}$$

from which the ecliptic coordinates may be recovered. Differentiation with respect to time gives the rates of change of the ecliptic coordinates in terms of the rates of change of the equatorial coordinates. The computation is accomplished by reference to a subroutine for the conversion of coordinates.

The equatorial coordinates $\alpha, \delta$ are related to the ecliptic coordinates $i, \Omega$ by the equations

$$\cos \delta \cos \alpha = + \sin i \sin \Omega \tag{33}$$

$$\cos \delta \sin \alpha = - \cos i \sin \epsilon - \sin i \cos \Omega \cos \epsilon \tag{34}$$

$$\sin \delta = + \cos i \cos \epsilon - \sin i \cos \Omega \sin \epsilon \tag{35}$$

from which the equatorial coordinates may be recovered. Differentiation with respect to time gives the rates of change of the equatorial coordinates in terms of the rates of change of the ecliptic coordinates. The computation is accomplished by reference to a subroutine for the conversion of coordinates.

Because of the equatorial bulge of the earth, its axis of rotation precesses with a period of 25725 years. The north pole describes a circle on the celestial sphere, and the vernal equinox advances toward the west along the ecliptic. In order to standardize the cartographic data, all equatorial coordinates are referred to the equinox of 1950.0.

The conversion of equatorial coordinates for one equinox into the equatorial coordinates for another equinox is accomplished with the aid of the equations in the Explanatory Supplement[41]. With minor changes the equations are as follows.

Let parameters $Q, D$ be defined in terms of the Besselian years $T_1, T_2$ of the two

equinoxes by the equations

$$Q = \frac{T_1 - 1950.0}{100} \tag{36}$$

$$D = \frac{T_2 - T_1}{100} \tag{37}$$

and let the angles $\phi_1, \phi_2, \theta$ be expressed in seconds of arc by the equations

$$\phi_1 = (2304.948 + 1.395\,Q)D + 0.302\,D^2 + 0.018\,D^3 \tag{38}$$

$$\phi_2 = (2304.948 + 1.395\,Q)D + 1.093\,D^2 + 0.018\,D^3 \tag{39}$$

$$\theta = (2004.255 - 0.852\,Q)D - 0.426\,D^2 - 0.042\,D^3 \tag{40}$$

Then the new equatorial coordinates $\alpha_2, \delta_2$ are related to the old equatorial coordinates $\alpha_1, \delta_1$ by the equations

$$\cos\delta_2 \cos(\alpha_2 - \phi_2) = -\sin\theta \sin\delta_1 + \cos\theta \cos\delta_1 \cos(\alpha_1 + \phi_1) \tag{41}$$

$$\cos\delta_2 \sin(\alpha_2 - \phi_2) = +\cos\delta_1 \sin(\alpha_1 + \phi_1) \tag{42}$$

$$\sin\delta_2 = +\cos\theta \sin\delta_1 + \sin\theta \cos\delta_1 \cos(\alpha_1 + \phi_1) \tag{43}$$

Arctangents are easily constructed from which the new coordinates may be derived. The computation is accomplished by reference to a subroutine for the change of equinox.

**Photography**

Photographs of celestial objects are given in the *Photographischer Himmelsatlas* of Haffner and Eisenhuth[9]. The photographs are relatively large and clear, but the scale and the orientation of the photographs must be determined from the known positions of recognizable stars.

Photographs of celestial objects are given in the *Atlas of Deep-Sky Splendors* by Vehrenberg[10]. Surrounding each photograph is a grid to indicate the equatorial coordinates. The grid determines the orientation of the photograph.

Photographs of the Northern Hemisphere have been prepared with high precision by the National Geographic Society–Palomar Observatory Sky Survey[11].

A photograph is a projection of a small area of the celestial sphere onto a plane perpendicular to the axis of the telescope. The photograph is a map in which a point on the surface of a sphere is projected through the center of the sphere onto a plane tangent to the sphere. The Cartesian coordinates $\Delta x, \Delta y$ in the map are expressed in terms of the deflection angle $\epsilon$ and the position angle $\theta$ by the equations

$$\frac{\Delta x}{a} = \tan\epsilon \cos\theta \qquad \frac{\Delta y}{a} = \tan\epsilon \sin\theta \tag{44}$$

where $a$ is the radius of the sphere. The position angle $\theta$ is measured counterclockwise from north. The coordinate $\Delta x$ is positive toward the north and the coordinate $\Delta y$ is positive toward the east. Required for the digitization of photographic data is a grid with lines of constant right ascension and declination.

Let the Cartesian coordinates $x, y, z$ of a point on the surface of the sphere be

expressed in terms of the spherical polar coordinates $\theta, \phi$ of the point by the equations

$$x = a \sin\theta \cos\phi \tag{45}$$

$$y = a \sin\theta \sin\phi \tag{46}$$

$$z = a \cos\theta \tag{47}$$

where $a$ is the radius of the sphere. The position vector $\mathbf{r}$ of the point on the sphere is given by the equation

$$\frac{\mathbf{r}}{a} = \sin\theta \cos\phi\, \mathbf{i} + \sin\theta \sin\phi\, \mathbf{j} + \cos\theta\, \mathbf{k} \tag{48}$$

where $\mathbf{i}, \mathbf{j}, \mathbf{k}$ are unit vectors in the directions of increasing $x, y, z$. The position vector $\mathbf{r}_0$ of the center of the map is given in terms of its spherical polar coordinates $\theta_0, \phi_0$ by the equation

$$\frac{\mathbf{r}_0}{a} = \sin\theta_0 \cos\phi_0\, \mathbf{i} + \sin\theta_0 \sin\phi_0\, \mathbf{j} + \cos\theta_0\, \mathbf{k} \tag{49}$$

The scalar product of these two vectors gives the cosine of the angle $\epsilon$ between them. The cosine is given by the equation

$$\cos\epsilon = \cos\theta_0 \cos\theta + \sin\theta_0 \sin\theta \cos(\phi - \phi_0) \tag{50}$$

Division of $\mathbf{r}$ by $\cos\epsilon$ extends $\mathbf{r}$ to the tangent plane, and subtraction of $\mathbf{r}_0$ gives the position vector

$$\Delta\mathbf{r} = \frac{\mathbf{r}}{\cos\epsilon} - \mathbf{r}_0 \tag{51}$$

of the point in the map. The coordinates $\Delta x, \Delta y$ are given by the scalar products of the position vector $\Delta\mathbf{r}$ and the unit vectors

$$-\cos\theta_0 (\cos\phi_0\, \mathbf{i} + \sin\phi_0\, \mathbf{j}) + \sin\theta_0\, \mathbf{k} \tag{52}$$

$$-\sin\phi_0\, \mathbf{i} + \cos\phi_0\, \mathbf{j} \tag{53}$$

The coordinates are given by the equations

$$\frac{\Delta x}{a} = -\frac{\sin(\theta - \theta_0) - 2\cos\theta_0 \sin\theta \sin^2\frac{1}{2}(\phi - \phi_0)}{\cos\theta_0 \cos\theta + \sin\theta_0 \sin\theta \cos(\phi - \phi_0)} \tag{54}$$

$$\frac{\Delta y}{a} = +\frac{\sin\theta \sin(\phi - \phi_0)}{\cos\theta_0 \cos\theta + \sin\theta_0 \sin\theta \cos(\phi - \phi_0)} \tag{55}$$

When the polar coordinates $\theta, \phi$ are identified with right ascension and declination $\alpha, \delta$ in accordance with the substitutions

$$\theta = \tfrac{1}{2}\pi - \delta \qquad\qquad \phi = \alpha \tag{56}$$

then the map coordinates $\Delta x, \Delta y$ are given by the equations

$$\frac{\Delta x}{a} = \frac{\sin(\delta - \delta_0) + 2 \sin \delta_0 \cos \delta \sin^2 \frac{1}{2}(\alpha - \alpha_0)}{\sin \delta_0 \sin \delta + \cos \delta_0 \cos \delta \cos(\alpha - \alpha_0)} \tag{57}$$

$$\frac{\Delta y}{a} = \frac{\cos \delta \sin(\alpha - \alpha_0)}{\sin \delta_0 \sin \delta + \cos \delta_0 \cos \delta \cos(\alpha - \alpha_0)} \tag{58}$$

The coordinate axes are oriented so that $\Delta x$ is measured to the north and $\Delta y$ is measured to the east of the center of the map.

If two stars can be recognized in the photograph, then their distance apart in the map of a unit sphere can be computed from their known positions. The radius for the actual map is the ratio between the measured distance in the actual photograph and the computed distance in the map of a unit sphere.

**Keplerian Orbit**

The gravitational force between two masses with spherical distributions of density is the same as though the masses were concentrated at their centers. The gravitational field of each spherical distribution of density is symmetric and is the same by Gauss' theorem as it would be if the mass were concentrated at its center. The force on each element of a distribution of density can be resolved into components parallel and perpendicular to the line of centers. Only the component parallel to the line of centers survives integration. The force is given by the equation

$$f = 2\pi GM \int\int \frac{(r - a \cos \theta)}{\{r^2 - 2ar \cos \theta + a^2\}^{\frac{3}{2}}} a^2 \sin \theta \, da \, d\theta \tag{59}$$

where $G$ is the gravitational constant, $M$ is a central mass, $\rho$ is the density, $a$ is the radius, and $\theta$ is the polar angle of an element of the distribution of density with center at the distance $r$ from the central mass. Integration with respect to $\theta$ is elementary and leads to the equation

$$f = \frac{4\pi GM}{r^2} \int \rho \, a^2 \, da \tag{60}$$

Thus the motion of spheres of finite radius is given by the Keplerian orbit as long as their densities are spherically symmetric.

The analysis of the Keplerian orbit is given in many texts. If two point masses $m_1, m_2$ attract each other with the inverse square law, then the force on each is equal to

$$f = \frac{Gm_1 m_2}{r^2} \tag{61}$$

where $G$ is the constant of gravitation and $r$ is the distance between the masses. Their center of mass moves with constant velocity, because the sum of their forces is zero. The position vectors $\mathbf{r}_1, \mathbf{r}_2$ of the masses with respect to their center of mass are given by the equations

$$\mathbf{r}_1 = + \frac{m_2}{m_1 + m_2} \mathbf{r} \qquad \mathbf{r}_2 = - \frac{m_1}{m_1 + m_2} \mathbf{r} \tag{62}$$

where $\mathbf{r}$ is the vector difference in position. The velocity vectors $\mathbf{v}_1, \mathbf{v}_2$ of the masses

with respect to their center of mass are given by the equations

$$\mathbf{v}_1 = + \frac{m_2}{m_1 + m_2} \mathbf{v} \qquad \mathbf{v}_2 = - \frac{m_1}{m_1 + m_2} \mathbf{v} \tag{63}$$

where $\mathbf{v}$ is the rate of change of $\mathbf{r}$.

Substitution in Newton's laws of motion leads to the equation

$$\frac{d\mathbf{v}}{dt} = - \frac{\mu}{r^2} \mathbf{n} \tag{64}$$

where $\mu$ is equal to $G(m_1 + m_2)$ and $\mathbf{n}$ is a unit vector in the direction of $\mathbf{r}$. The vector $\mathbf{r} \times \mathbf{v}$ satisfies the equation

$$\frac{d}{dt}(\mathbf{r} \times \mathbf{v}) = 0 \tag{65}$$

because $d\mathbf{v}/dt$ is in the direction of $\mathbf{r}$. A constant vector $\mathbf{h}$ is defined by the equation

$$\mathbf{h} = \mathbf{r} \times \mathbf{v} = r^2 \mathbf{n} \times \frac{d\mathbf{n}}{dt} \tag{66}$$

The vector $\mathbf{h}$ is twice the rate at which the vector $\mathbf{r}$ sweeps out area, and is normal to the plane of the orbit.

Expansion of a vector triple product leads to the equation

$$\frac{d}{dt}(\mathbf{h} \times \mathbf{v}) = \mathbf{h} \times \frac{d\mathbf{v}}{dt} = - \mu \frac{d\mathbf{n}}{dt} \tag{67}$$

Integration gives the equation

$$\mathbf{h} \times \mathbf{v} = - \mu(\mathbf{n} + \mathbf{e}) \tag{68}$$

where $\mathbf{e}$ is a constant of integration. Conversion of a scalar–vector triple product leads to the equation

$$- \mathbf{r} \cdot \mathbf{h} \times \mathbf{v} = \mu r(1 + \mathbf{e} \cdot \mathbf{n}) = \mathbf{h} \cdot \mathbf{r} \times \mathbf{v} = h^2 \tag{69}$$

Let the polar angle $\theta$ between $\mathbf{e}$ and $\mathbf{n}$ be determined by the equation

$$\mathbf{e} \cdot \mathbf{n} = e \cos \theta \tag{70}$$

where $e$ is the magnitude of $\mathbf{e}$. The equation of a point in the orbit is

$$r = \frac{h^2}{\mu(1 + e \cos \theta)} \tag{71}$$

which is the fundamental equation of a conic section.

If $e < 1$ the orbit is an ellipse with the eccentricity $e$, and with the line of apsides in the direction $\mathbf{e}$. The semimajor axis $a$ is derived from the sum of values of $r$ for $\theta$ equal to 0 and $\pi$. The value of $a$ is given by the equation

$$a = \frac{h^2}{\mu(1 - e^2)} \tag{72}$$

The center of the ellipse is at a distance from the focus equal to the difference between the semimajor axis $a$ and the value of $r$ for $\theta$ equal to zero. The center is at the

distance $ea$ from the focus. The semiminor axis $b$ is derived from the point where

$$\cos\theta = -e \qquad \text{and} \qquad r = a \tag{73}$$

The value of $b$ is given by the equation

$$b = a\sqrt{1 - e^2} \tag{74}$$

The equation of a point in the orbit is

$$r = \frac{a(1 - e^2)}{1 + e\cos\theta} \tag{75}$$

The polar angle $\theta$ is the true anomaly of the point in the orbit.

Let the origin of coordinates be shifted to the center of the ellipse. The Cartesian coordinates $x, y$ of a point on the ellipse are given in terms of a parametric angle $\phi$ by the equations

$$x = a\cos\phi \qquad y = b\sin\phi \tag{76}$$

The distance from the focus to the point is given by the equation

$$r = \sqrt{(a\cos\phi - ea)^2 + b^2\sin^2\phi} = a(1 - e\cos\phi) \tag{77}$$

The parametric angle $\phi$ is the eccentric anomaly of the point in the orbit.

The true anomaly is related to the eccentric anomaly by the equation

$$\tan\theta = \frac{\sin\phi\sqrt{1 - e^2}}{\cos\phi - e} \tag{78}$$

from which the true anomaly is recovered by the computation of an arctangent.

The radius from the center to the point sweeps out an area equal to $\frac{1}{2}ab\phi$. The point forms a triangle with the center and the focus. The area of the triangle is $\frac{1}{2}eab\sin\phi$. The radius from the focus to the point sweeps out an area equal to the difference. The area is given by the equation

$$\tfrac{1}{2}ab(\phi - e\sin\phi) = \tfrac{1}{2}ht \tag{79}$$

where $t$ is the elapsed time since the point passed through the apse. The parametric angle $\phi - e\sin\phi$ is the mean anomaly of the point in the orbit. The eccentric anomaly is recovered from the mean anomaly by a Newton–Raphson iteration.

The period $P$ of the orbit is the time for the angle $\phi$ to increase by $2\pi$. The period is given by the equation

$$P = \frac{2\pi a^2}{h}\sqrt{1 - e^2} = \frac{2\pi a^{\frac{3}{2}}}{\mu^{\frac{1}{2}}} \tag{80}$$

The period is proportional to the three-halves power of the semimajor axis. The rate of change of the eccentric anomaly is given by the equation

$$\frac{d\phi}{dt} = \frac{\frac{2\pi}{P}}{1 - e\cos\phi} \tag{81}$$

The Cartesian components of velocity in the orbit are given by the equations

$$\frac{dx}{dt} = -\frac{2\pi a}{P}\frac{\sin\phi}{(1-e\cos\phi)} \tag{82}$$

$$\frac{dy}{dt} = +\frac{2\pi b}{P}\frac{\cos\phi}{(1-e\cos\phi)} \tag{83}$$

Scalar multiplication of the velocity by unit vectors with the components

$$\left(\frac{a\cos\phi - ea}{r}, +\frac{b\sin\phi}{r}\right) \tag{84}$$

$$\left(-\frac{b\sin\phi}{r}, \frac{a\cos\phi - ea}{r}\right) \tag{85}$$

resolves the velocity into components parallel and perpendicular to the radius vector from the focus to the point on the ellipse. The components of velocity are given by the equations

$$\frac{dr}{dt} = \frac{2\pi a}{P}\frac{e\sin\phi}{(1-e\cos\phi)} \tag{86}$$

$$r\frac{d\theta}{dt} = \frac{2\pi a}{P}\frac{\sqrt{1-e^2}}{(1-e\cos\phi)} \tag{87}$$

from which the rate of change of the true anomaly may be derived.

If $e > 1$ the orbit is an hyperbola with asymptotes at the angles where

$$\cos\theta = -\frac{1}{e} \tag{88}$$

The magnitude of the vector $\mathbf{r}\times\mathbf{v}$ is given by the equation

$$h = \sigma v_\infty \tag{89}$$

where $\sigma$ *is the projection of* $\mathbf{r}$ *on a line perpendicular to* $\mathbf{v}$ and $v_\infty$ is the magnitude of $\mathbf{v}$ at $\mathbf{r}\to\infty$. In the limit the velocity $\mathbf{v}$ lies on an asymptote and $\sigma$ is the distance from the focus to the asymptote, while the unit vector $\mathbf{n}$ is orthogonal to the sum $\mathbf{n}+\mathbf{e}$ and the vectors $\mathbf{n}$ and $\mathbf{e}$ are the sides of a right triangle. The magnitude of the vector $\mathbf{h}\times\mathbf{v}$ is given by the equation

$$hv_\infty = \mu\sqrt{e^2-1} \tag{90}$$

Solution for the eccentricity $e$ leads to the equation

$$e = \sqrt{1+\frac{\sigma^2 v_\infty^4}{\mu^2}} \tag{91}$$

which defines the parameters of the hyperbola in terms of the separation of path $\sigma$ and the velocity of approach $v_\infty$ of the two masses in orbit.

Actual orbits are non-Keplerian because of perturbations by equatorial bulges and by extraneous bodies. The Keplerian orbit does provide a qualitative system for cartography if the apsides of the Keplerian orbit are assumed to precess at the same rate as the apsides of the true orbit. Both orbits could be made to coincide at two points per period.

### Planets and Satellites

Data on the radii and the rotations of planets are to be found in the Explanatory Supplement[41]. Radar data on radii have been published by Ash, Shapiro, and Smith[44]. Radar data on rotations have been published, in the case of Mercury by Colombo and Shapiro[45], and in the case of Venus by Carpenter[46]. New data on the masses of the outer planets and Pluto have been published by Seidelmann, Klepczynski, Duncombe, and Jackson[47-50].

Data for the use of precessing Keplerian orbits in the simulation of planetary orbits are given in the Explanatory Supplement[41]. Data for the orbits of the Galilean satellites of Jupiter are given in the thesis by Marsden[43].

The hierarchy of reference planes in a geocentric representation include

1. The equator of the earth.
2. The plane of the ecliptic.
3. The orbit of the planet.
4. The equator of the planet.
5. The orbit of the satellite.
6. The equator of the satellite.

For some satellites the equator of the planet is replaced by a Laplacian plane, which is orthogonal to the axis of precession of the satellite. Each reference plane is at an angle of inclination with respect to the preceding plane. The reference axis for azimuth angles is the ascending node of each plane with respect to the preceding plane.

The plane of the ecliptic is used most often for the reference plane of a heliocentric representation. The physical and the orbital data for the planets in the present system are expressed as inclinations and longitudes for which the plane of the ecliptic is the reference plane and the vernal equinox is the reference axis. The orbital data for the satellites are expressed as inclinations and longitudes for which the equator of the planet is the reference plane and the ascending node of the equator of the planet on the ecliptic is the reference axis. Data for the epoch and the equinox of 1950.0 are given in the celestial catalog for planets and satellites.

The accurate computation of the orbits of the moon and the planets is accomplished through a step-by-step integration of the equations of motion in a Cartesian heliocentric coordinate system. The accurate computation has been described by Oesterwinter and Cohen[51].

### Binaries

Many stars consist of two or more companions. Visual binaries are so nearby that individual companions can be resolved. Observations of position and velocity over a period of time determine the elements of the orbits of the companions about a common center of mass. Spectroscopic binaries are too far away to permit resolution into individual companions, but Doppler shifts and mixed types in the spectra reveal the presence of two companions. Eclipsing binaries have orbits at such a small inclination to the line of sight that one companion periodically eclipses the other. Data for binary stars are given in the *Atlas of the Heavens* by Becvar[38]. A collection of orbital data is to be found in a *Catalog of Visual Binary Orbits* by Worley[52].

The reference plane for binary stars is the plane perpendicular to the line of sight, and the reference axis is the north meridian. The orientation of the orbit is defined by the inclination of the orbit plane to the reference plane and by the position angle of the ascending node of the orbit plane with respect to the reference plane.

## AXIS CONVERSION

The conversion of coordinates which follows a change of axes can be computed with the aid of the following subroutines.

SUBROUTINE CHAXES (Q1, F1, X0, Q0, F0, Q2, F2)

**********

FORTRAN SUBROUTINE TO CHANGE AXES OF POLAR COORDINATES

**********

The polar coordinates $\theta_1, \phi_1$ of the point with respect to the initial axes are given in the arguments Q1, F1. The polar coordinates $\theta_0, \phi_0$ of the final pole with respect to the initial axes are given in the arguments Q0, F0. The azimuth $\chi_0$ of the origin of azimuth as measured from the ascending node of the final equator on the initial equator is given in the argument X0. The polar coordinates $\theta_2, \phi_2$ of the point with respect to final axes are given in the functions Q2, F2. All angles are expressed in degrees and decimals.

SUBROUTINE CVEQEC (AA, RA, AD, RD, AE, RE, AI, RI, AN, RN)

**********

CONVERSION OF EQUATORIAL COORDINATES INTO ECLIPTIC COORDINATES

**********

The equatorial coordinates $\alpha, \delta$ are given in the arguments AA, AD and the rates of change of $\alpha, \delta$ are given in the arguments RA, RD. The obliquity $\epsilon$ is given in the argument AE, and the rate of change of $\epsilon$ is given in the argument RE. The ecliptic coordinates $i, \Omega$ are given in the functions AI, AN, and the rates of change of $i, \Omega$ are given in the functions RI, RN. All angles are expressed in degrees and decimals.

SUBROUTINE CVECEQ (AI, RI, AN, RN, AE, RE, AA, RA, AD, RD)

**********

CONVERSION OF ECLIPTIC COORDINATES INTO EQUATORIAL COORDINATES

**********

The ecliptic coordinates $i, \Omega$ are given in the arguments AI, AN and the rates of change of $i, \Omega$ are given in the arguments RI, RN. The obliquity $\epsilon$ is given in the argument AE, and the rate of change of $\epsilon$ is given in the argument RE. The equatorial coordinates $\alpha, \delta$ are given in the functions AA, AD, and the rates of change of $\alpha, \delta$ are given in the functions RA, RD. All angles are expressed in degrees and decimals.

SUBROUTINE CHEQNX (T1, A1, D1, T2, A2, D2)

**********

FORTRAN SUBROUTINE TO CHANGE EQUINOX OF EQUATORIAL COORDINATES

**********

The epoch $T_1$ of the initial equinox is given in argument T1. The right ascension and declination $\alpha_1, \delta_1$ of the point with respect to the initial equinox are given in the arguments A1, D1. The epoch $T_2$ of the final equinox is given in argument T2. The right ascension and declination $\alpha_2, \delta_2$ of the point with respect to the final equinox are given in the functions A2, D2. Epochs are expressed in Besselian years, and angles are expressed in degrees and decimals.

SUBROUTINE CVEQMP (AR, DN, A0, D0, DX, DY)

**********

FORTRAN CONVERSION OF EQUATORIAL COORDINATES INTO MAP COORDINATES

**********

The right ascension and declination $\alpha, \delta$ of a point in the map are given in the arguments AR, DN. The right ascension and declination $\alpha_0, \delta_0$ of the center of the map are given in the arguments A0, D0. The Cartesian coordinates $\Delta x, \Delta y$ in the map of a unit sphere are given in the functions DX, DY. All angles are expressed in degrees and decimals.

SUBROUTINE CVMATA (AM, AE, PH, TH)

**********

FORTRAN SUBROUTINE TO CONVERT MEAN ANOMALY INTO TRUE ANOMALY

**********

The mean anomaly is given in argument AM, and the eccentricity is given in argument AE. The eccentric anomaly is given in the function PH, and the true anomaly is given in the function TH. All angles are in the same cycle. All angles are in degrees and decimals.

## STELLAR CARTOGRAPHY

### Nomenclature

An important part of celestial cartography is a list of names of stars and nebulae with summaries of their properties. Many bright stars have special names. In the Bayer system, each star is designated by Greek letter and constellation, while in the Flamsteed system, each star is designated by catalog number and constellation. A star may have many designations, which are the entry numbers of the star in different catalogs. The star may be designated by its number in the Durchmusterung, in the Henry Draper Catalog, in the Boss General Catalog, or in the Yale Catalog of Bright Stars. A nebula may be designated by its number in the Messier Catalog, or in the Dreyer New General Catalog.

### Position and Proper Motion

Star positions in right ascension and declination and proper motions in right ascension and declination are listed in various catalogs for the epoch and equinox of 1950.0. A standard reference for many years was the *General Catalog* by Boss[32] with a listing of 33342 stars. A source of recent data is the *Star Catalog* of the Smithsonian Astrophysical Observatory[33] with a listing of 258997 stars.

The components of proper motion are actually the rates of change of right ascension and declination $\dot{\alpha}, \dot{\delta}$ and the great circle proper motion is given by the square root of the sum of squares of $\dot{\alpha} \cos \delta, \dot{\delta}$.

### Parallax

As the earth revolves around the sun the apparent position of a star describes an ellipse with respect to background stars. The parallax of the star is the angular deviation of the apparent position of the star from the position which the star would have if it were viewed from the sun. The distance to a star is one parsec if the radius of the earth's orbit subtends 1" of arc at the star.

The distance to a star may be converted from parsecs to kilometers with the aid of the equivalence

$$1.0 \text{ parsec} = 3.085678 \times 10^{13} \text{ kilometers} \tag{92}$$

The proper motion of a star may be converted into velocity with the aid of the equivalence

$$1.0 \frac{(\text{pc})(")}{(\text{yr})} = 4.740573 \frac{(\text{km})}{(\text{sec})} \tag{93}$$

These conversion factors are required for the reduction of catalog data to a single system of coordinates.

**Starlight**

In the beginning the apparent magnitudes of stars were assigned by visual estimation. When photometers became available, it was possible to compare the brightness of two stars. The light of the brighter star was dimmed through the adjustment of a shutter until both stars appeared to be equally bright. The original assignment of magnitudes was found to obey an empirical law which has been adopted as the standard. If $m_1, m_2$ are the apparent magnitudes of two stars and if $I_1, I_2$ are their apparent intensities, then the magnitudes and the intensities are related by the equation

$$m_1 - m_2 = -2.5 \log_{10} \frac{I_1}{I_2} \tag{94}$$

Thus a 5-unit difference in magnitude corresponds to a 100-fold ratio of brightness.

Because of the inverse square law, the apparent magnitude of a star depends upon its distance. The absolute magnitude of a star is that apparent magnitude which the star would have if it were at a distance of 10 parsecs. The apparent magnitude $m$ is related to the absolute magnitude $M$ and the parallax $\pi$ by the equation

$$M = m + 5 + 5 \log_{10} \pi \tag{95}$$

The difference $m - M$ is the distance modulus of the star.

A sequence of stars can be arranged in the order of increasing magnitude. The sequence depends upon whether the photometric instrumentation is bolometric, visual, photographic, photoelectric, or monochromatic. The bolometric magnitude of the sun is defined to be equal to the visual magnitude of the sun. The photographic and photoelectric magnitudes of an A0 star are defined to be equal to the visual magnitude of the A0 star. The photoelectric magnitudes of other stars deviate from their visual magnitudes because they have a different color from the color of the standard stars. The amount of deviation is the color index.

The apparent magnitude of a star can be derived from the integral of the product of the spectral intensity and the instrumental sensitivity. The bolometric magnitude is determined by the entire energy in the spectrum, and the sensitivity is unity for all wave lengths. The visual magnitude depends upon whether the visual photometry is under photopic or scotopic conditions of observation. For photopic photometry the sensitivity is a maximum at 5550Å while for scotopic photometry the sensitivity is a maximum at 5100Å. For photography with blue-sensitive plates the sensitivity is a maximum at 4300Å. For photoelectric photometry the sensitivity depends upon the combination of filter and cathode in the photoelectric instrumentation. In the $U, B, V$ system the ranges of sensitivity are centered around 3500Å, 4350Å, 5550Å respectively.

The color of the star is specified by the color index $B - V$ or by the color index $U - B$.

An important variable in the measurement of stellar magnitude is the absorption of a ray of starlight by the atmosphere. The amount of absorption depends upon the state of the weather and upon the length of path in the atmosphere. The length of path varies like the secant of the zenith angle. Measurements at different times in the night with different zenith angles provide data which can be extrapolated to zero length of path. The extrapolation is accurate only for monochromatic radiation because the atmospheric absorption varies with wave length.

Spectral Type

A star is formed in the gravitational collapse of a globule of gas and dust. The interior of the star is heated by compression until thermonuclear reactions begin to occur. The heat which is liberated in the interior is transported to the surface where it is radiated into space. The spectrum of a star is the distribution of energy in the radiation which escapes from the surface layers of the star. The color which is absorbed or emitted with the greatest efficiency moves the least distance between emission and absorption. It has the least intensity in the spectrum because it comes from the outermost coolest layers of the star. Especially efficient for absorption and emission are atoms in the outer layers.

The distribution of energy in the radiation in a star deviates from the distribution of energy in a black body. It is the deviation of distribution which maintains the outward transportation of the radiation. An assignment of temperature to the gas should be made only as a measure of the total energy content. The effective temperature of a star is the temperature of that black body which would have the same total energy. The color of the star shifts from red to blue with increasing temperature.

The atmospheres of stars are composed of molecules, atoms, ions, electrons, and photons. The rate of absorption of photons by each constituent is proportional to the concentration of the constituent. The concentration of a constituent is a kinetic balance between the rates of the reactions which liberate and eliminate the constituent. Reactions in which there is no change in the number of reactants depend upon the temperature, while reactions in which there is a change in the number of reactants depend upon both pressure and temperature. At equilibrium the concentrations of the reactants are determined by equilibrium quotients. A decrease of pressure favors dissociation and ionization.

An important feature of stellar spectra is the Balmer series for hydrogen. Important wave lengths in the Balmer series are given in the following table[62].

| Hα | Hβ | Hγ | Hδ | Series Limit |
|---|---|---|---|---|
| 6562.82Å | 4861.33Å | 4340.47Å | 4101.74Å | 3645.98Å |

At the series limit there is a Balmer discontinuity in the spectrum. As temperature rises, molecules are dissociated into atoms, and atoms are ionized into ions. Metals are ionized first, then hydrogen is ionized next, and helium is ionized last. The temperature of the star may be estimated from the relative strengths of the absorption lines of atoms with different ionization potentials. The density of the star may be estimated from the broadening of absorption lines by interatomic collisions.

The evolution of stars of various masses has been computed theoretically. Although the theoretical models are based upon simplifying assumptions, they serve as guidance for the interpretation and coordination of observations.

The spectra of stars can be correlated with their positions in a Hertzsprung–Russell

diagram where the logarithm of luminosity is plotted against the logarithm of effective temperature. Young stars fall on the zero-age main sequence while red giants fall on the red giant branch. The most massive stars are the hottest and the bluest. They evolve the soonest from the main sequence to the giant branch. Eventually they fall back twice along the horizontal branch. They may end as white dwarfs or neutron stars.

The spectra of stars can be correlated with their positions in a Hertzsprung-Russell diagram where absolute magnitude is plotted against color index. The basis for the classification of a star is a visual comparison of its spectrum with the spectra of stars with absolute magnitudes which are known from trigonometric parallax. Especially useful for the correlation of absolute magnitude with color index are clusters of stars all with the same age and distance but with a range of masses.

As the stars evolve away from the main sequence they expand in radius. The temperature and pressure at their surfaces decrease. Some lines in the spectra of the stars are sensitive to temperature while others are sensitive to both pressure and temperature. The spectra can be arranged in sequences with progressive variations in line intensity. The sequences are illustrated in the *Atlas of Stellar Spectra* by Morgan, Keenan, and Kellman[63].

In the classification of stars in the Morgan-Keenan system, each star is assigned a color step with one of the letters O, B, A, F, G, K, M. For finer classification within a step, a numeral is appended to the letter. Each star is assigned a luminosity class with one of the numerals I, II, III, IV, V. For finer classification within a class a letter a or b is appended to the numeral.

Tables to express the relationship between absolute magnitude and color index for each luminosity class have been published by Allen[60], by Keenan[67], and by Blaauw[68]. The spacing between the absolute magnitudes for the various luminosity classes is too large to permit the recovery of the absolute magnitudes of individual stars from their spectroscopic classifications. The only systematic tabulation of individual absolute magnitudes in the modern literature appears to be in the *Catalog of the Heavens* by Becvar[38].

### Apparent Magnitude

The visual magnitude $V$ and the color index $B - V$ are given for bright stars in the *Catalog of Bright Stars* by Hoffleit[34]. The apparent magnitudes in the $U, B, V$ system for many of these stars are to be found in *Communication No.* 63 of the Lunar and Planetary Laboratory by Johnson, Mitchell, Iriarte, and Wisniewski[85], and in the *Publication No.* 21 of the Naval Observatory by Blanco, Demers, Douglass, and Fitzgerald[35].

### Spectral Standards

A few stars have been elected to membership in a set of standard stars[74,75]. The sun is a representative G2 V star and Alpha Lyrae or Vega is a representative A0 V star. Evidence that these stars are not perfectly constant has been published by Johnson[93,94].

The spectrum of the sun has been measured by a NASA team whose principal investigator was Thekaekara[72,73]. They observed the sun from an aircraft at high altitude. They used a quartz iodine lamp and commercial black bodies for reference standards. They have tabulated their results in the form of an histogram.

The solar constant outside the earth's atmosphere is

$$0.1353 \frac{(\text{watt})}{(\text{cm})^2} = 1.940 \frac{(\text{cal})}{(\text{sec})(\text{cm})^2} \tag{96}$$

and the astronomical unit is

$$149597900 \text{ km} \tag{97}$$

whence the radiant flux from the sun is

$$3.80 \times 10^{33} \frac{(\text{erg})}{(\text{sec})} \tag{98}$$

The radiant intensity of a black body is given by the formula

$$\sigma T^4 \tag{99}$$

where the Stefan–Boltzmann constant $\sigma$ is

$$5.66961 \times 10^{-5} \frac{(\text{erg})}{(\text{sec})(\text{cm})^2(^\circ\text{K})^4} \tag{100}$$

The effective temperature of the sun is the temperature of that black body which would have the same radiant intensity. The radius of the sun is

$$695992 \text{ km} \tag{101}$$

whence the effective temperature is

$$5762^\circ\text{K} \tag{102}$$

The luminosity of a star is the radiant flux of the star.

The photopic visual sensitivity is tabulated on page 87 of the *Smithsonian Physical Tables*[58], and the energy distribution in the solar spectrum has been published by Thekaekara[73]. The mechanical equivalent of light[60] is

$$680 \frac{(\text{lumens})}{(\text{watt})} \tag{103}$$

and the luminance of a star of zero apparent visual magnitude outside the atmosphere[60] is

$$2.65 \times 10^{-10} \frac{(\text{lumens})}{(\text{cm})^2} \tag{104}$$

With these data it may be determined that the apparent visual magnitude of the sun is −26.70 just outside the atmosphere, and the absolute visual magnitude of the sun is +4.87. That the photovisual magnitude of the sun is −26.73 has been reported by Stebbins and Kron[71].

The spectrum of the sun is illustrated in Appendix D.

The distribution of absolute energy in the spectrum of Alpha Lyrae has been determined by Oke and Schild[81]. They compared the light of the star with the light of calibrated lamps and black bodies of known temperature. They used nominal corrections for atmospheric extinction at their observatory. The various sources of atmospheric extinction have been resolved by Hayes and Latham[83]. They have corrected measurements by Hayes[60] to give absolute spectral energy. The distribution of energy in the spectrum of Alpha Lyrae has been recalibrated by Tüg, White, and Lockwood[84].

They compared the light of the star with the light of newly calibrated black body cavities. A thirteen-color photometry of 1380 stars has been cataloged by Johnson and Mitchell[89]. They give a method which converts the thirteen magnitudes into absolute intensities at nominal wave lengths. An illustration of the spectrum of Alpha Lyrae in a book by Dufay[62] shows that interpolation between nominal wave lengths is of doubtful value because of deep absorption lines.

An interferometer is used by Johnson[90-92] in an elegant method of spectrometry. Starlight from the telescope is split into two equal beams by a half-silvered mirror. The beams are reflected by mirrors and are recombined at a detector. If the optical path length is the same for both beams, then all colors are reinforced equally. If one mirror is moved, the difference in phase for each color depends upon the wave length. Interference between the beams is measured for a sequence of positions of one mirror. The displacement between positions of the mirror is one quarter wave length of a reference standard. The wave length of the reference standard is 3164.3Å, which is half the wave length of a helium-neon laser. An interferogram is the detector current for $2^{14}$ positions of the mirror. Then a fast Fourier transform of order $2^{14}$ can be applied to the interferogram to obtain spectral intensities at 8192 discrete frequencies. The sampling of the interferogram at $N$ frequencies is equivalent to the application of a weighting factor of $\sin N\alpha / \sin \alpha$ to a continuous spectrum, where the relative deviation $\alpha$ from one discrete frequency is a multiple of $(1/N)\pi$ at any other discrete frequency. The advantage of the interferometer is that it uses all of the light from the star, whereas a monochromator uses only that fraction which is deflected through a narrow slit. Unfortunately, filtering in the instrumentation eliminated all wave lengths short of 4000Å and all wave lengths beyond 10000Å.

The spectral data for Alpha Lyrae are compared in Appendix D.

At least seven-color photometry would be required for an accurate determination of distance modulus, because the spectrum is determined by the following properties of the star.

1. Mass.
2. Angular Momentum.
3. Age.
4. Helium Content.
5. Metal Content.
6. Interstellar Absorption.
7. Distance.

Although multicolor photometric data do exist, they do not seem to have led yet to a systematic improvement in distance moduli.

**Variables**

A number of stars pulsate in luminosity. The Cepheid variables occur in a narrow band between the main sequence and the giant branch. They have a period--luminosity relationship. The RR Lyrae variables occur in a narrow gap in the horizontal branch. They have a uniform absolute magnitude. The presence of variable stars in a stellar system helps to establish a distance modulus for the system.

**Distance**

The parallax of the nearest stars can be observed directly, and the distance can be determined by trigonometry. A collection of trigonometric parallaxes is to be found in the *General Catalog of Trigonometric Stellar Parallaxes* by Jenkins[36].

Most stars are too far away and their distances must be derived from their distance moduli. The apparent magnitude of a star can be measured directly, but the absolute magnitude must be estimated by spectroscopy. A correction must be applied for interstellar absorption.

That trigonometric parallax has a probable error of 0.028" has been concluded by Strand[30]. Distances to stars on the main sequence can be determined to a probable error of ± 15% from spectroscopic parallax, but distances to stars on the giant branch have maximum errors of 80% because of the wide separation between luminosity classes in the Hertzsprung–Russell diagram. Where trigonometric and spectroscopic data both are available for the same star, a weighted mean has been computed with weights inversely proportional to the squares of the nominal errors. The mean parallaxes are given in the celestial catalog.

### Radial Velocity

The absorption lines in the spectrum of a star are shifted because the star has a radial velocity relative to the earth. That radial velocity has a probable error of 4.5 (km)/(sec) has been concluded by Petrie[31]. A collection of radial velocities is to be found in the *General Catalog of Stellar Radial Velocities* by Wilson[37].

## CLUSTER CARTOGRAPHY

The gravitational collapse of a cloud of gas and dust may create a number of stars which move together thereafter for a period of time. Interactions between the stars in a cluster and the stars in the field maintain a random distribution of velocity among the stars. The probability that any star is a member of the cluster depends upon both the position and the velocity of the star. The membership of a cluster does not remain constant because there are captures and escapes of stars between the cluster and the field. The density of stars in a cluster fades away gradually with distance from the center of the cluster. The mixture of stars is not uniform, and the most luminous stars tend to congregate near the center of the cluster. A list of clusters is to be found in a *Catalog of Star Clusters and Associations* by Alter, Ruprecht, and Vanysek[103].

Galactic clusters contain a few hundred stars. A few galactic clusters have received intensive study because they provide the basis for the experimental determination of the zero–age main sequence in the Hertzsprung–Russell diagram. A list of galactic clusters is to be found in a *Catalog of Galactic Clusters* by Hogg[128].

The distributions of stars in galactic clusters are determined from observations of the positions and magnitudes of the individual stars. The mass and the luminosity of a cluster can be computed from the number of stars with the aid of nominal relations between mass and luminosity.

For each cluster there is a file of positional data and a file of photometric data. Studies of proper motion have been limited to the establishment of membership for each cluster. Unless the cluster contains many members bright enough to be listed in the general catalogs, it is not possible to determine the proper motion of the cluster with respect to a nonrotating reference frame.

Root mean square radii for galactic clusters have been computed from the summation of squares of the radii of the positions of the individual stars as published in the literature[104–127]. The mean radii are listed in the celestial catalog.

Trigonometric distances to galactic clusters are available for a few of the nearest clusters. The apparent rate of contraction of a cluster can be combined with the rate of recession of the cluster to determine its distance by perspective. The accuracy of the determination depends upon the assumption that the average motion of the stars is parallel to a line toward an apex on the celestial sphere. Photometric distances to galactic clusters are based on the correlation of the $U, B, V$ magnitudes of all of the stars in the cluster with the zero-age main sequence. The magnitudes in the presence of interstellar reddening have excesses relative to the magnitudes for an absence of interstellar reddening. The excesses in $B - V$ and $U - B$ are determined by the amount of displacement which is required in order to bring the stars into coincidence with the main sequence in a plot of $U - B$ against $B - V$. The excess in $V$ then is three times the excess in $B - V$. The distance is derived from the corrected distance modulus.

Globular clusters contain several thousand stars. A few globular clusters have received intensive study because they contribute to an understanding of galactic structure. Lists of globular clusters are to be found in catalogs of globular clusters by Hogg[128] and by Arp[129].

The distributions of stars in globular clusters are determined from observations of the integrated luminosity through straight slits or circular apertures. The total luminosity is determined in a schraffierkassette where the image of the cluster is moved back and forth over a photographic plate in a raster fine enough to make the exposure uniform. The number of stars and the mass of a cluster can be computed from the luminosity with the aid of nominal relations between luminosity and color index.

Globular clusters have been observed through concentric apertures and have been scanned with offset apertures. The most thoroughly surveyed clusters are Omega Centauri and 47 Tucanae, for which there are photoelectric data by Gascoigne and Burr[131]. A thoroughly surveyed elliptical galaxy is NGC 3379, for which there are photoelectric data by Miller and Prendergast[135]. Photoelectric data for 67 globular clusters have been published by Kron and Mayall[133]. Star counts of 54 globular clusters have been published by King, Hedemann, Hodge, and White[140].

An analysis of the surface density in the image of a cluster has been published in a series of papers by King[136-141]. In the first paper there is an empirical formula which is based upon the assumption that surface density varies as the square of the distance from the edge of the image. If the space density in a cluster varied linearly with distance from the boundary of the cluster, then the surface density in the image would vary as the three-halves power of the distance from the edge of the image because of the curvature of the boundary of the cluster. In the third paper there is a theoretical formulation which is based upon the assumption that the random velocities of the stars have a truncated Maxwellian distribution with isotropy. The actual distribution must be anisotropic in order that the stars are scattered outward against the inward acceleration of the gravitational field. The observations of clusters were well represented by a series of models with only two parametrs. One parameter was a core radius and the other parameter was the boundary radius. In papers by Peterson and King[141,142] there are values of the radii for the theoretical models in the third paper.

For the diameter of a cluster, various authors have quoted the diameter of aperture which transmits an arbitrary fraction of light such as one-fifth, one-half, or nine-tenths of the total light. The diameter of aperture for total light is indeterminate. A more meaningful measure of the diameter of a cluster would be the root mean

square radius $\mathcal{R}$, as defined by the equation

$$\mathcal{R}^2 = \frac{\sum m_i r_i^2}{\sum m_i} \tag{105}$$

where $m_i$ and $r_i$ are the mass and the distance of the $i$th star from the center of the image. Insofar as there is a surface density $\sigma(r)$ at the distance $r$ from the center of the image, the mean square radius is given by the equation

$$\mathcal{R}^2 = \frac{2\pi \int_0^\infty \sigma(r)\, r^3\, dr}{2\pi \int_0^\infty \sigma(r)\, r\, dr} \tag{106}$$

In the case of a circular aperture, an integration by parts gives the equation

$$2\pi \int_0^\infty \sigma(r)\, r^3\, dr = 4\pi \int_0^\infty r \int_r^\infty \sigma(s)\, s\, ds\, dr \tag{107}$$

It is just the integral under the integral sign which is observed through apertures of various radii.

Insofar as the cluster has spherical symmetry, a one–dimensional, two–dimensional, or three–dimensional evaluation of the sum of squares of coordinates gives truly once, twice, or thrice the evaluation of the sum of squares of one coordinate. Not only is the summation of squares of radii important in the evaluation of moments of inertia but it gives also the function which appears in the time–dependent form of the virial theorem.

Let the globular cluster have spherical symmetry and let $r, \phi, z$ be cylindrical polar coordinates with origin at the center of symmetry and with axis along the line of sight. Let $n$ be the number of stars per unit volume in a cluster of radius $a$, and let $N$ be the number of stars which are visible through an aperture of radius $r$. Then $N$ is related to $n$ in accordance with the equation

$$N = 4\pi \int_0^r \int_0^{\sqrt{a^2 - s^2}} n\, dz\, s\, ds \tag{108}$$

Let $n$ be expressed by the series expansion

$$n = \sum_{k=1}^{\infty} c_k \frac{1}{\kappa \sqrt{r^2 + z^2}} \sin \kappa \sqrt{r^2 + z^2} \tag{109}$$

where the parameter $\kappa$ is defined by the equation

$$\kappa a = k\pi \tag{110}$$

Let $N_k$ be the result of the substitution of the $k$th function into the integral for $N$. Then $N$ is given by the equation

$$N = \sum_{k=1}^{\infty} c_k N_k \tag{111}$$

The functions $N_k$ were evaluated at thirty–six radii $r_i$ by sixteen point Gaussian integration, and the coefficients were determined by matrix inversion.

The total number of stars is the value of $N$ for $r = a$. The mean square radius $\mathcal{R}^2$

can be computed in terms of either cylindrical coordinates or spherical coordinates as expressed by the equation

$$\mathcal{R}^2 = \frac{\int_0^a \int_0^{\sqrt{a^2-r^2}} n\, r^3\, dz\, dr}{\int_0^a \int_0^{\sqrt{a^2-r^2}} n\, r\, dz\, dr} = \frac{2}{3} \frac{\int_0^a n\, r^4\, dr}{\int_0^a n\, r^2\, dr} \tag{112}$$

The integration in spherical coordinates is accomplished with the aid of the equations

$$\int_0^\pi r \sin kr\, dr = \frac{(-1)^{k+1}\pi}{k} \tag{113}$$

and

$$\int_0^\pi r^3 \sin kr\, dr = \left[\pi^2 - \frac{6}{k^2}\right] \frac{(-1)^{k+1}\pi}{k} \tag{114}$$

These equations are useful for checking the series expansions of functions whose integrations can be evaluated directly. The matrix whose elements are $N_k(r_i)$ can be inverted once and for all. The inverse matrix then can be applied to the surface density at the 36 radii $r_i$ to obtain the coefficients of an expansion of space density in a series of the Helmholtz functions.

Root mean square radii of globular clusters have been estimated on the basis of the core radii and boundary radii in the papers by Peterson and King[141,142]. These data for radii go with the theoretical models in the third paper by King. Inasmuch as there are no data for mean square radii for these models, the empirical formula in the first paper by King has been generalized so as to simulate the theoretical curves. Both radii and the exponent were allowed to vary with concentration in such a way as to optimize the simulation of the theoretical curves. The general empirical formula was calibrated directly by comparisons with the data for a few clusters and the galaxy NGC 3379. Integrations with fractional exponents can be expressed in terms of the incomplete beta function for which there are now standard computing subroutines. The mean radii are listed in the celestial catalog.

Photometric estimates of distances to globular clusters are based on the 25 brightest stars or on the RR Lyrae type variable stars in the horizontal branch of the Hertzsprung–Russell diagram. Nominal corrections for interstellar reddening are proportional to the secant of the angle between the line of sight and the pole of the galactic equator. Data on magnitudes and distances are summarized in the papers by Peterson and King.

Determinations of the radial velocity from the spectra of 70 globular clusters have been summarized by Kinman[149].

## GALACTIC CARTOGRAPHY

The ultimate challenge is the cartography of a galaxy from a viewpoint which can never be reached by human eye.

The Milky Way is the visible evidence of the galaxy in which the solar system is located. The galaxy is composed of gas, dust, and stars. Part of the material is concentrated in a flat disk, part is concentrated in a central nucleus, and part is

distributed over a spherical volume of which the disk is the equatorial plane. The material in the disk circulates around the nucleus with an angular velocity which diminishes with distance from the center. The primary structure of the disk is a pair of arms which spiral outward from the center. In the outer reaches of the galaxy there is a splitting of the arms into spurs and branches and there are detached arms with no connection to the inner spiral structure. The secondary structure of the spiral galaxy consists of clouds which are strung out along the arms, and filaments which stretch across the space between the arms.

The stars in the spiral arms are young blue stars and are designated as population I stars. They are relatively rich in metals. The stars in the central nucleus and in the globular clusters are old red stars and are designated as population II stars. They are relatively free of metals.

Much of the interstellar gas is H I or neutral hydrogen. Imbedded in the neutral hydrogen are nebulae of H II or ionized hydrogen. The nebulae are luminous because the ultraviolet light from nearby stars generates fluorescence in the hydrogen. The H II regions illuminate the spiral arms of the galaxy.

Modern determinations[96] of the orientation of the plane of the galaxy are founded on the line of concentration of radio and infrared radiation from the celestial sphere. The direction to the pole of the galactic coordinates is defined by

$$\alpha = 12^h\ 49^m.0 \qquad \delta = +\ 27^\circ\ 24' \tag{115}$$

The center of the galaxy is assumed to be in the direction of Sagittarius A, and is the direction of zero galactic longitude. The direction of the center is defined by

$$\alpha = 17^h\ 42^m.4 \qquad \delta = -\ 28^\circ\ 55' \tag{116}$$

The distance to the center is 10 kpc. The material of the galaxy rotates in a clockwise direction around the pole of the galactic coordinates. The arms of the galaxy rotate in the same direction at a slower rate.

The velocity of the sun deviates from the mean velocity of the stars in the neighborhood of the sun. The velocity of the sun with respect to the local standard of rest is 15.4 (km)/(sec) toward an apex with galactic coordinates

$$l^{II} = 51^\circ \qquad b^{II} = +\ 23^\circ \tag{117}$$

The solar velocity is added to the apparent velocities of stars to obtain the stellar velocities with respect to the local standard of rest.

Let the vector velocity $\mathbf{v}$ be the velocity of a point in the mean circular motion. The rotational velocity $v(\varpi)$ of the point is a function of the distance $\varpi$ of the point from the center of the galaxy. The local motion at the sun is a combination of a rate of rotation and a rate of shear. Let $\mathbf{n}$ be a unit vector in the direction to the center of the galaxy, and let $\mathbf{s}$ be a unit vector in the direction of motion around the center. The components of the space velocity $\mathbf{v}$ are given by the equations

$$\mathbf{n} \cdot \mathbf{v} = -\frac{v(\varpi)}{\varpi} r \cos b \sin l \tag{118}$$

$$\mathbf{s} \cdot \mathbf{v} = v(\varpi) - \frac{dv(\varpi)}{d\varpi} r \cos b \cos l \tag{119}$$

where $r, b, l$ are heliocentric galactic coordinates. The variation with respect to $l$ of the components of $\mathbf{v}$ leads to values of $v(\varpi)$ and its derivative $dv(\varpi)/d\varpi$.

The rotation at the position of the sun is expressed in terms of Oort's constants $A, B$

by the equations

$$\frac{v(\varpi)}{\varpi} = B - A \qquad \frac{dv(\varpi)}{d\varpi} = A + B \tag{120}$$

Modern values for Oort's constants are given by the equations

$$A = +15\,\frac{(\text{km})}{(\text{sec})(\text{kpc})} \qquad B = -10\,\frac{(\text{km})}{(\text{sec})(\text{kpc})} \tag{121}$$

The velocity in the circular motion at the sun is 250 (km)/(sec).

In the neutral hydrogen atom there is coupling between the nuclear spin and the electron spin. There is a hyperfine splitting of the nuclear energy according to whether the spins are parallel or antiparallel. Transitions between the energy levels emit or absorb photons with a wavelength of 21 cm. The radiation from a source which is moving with respect to an observer is shifted by the Doppler effect. The radiation at the sun comes from clouds of hydrogen gas in the galaxy.

The simplest interpretation of the 21 cm radiation is based on the assumption that the source which is emitting the radiation is moving in a circle concentric with the galaxy. The rotational velocity $v(\varpi)$ of the source is a function of the distance $\varpi$ of the source from the center of the galaxy. The center, the source, and the sun are at the corners of a triangle. By the cosine law, the distance $\varpi$ from the center of the galaxy is related to the distance $r$ from the sun by the equation

$$\varpi^2 = a^2 + r^2 - 2ar\cos l \tag{122}$$

where $a$ is the distance of the sun from the center of the galaxy and $l$ is the galactic longitude of the source. By the sine law, the difference $\delta v$ between the components of velocity of sun and source in the direction of $r$ is given by the equation

$$\delta v = \left\{\frac{v(a)}{a} - \frac{v(\varpi)}{\varpi}\right\} a\sin l \tag{123}$$

The distance $r$ is given in terms of the distance $\varpi$ by the equation

$$r = a\cos l \pm \sqrt{\varpi^2 - a^2\sin^2 l} \tag{124}$$

Then the intensity $I$ in the Doppler spectrum is related to the luminosity $L$ per unit volume in the direction of the source by the equation

$$I = -\frac{L}{|a\sin l|}\,\frac{\varpi}{\sqrt{\varpi^2 - a^2\sin^2 l}}\,\frac{1}{\dfrac{d}{d\varpi}\left(\dfrac{v(\varpi)}{\varpi}\right)} \tag{125}$$

If the galactic longitude is between $-90°$ and $+90°$, then $\varpi \geq a\sin l$. At the point where

$$\varpi = |a\sin l| \qquad \text{and} \qquad r = a\cos l \tag{126}$$

the intensity $I$ is infinite. The rotational velocity is given by the equation

$$v(\varpi) = v(a)\sin l - \delta v \tag{127}$$

Thus the rotation curve for $\varpi < a$ can be deduced from the Doppler shift at the maximum of intensity. For other values of $\varpi$ the luminosity $L$ can be deduced from the intensity $I$ provided the rotation curve nowhere is tangent to a line through the origin of the rotation curve. The intensity $I$ is a superposition of spectra for which $r < a\cos l$ and spectra for which $r > a\cos l$. Resolution of this ambiguity requires a

measure of ingenuity.

If the galactic longitude is between 90° and 270°, then $\varpi \geq a$. Interpretation of luminosity $L$ in terms of intensity $I$ requires an independent evaluation of the rotation curve. For sufficiently large values of the distance $\varpi$ the rotational velocity $v(\varpi)$ varies like $1/\sqrt{\varpi}$ in accordance with Keplerian law.

In the limiting case of a flat disk with circular symmetry, a surface density $\sigma(\varpi)$ can be deduced from the rotational velocity $v(\varpi)$. For circular motion without interactions between stars the gravitational potential $\varphi(a)$ is given by the equation

$$\varphi(a) = -\int_a^\infty \frac{v^2(\varpi)}{\varpi}\, d\varpi \tag{128}$$

For a circular distribution of surface density the gravitational potential $\varphi(a)$ is given by the equation

$$\varphi(a) = -G \int\int \frac{\sigma(\varpi)\, \varpi\, d\varpi\, d\phi}{\sqrt{(a + \varpi\cos\phi)^2 + \varpi^2 \sin^2\phi}} \tag{129}$$

where $\varpi, \phi$ are polar coordinates with pole at the center of the disk. The substitutions

$$k = \frac{\sqrt{4a\varpi}}{a + \varpi} \qquad \text{and} \qquad \phi = 2\theta \tag{130}$$

replace the integration with respect to $\phi$ by the complete elliptic integral of the first kind $K$, which is defined by the equation

$$K = \int_0^{\frac{\pi}{2}} \frac{d\theta}{\sqrt{1 - k^2 \sin^2\theta}} \tag{131}$$

The gravitational potential is given by the equation

$$\varphi(a) = -4G \int \frac{K}{a + \varpi}\, \sigma(\varpi)\, \varpi\, d\varpi \tag{132}$$

The modulus $k$ satisfies the inequality

$$k^2 \leq 1 \tag{133}$$

If $\varpi = a$, the modulus $k = 1$, and the elliptic integral $K$ has a logarithmic singularity, but integration through the singularity is convergent.

The determination of surface density for a specified rotation curve requires the solution of an integral equation. If the surface density is approximated by an histogram, then the differences between uniform disks of successively incremented radii provide the kernel function for the integral equation.

Elaborate contour maps of the intensity of the 21 cm line of hydrogen have been prepared by Kerr[155-157] and by Westerhout[158]. The latest interpretation of the contour maps in terms of galactic structure has been made by Simonson[162,163]. He has adjusted and tested a model of the spiral structure until it reproduced the main features of the intensity distribution. The spiral arms are simulated in the model by simple spiral lines with branching and detachment. The latest construction of a rotation curve for the galaxy has been made by Sinha[164]. He has simulated the mass of the galaxy with a nucleus, a bulge, and a disk. The rotation curve has a minimum near a radius of 3 kpc and two maxima.

Unfortunately, the motion in the galaxy is turbulent. For a root mean square random

velocity of 15 (km)/(sec), a cell radius of 1.4 pc per star, a galactic radius of 10 kpc, and a peripheral velocity of 250 (km)/(sec), the Reynolds number is given by the approximation

$$\mathcal{R}e \sim 200000 \tag{134}$$

Thus the Reynolds number is well above the critical value of 400 for which there should be turbulent flow. Convective transport of angular momentum outward from the galactic nucleus must contribute to a gradual expansion of the galaxy. The addition of local turbulent velocity to the circular velocity of the hydrogen displaces the apparent position of the source of the 21 cm line. It is assumed that an average of local perturbations of density and velocity is expressible by simple spirals.

## CELESTIAL CATALOG

There are many catalogs which summarize the properties of celestial objects. Each of the small catalogs gives most of the properties of each star, while each of the large catalogs lists only one property of many stars. The objective of the preparation of a catalog for the present project was to collect in one place a full set of data for each of the stars in the Nautical Almanac. It was of interest to determine whether planets, clusters, and galaxies could be fitted into a catalog of stars. For each celestial object there are several cards of data which cover physical properties, positional data, and orbital elements. All data in this catalog are reduced to the epoch and equinox of 1950.0, and are in machine readable format.

In the meantime, positional data and spectral data for 19045 stars have been collected in a computer file by W. Stein[39] in this laboratory. The ultimate source of astronomical data will be the National Astronomical Data Center which is being established by the National Aeronautics and Space Administration at Goddard Space Flight Center.

## CONSTELLATIONS

In the beginning each constellation was assigned an area on the celestial sphere. Boundaries between constellations were assigned by Delporte[95]. The boundaries were circles and meridians in the equatorial coordinates of 1875. The boundaries have precessed already since that date to an appreciable extent. The boundaries in the equatorial coordinates of 1950.0 have been computed at close enough intervals to provide smooth curves in conventional maps.

## MILKY WAY

Panoramic photography of the Milky Way is available in various publications such as the *Photographischer Himmelsatlas* of Haffner and Eisenhuth[9].

Isophotes of the Milky Way have been published by Roach and Megill[97], but these deviate in obvious detail from the panoramic photography. The isophotes were derived from extrapolations of star counts beyond the eighteenth magnitude into the ranges of bright nebulae and faint stars where individual stars cannot be resolved.

Isophotes of the Milky Way have been published by Elsässer and Haug[98], and these

are in better agreement with the panoramic photography. The isophotes were derived from photoelectric determinations of the brightness of the Milky Way in the visual and in the blue ranges of sensitivity. The isophotes have been corrected by the subtraction of the contribution of zodiacal light. They are not in a form which is convenient for digitization.

A series of isophotometric maps of the Southern Milky Way in red, yellow, and green has been prepared by Johnson[99]. Unfortunately, the isophotes cannot be used as the basis of a complete map. Not only does the intensity for each isophote vary from map to map, but the isophotes do not nest together in those common areas where successive maps overlap.

An elaborate system of contour maps has been prepared by Pannekoek and Koelbloed[100-102]. The brightness of the Milky Way is expressed as the equivalent number of stars of tenth photographic magnitude per square degree. The isophotes for the Northern Milky Way were based upon photographic plates which were prepared at Heidelberg in the northern hemisphere, while the isophotes for the Southern Milky Way were based upon photographic plates which were prepared at Lembang and at Mazelspoort in the southern hemisphere. The plates were prepared with the telescope out of focus so that the point images of stars were expanded into disc images of finite diameter. The brightest stars stood out as individual discs while the clouds of stars merged into continuous background. The variation of the density of individual discs with the magnitudes of their stars served to calibrate the photographic plates.

The isophotes evidently include the zodiacal light with the starlight. The zodiacal light depends qualitatively on the inclination of the ecliptic to the galactic equator. It is a maximum where the ecliptic and the galactic equators intersect. Otherwise it may be in the range 20 to 60 stars of 10th photographic magnitude or in the range 30 to 90 stars of 10th visual magnitude per square degree. The extent to which this amount of light can move the isophotes is inversely related to the gradient of brightness near the isophotes.

Two sets of maps for the two hemispheres overlap at the extreme ends of their ranges, and a comparison between them shows that they are only approximately in agreement. The extremes of range are perhaps the most uncertain parts of each range because they are derived from that part of the Milky Way which would be nearest to the horizon.

Several bright stars are free of isophotes in the maps of Johnson, but these stars are looped by isophotes in the maps of Pannekoek and Koelbloed. Some halation probably was included in the contour maps and is avoided in the present interpretation wherever it can be recognized.

The apparent flux of energy from a star is defined uniquely as a function of magnitude for bolometric magnitude. The apparent flux of energy is defined for visual magnitude and for photographic magnitude if the instrumental sensitivities coincide with international standards of sensitivity. The amount of starlight from a unit solid angle of the sky can be expressed as the equivalent number of stars of a given magnitude which would give the same amount of starlight. The ratio of the number for a given visual magnitude to the number for the same photographic magnitude varies with galactic coordinates. The ratio is greater than average near the galactic plane while the ratio is less than average near the galactic poles. The ratio is especially large in the densest star clouds, where a large ratio is attributed to a weakening and reddening of the starlight during its passage through interstellar gas and dust. For the same total starlight from all directions the number of stars of a given visual magnitude is twice the number of stars of the same photographic magnitude.

The isophote for an apparent brightness of 150 stars of the 10th photographic magnitude per square degree has been selected to represent the Milky Way. It is estimated that this isophote corresponds approximately to 320 stars of the 10th visual magnitude per square degree. Unfortunately, the isophote is not confined entirely to the mapped areas, and a slight amount of extrapolation was necessary with the photographs as a guide.

The isophote which has been selected to outline the Milky Way delineates all the major star clouds and dark nebulae as illustrated in the panoramic photography, and it concentrates the starlight into clouds to an extent which is not evident in traditional representations.

The Cartesian coordinates of the maps of isophotes were galactic coordinates in the coordinate system of 1880.0. The pole of the galactic coordinates was at 190° right ascension and at 30° declination. The galactic longitude was measured from the ascending node of the galactic equator. The right ascension and the declination were recovered from the galactic latitude and longitude. The equatorial coordinates for the equinox of 1880.0 were converted finally into equatorial coordinates for the equinox of 1950.0 by reference to the subroutine for the change of equinox.

## MAGELLANIC CLOUDS

The Magellanic Clouds are satellites of the Milky Way. Isophotes of the clouds have been plotted by de Vaucouleurs[165,166]. They are irregular barred galaxies with incipient arms. Each bar is at the center of a rotating envelope of hydrogen. The major axis of the hydrogen in the large cloud is at a position angle of 165° while the axis of the bar is at a smaller position angle. The plane of the hydrogen is inclined at an angle of 63° to the line of sight, and the hydrogen in the northwest is receding.

The visible bar of each cloud is displayed with a background grid of parallels and meridians in photographs by Vehrenberg[10]. A polygonization has been selected to illustrate the boundary of the most visible region in each photograph.

## ANDROMEDA GALAXY

The nearest spiral galaxy is in the Andromeda constellation. It is designated NGC 224 or M31. It has an elliptical image with the major axis at a position angle of 38°. A pair of elliptical galaxies are satellites of the spiral galaxy. A satellite southeast of the major axis is designated NGC 221 or M32, while a satellite northwest of the major axis is designated NGC 205. Isophotes of the galaxies have been plotted by de Vaucouleurs[167]. The isophotes do not show the spiral structure. The positions of emission nebulae in the galaxy have been recorded by Baade and Arp[168]. The positions of the emission nebulae have been correlated by Arp[169] with a pair of spiral arms in a plane at 16° to the line of sight. In the plane of the galaxy the spirals are expressed by the equation

$$r = 30' e^{0.13\theta} \tag{135}$$

where $r$ is the angular distance from the center of the galaxy and $\theta$ is the azimuth angle with respect to the major axis. The emission nebulae do not all fall on the mathematical spiral. There is evidence of distortion and branching of the spiral arms. Arguments that the distortion is evidence for warping of the plane of the galaxy are

not convincing. The galaxy M32 must be between us and the plane of M31 because its apparent direction is inside the perimeter of M31, but just how close it is to the plane of M31 is not known with enough accuracy. Contour maps of the atomic hydrogen in the galaxy have been prepared by Argyle[170] and by Roberts[171,172]. The maps do not show the local distortion of the spiral arms. The hydrogen is concentrated in a ring at a distance of 52' from the center of the galaxy. The hydrogen is receding on the northeast side of the galaxy. A rotation curve for the galaxy has been published by Rubin and Ford[173,174]. The rotation curve has a minimum near 10' from the center and two maxima.

A photograph of the galaxy has been published by Haffner and Eisenhuth[9], and a transparency has been purchased from the Hale Observatories. Inspection of the photographs indicates that there are branchs of the spiral arms and filaments between the spiral arms. Dark lanes can be perceived between the spiral arms. The appearance of the galaxy indicates that the northwest edge is the nearest and the spiral arms trail the angular velocity.

The scale of a photograph has been determined from the positions of stars in the field of view. A grid of lines at one minute intervals of right ascension and declination was plotted to scale for comparison with the photograph. The outlines of the most prominent dark lanes have been transferred to the grid. The periphery of the visible images of the galaxy and its satellites have been simulated by ellipses.

## DISCUSSION

There was a spectacular decrease in the time for the extraction of data when the use of format statements with character data was replaced by the use of shift statements with binary data. The extraction of data is only part of the cartographic computation, and the times for selection and transformation remained the same.

In the original publication by Delporte there was a small projection of the constellation Norma into the constellation Lupus, but this projection is assigned to Circinus in the present repertory in conformity with modern star charts[12-14].

The radii of globular clusters are difficult to define. The edge of the image is hidden in the background of fog and stars. The number of stars which are counted in a photographic plate increases and expands with increase in the time of exposure of the photographic plate. The distribution of radiance differs from the distribution of number. The most massive stars, which congregate near the center of the cluster, dominate the radiance. The distribution of mass is intermediate between the distribution of radiance and the distribution of number. There is evidence that many clusters have composite structures with dense nuclei and diffuse halos. It is possible that the image of a cluster is composed of concentric disks with a density which varies as the three-halves power of distance from the edge of each disk. That M3 and M15 have composite structures has been reported by Da Costa and Freeman[144], and by Newell and O'Neil[145].

An expression of density as a series of Helmholtz functions gives greater flexibility than a two-parameter representation. The advantage of the use of Helmholtz functions in a series for density is that a series for gravitational potential then is available instantly. The disadvantage of the use of Helmholtz functions is that the series converge slowly when the density function has a small central core.

An interesting feature of the Helmholtz representation is that if the density were expressed directly at the discrete space radii, then the matrix to determine the

coefficients would be singular, because the highest order Helmholtz function is zero at each discrete radius. The singularity is removed from the matrix for the determination of coefficients as the result of integration with respect to $r$, $z$, because the integration gives linearly independent values at the discrete radii.

## CONCLUSION

There can be a 50-fold increase in the speed of extraction of data when the use of format specifications with character data is replaced by the use of shift instructions with binary data.

The difference in magnitude between luminosity classes is too great for spectral classification to be an adequate base for three-dimensional cartography.

## BIBLIOGRAPHY


1. *Cache, Oklahoma.*
   U. S. Army Engineer Topographic Laboratories, Fort Belvoir, Virginia, 1972.

2. *Transformation of Terrestrial Survey Data to Doppler Satellite Datum.*
   R. J. Anderle, Journal of Geophysical Research, **79**, 5319 (1974)

3. *The Plotting of Maps on a CRT Printer.*
   A. V. Hershey, Naval Weapons Laboratory, Dahlgren, Virginia, Report No. 1844 (May, 1963)

4. *Cartographic Symbology.*
   A. V. Hershey, Proceedings of International Conference on Automation in Cartography, Reston, Virginia, December, 1974, p. 215, (American Congress on Surveying and Mapping, Falls Church, Virginia, 1976)

5. *A Computer System for Scientific Typography.*
   A. V. Hershey, Computer Graphics and Image Processing, 1, 373 (1972)

6. *Cartographic Data Bases.*
   E. L. Robe, Proceedings of International Conference on Automation in Cartography, Reston, Virginia, December, 1974, p. 152, (American Congress on Surveying and Mapping, Falls Church, Virginia, 1976)

7. *World Data Bank II: Content, Structure, and Application.*
   D. E. Anderson, J. L. Angel, and A. J. Gorny, Proceedings of the First International Advanced Study Symposium on Topological Data Structures for Geographic Information Systems, Harvard University, October, 1977.

8. *Map Projection Equations.*
   F. Pearson II, Naval Surface Weapons Center, Dahlgren, Virginia, Report TR-3624 (March, 1977)

9. *Das Weltall im Bild Photographischer Himmelsatlas.*
   H. Haffner, and A. Eisenhuth, (Styria, Graz, Austria, 1967)

10. *Atlas of Deep Sky Splendors.*
    H. Vehrenberg, (Sky Publishing Corporation, Cambridge, Massachusetts, 1967)

11. *The National Geographic Society–Palomar Observatory Sky Survey.*
    Robinson Laboratory of Astrophysics, (California Institute of Technology, Pasadena, California, 1952)

12. *A Map of the Heavens.*
    (National Geographic Society, Washington, August, 1970)

13. *A Star Atlas and Reference Handbook.*
    A. P. Norton, (Gall and Inglis, Edinburgh, 1966)

14. *Atlas Coeli 1950.0.*
    A. Becvar, (Ceskoslovenske Akademie Ved, Praha, 1962)

15. *Photographic Lunar Atlas.*
    Edited by G. P. Kuiper, (University of Chicago Press, Chicago, 1960)

16. *The Earth's Moon.*
    (National Geographic Society, Washington, February, 1969)

17. *Lunar Earthside Chart.*
Aeronautical Chart and Information Center, (U. S. Government Printing Office, Washington, D. C. 1970)

18. *Lunar Farside Chart.*
Aeronautical Chart and Information Center, (U. S. Government Printing Office, Washington, D. C. 1970)

19. *Lunar Polar Chart.*
Aeronautical Chart and Information Center, (U. S. Government Printing Office, Washington, D. C. 1970)

20. *Astronomy: Fundamentals and Frontiers.*
R. Jastrow, and M. H. Thompson, (John Wiley & Sons, New York, 1977)

21. *Stars and Stellar Systems. I. Telescopes.*
G. P. Kuiper, and B. M. Middlehurst, Editors, (The University of Chicago Press, Chicago, 1960)

22. *Stars and Stellar Systems. II. Astronomical Techniques.*
W. A. Hiltner, Editor, (The University of Chicago Press, Chicago, 1962)

23. *Stars and Stellar Systems. III. Basic Astronomical Data.*
K. Aa. Strand, Editor, (The University of Chicago Press, Chicago, 1963)

24. *Stars and Stellar Systems. IV. Clusters and Binaries.*
(Unpublished)

25. *Stars and Stellar Systems. V. Galactic Structure.*
A. Blaauw, and M. Schmidt, Editors, (The University of Chicago Press, Chicago, 1965)

26. *Stars and Stellar Systems. VI. Stellar Atmospheres.*
J. L. Greenstein, Editor, (The University of Chicago Press, Chicago, 1960)

27. *Stars and Stellar Systems. VII. Nebulae and Interstellar Matter.*
B. M. Middlehurst, and L. H. Aller, Editors, (The University of Chicago Press, Chicago, 1968)

28. *Stars and Stellar Systems. VIII. Stellar Structure.*
L. H. Aller, and D. B. McLaughlin, Editors, (The University of Chicago Press, Chicago, 1965)

29. *Stars and Stellar Systems. IX. Galaxies and the Universe.*
A. Sandage, M. Sandage, and J. Kristian, Editors, (The University of Chicago Press, Chicago, 1975)

30. *Trigonometric Stellar Parallaxes.*
K. Aa. Strand, Stars and Stellar Systems, **3**, 55 (1963)

31. *Radial Velocities.*
R. M. Petrie, Stars and Stellar Systems, **3**, 64 (1963)

32. *General Catalog.*
B. Boss, (Carnegie Institution of Washington, Washington, 1937)

33. *Star Catalog.*
Smithsonian Astrophysical Observatory, (Smithsonian Institution, Washington, 1966)

34. *Catalog of Bright Stars.*
D. Hoffleit, (Yale University Observatory, New Haven, Connecticut, 1964)

35. *Photoelectric Catalog.*
V. M. Blanco, S. Demers, G. G. Douglass, and M. P. Fitzgerald, Publications of the United States Naval Observatory, Volume 21, (Government Printing Office, Washington, 1970)

36. *General Catalogue of Trigonometric Stellar Parallaxes.*
L. F. Jenkins, (Yale University Observatory, New Haven, Connecticut, 1963)

37. *General Catalog of Stellar Radial Velocities.*
R. E. Wilson, (Carnegie Institution of Washington, Washington, D. C. 1953)

38. *Atlas of the Heavens. II. Catalog 1950.0.*
A. Becvar, (Sky Publishing Corporation, Cambridge, Massachusetts, 1964)

39. *Introduction to the Dahlgren General Catalog.*
W. L. Stein, and J. C. Rudisill, Naval Surface Weapons Center, Dahlgren, Virginia, Report TR-3607 (February, 1977)

40. *The Observer's Handbook.*
R. J. Northcott, Editor, (The Royal Astronomical Society of Canada, Toronto, 1970)

41. *Explanatory Supplement to the Ephemeris.*
The Nautical Almanac Offices of the United Kingdom and the United States of America, (Her Majesty's Stationery Office, London, 1961)

42. *The American Ephemeris and Nautical Almanac.*
U. S. Naval Observatory, (U. S. Government Printing Office, Washington, 1950)

43. *The Motions of the Galilean Satellites of Jupiter.*
B. G. Marsden, (PhD Thesis, Yale University, New Haven, 1966)

44. *Astronomical Constants and Planetary Ephemerides Deduced from Radar and Optical Observations.*
M. E. Ash, I. I. Shapiro, and W. B. Smith, Astronomical Journal, 72, 338 (1967)

45. *The Rotation of the Planet Mercury.*
G. Colombo, and I. I. Shapiro, Astrophysical Journal, 145, 296 (1966)

46. *A Radar Determination of the Rotation of Venus.*
R. L. Carpenter, Astronomical Journal, 75, 61 (1970)

47. *The Mass of Jupiter and the Motion of Four Minor Planets.*
W. J. Klepczynski, Astronomical Journal, 74, 774 (1969)

48. *The Masses of Saturn and Uranus.*
W. J. Klepczynski, P. K. Seidelmann, and R. L. Duncombe, Astronomical Journal, 75, 739 (1970)

49. *The Mass of Neptune and the Orbit of Uranus.*
P. K. Seidelmann, R. L. Duncombe, and W. J. Klepczynski, Astronomical Journal, 74, 776 (1969)

50. *Determination of the Mass of Pluto.*
P. K. Seidelmann, W. J. Klepczynski, R. L. Duncombe, and E. S. Jackson, Astronomical Journal, **76**, 488 (1971)

51. *New Orbital Elements for Moon and Planets.*
C. Oesterwinter, and C. J. Cohen, Celestial Mechanics, **5**, 317 (1972)

52. *A Catalog of Visual Binary Orbits.*
C. E. Worley, Publications of the United States Naval Observatory, **18(III)**, 4 (1963)

53. *Automatic Orbit Computation for Visual Binaries.*
R. Wielen, Astronomical Journal, **67**, 599 (1962)

54. *Alpha and Proxima Centauri.*
C. Gasteyer, Astronomical Journal, **71**, 1017 (1966)

55. *Dynamics of the Triple System Zeta Aquarii.*
R. S. Harrington, Astronomical Journal, **73**, 508 (1968)

56. *Smithsonian Physical Tables (9th Edition).*
W. E. Forsythe, (Smithsonian Institution, Washington, D. C. 1954)

57. *American Institute of Physics Handbook.*
D. E. Gray, Editor, (McGraw-Hill, New York, Third Edition, 1972)

58. *Miscellaneous Physical Tables. Planck's Radiation Functions and Electronic Functions.*
A. N. Lowan, (National Bureau of Standards, Work Projects Administration, New York, 1941)

59. *Determination of e/h, using Macroscopic Quantum Phase Coherence in Superconductors: Implications for Quantum Electrodynamics and the Fundamental Physical Constants.*
B. N. Taylor, W. H. Parker, and D. N. Langenberg, Reviews of Modern Physics, **41**, 375 (1969)

60. *Astrophysical Quantities.*
C. W. Allen, (Athelone Press, London, 1963)

61. *The Hertzsprung-Russell Diagram from Photoelectric Observations of Nearby Stars.*
P. P. Parenago, International Astronomical Union Symposium No. 10 (1959) p. 11.

62. *Introduction to Astrophysics: the Stars.*
J. Dufay, (Dover Publications, Inc., New York, 1964)

63. *An Atlas of Stellar Spectra.*
W. W. Morgan, P. C. Keenan, and E. Kellman, (University of Chicago Press, Chicago, 1943)

64. *A Photometric System.*
H. L. Johnson, Annales d'Astrophysique, **18**, 292 (1955)

65. *Fundamental Stellar Photometry for Standards of Spectral Type on the Revised System of the Yerkes Spectral Atlas.*
H. L. Johnson, and W. W. Morgan, Astrophysical Journal, **117**, 313 (1953)

66. *Photometric Systems.*
H. L. Johnson, Stars and Stellar Systems, **3**, 204 (1963)

67. *Classification of Stellar Spectra.*
P. C. Keenan, Stars and Stellar Systems, **3**, 78 (1963)

68. *The Calibration of Luminosity Criteria.*
A. Blaauw, Stars and Stellar Systems, **3**, 383 (1963)

69. *Quantitative Classification Methods.*
B. Strömgren, Stars and Stellar Systems, **3**, 123 (1963)

70. *U–B and B–V Colors of Black Bodies.*
H. Arp, Astrophysical Journal, **133**, 874 (1961)

71. *Six-Color Photometry of Stars. X. The Stellar Magnitude and Color Index of the Sun.*
J. Stebbins, and G. E. Kron, Astrophysical Journal, **126**, 266 (1957)

72. *The Solar Constant and the Solar Spectrum Measured from a Research Aircraft at 38000 Feet.*
M. P. Thekaekara, Principal Investigator, Goddard Space Flight Center Report No. NASA TR R-351, October, 1970.

73. *Solar Energy Outside the Earth's Atmosphere.*
M. P. Thekaekara, Solar Energy, **14**, 109 (1973)

74. *Standard Stars for Photoelectric Spectrophotometry.*
J. B. Oke, Astrophysical Journal, **131**, 358 (1960)

75. *Photometric Standard Stars.*
A. W. J. Cousins, Royal Observatory Annals, Number 7, (Royal Greenwich Observatory, Herstmonceux, 1971)

76. *Absolute Measures of Stellar Radiation.*
R. V. Willstrop, Monthly Notices of the Royal Astronomical Society, **121**, 17 (1960)

77. *Absolute Measures of Stellar Radiation II.*
R. V. Willstrop, Royal Astronomical Society Memoirs, **69**, 83 (1965)

78. *Extra-Atmospheric Spectrophotometric Standards. Energy Distribution in the Spectra of Selected Stars in CGS Units.*
A. V. Kharitonov, Soviet Astronomy-AJ, **7**, 258 (1963)

79. *Ultraviolet Spectrophotometry of Some Hot Stars.*
I. N. Glushneva, Soviet Astronomy-AJ, **8**, 163 (1964)

80. *An Absolute Spectrophotometric Calibration of the Energy Distribution of Twelve Standard Stars.*
D. S. Hayes, Astrophysical Journal, **159**, 165 (1970)

81. *The Absolute Spectral Energy Distribution of Alpha Lyrae.*
J. B. Oke, and R. E. Schild, Astrophysical Journal, **161**, 1015 (1970)

82. *Measurements of the Monochromatic Flux from Vega in the Near-Infrared.*
D. S. Hayes, D. W. Latham, and S. H. Hayes, Astrophysical Journal, **197**, 587 (1975)

83. *A Rediscussion of the Atmospheric Extinction and the Absolute Spectral-Energy Distribution of Vega.*
D. S. Hayes, and D. W. Latham, Astrophysical Journal, **197**, 593 (1975)

84. *Absolute Energy Distributions of α Lyrae and 109 Virginis from 3295A to 9040A.*
H. Tüg, N. M. White, and G. W. Lockwood, Astronomy and Astrophysics, **61**, 679 (1977)

85. *UBVRIJKL Photometry of the Bright Stars.*
H. L. Johnson, R. I. Mitchell, B. Iriarte, and W. Z. Wisniewski, Communication No. 63 of the Lunar and Planetary Laboratory, (University of Arizona, Tucson, Arizona, 1966)

86. *Eight-Color Narrow-Band Photometry of 985 Bright Stars.*
H. L. Johnson, R. I. Mitchell, and A. S. Latham, Communication No. 92 of the Lunar and Planetary Laboratory, (University of Arizona, Tucson, Arizona, 1967)

87. *Thirteen-Color Narrow-Band Photometry of One Thousand Bright Stars.*
R. I. Mitchell, and H. L. Johnson, Communication No. 132 of the Lunar and Planetary Laboratory, (University of Arizona, Tucson, Arizona, 1969)

88. *Stellar Irradiance Catalog.*
H. L. Johnson, (University of Arizona, Tucson, 1972)

89. *Thirteen-Color Photometry of 1380 Bright Stars.*
H. L. Johnson, and R. I. Mitchell, Revista Mexicana de Astronomia y Astrofisica, **1**, 299 (1975)

90. *A New Michelson Spectrophotometer System.*
H. L. Johnson, Revista Mexicana de Astronomia y Astrofisica, **2**, 219 (1977)

91. *An Atlas of Stellar Spectra. I.*
H. L. Johnson, Revista Mexicana de Astronomia y Astrofisica, **2**, 71 (1977)

92. *An Atlas of Stellar Spectra. II.*
H. L. Johnson, Revista Mexicana de Astronomia y Astrofisica, **4**, 3 (1978)

93. *The Sun as a Variable Star.*
H. L. Johnson, and B. Iriarte, Lowell Observatory Bulletin No. 96, **4**, 99 (1959)

94. *The Mystery of Vega.*
W. Z. Wisniewski, and H. L. Johnson, Sky and Telescope, **57**, 4 (1979)

95. *Délimitation Scientifique des Constellations.*
E. Delporte, (Cambridge University Press, London, 1930)

96. *The New I. A. U. System of Galactic Coordinates (1958 Revision)*
A. Blaauw, C. S. Gum, J. L. Pawsey, and G. Westerhout, Monthly Notices of the Royal Astronomical Society, **121**, 123 (1960)

97. *Integrated Starlight over the Sky.*
F. E. Roach, and L. R. Megill, Astrophysical Journal, **133**, 228 (1961)

98. *Über eine Lichtelektrische Flächenphotometrie der Südlichen und Nördlichen Milchstrasse in Zwei Farben und die Struktur des Galaktischen Systems.*
H. Elsässer, and U. Haug, Zeitschrift für Astrophysik, **50**, 121 (1960)

99. *An Absolute Isophotometry of the Southern Milky Way and Two Fields in Orion.*
H. M. Johnson, Memoir No. 15 of Mount Stromlo Observatory, (The Australian National University, Canberra, Australia, May, 1960)

100. *Photographic Photometry of the Southern Milky Way.*
A. Pannekoek, and D. Koelbloed, Publications of the Astronomical Institute of the University of Amsterdam, No. 9, (1949)

101. *Die Südliche Milchstrasse.*
A. Pannekoek, Annalen von der Bosscha-Sterrenwacht, Lembang, Java, 2, A1 -A79 (1932)

102. *Photographische Photometrie der Nördlichen Milchstrasse.*
A. Pannekoek, Publications of the Astronomical Institute of the University of Amsterdam, No. 3, (1933)

103. *Catalog of Star Clusters and Associations.*
G. Alter, J. Ruprecht, and V. Vanysek, Czechoslovak Academy of Sciences, Prague, (Plenum Press, Inc., New York, 1958)

104. *Photometric Data for the Old Galactic Cluster NGC 188.*
A. Sandage, Astrophysical Journal, **135**, 333 (1962)

105. *New Photometric Data for the Old Galactic Cluster NGC 188. The Presence of a Gap, Chemical Composition, and Distance Modulus.*
O. J. Eggen, and A. Sandage, Astrophysical Journal, **158**, 669 (1969)

106. *A Spectroscopic Study of NGC 188.*
J. L. Greenstein, and P. C. Keenan, Astrophysical Journal, **140**, 673 (1964)

107. *Proper Motions, Membership, and Stellar Content of the Old Cluster NGC 188.*
A. R. Upgren, W. S. Mesrobian, and S. J. Kerridge, Astronomical Journal, **77**, 74 (1972)

108. *Investigations on Proper Motion. XXII. The Proper Motion of the Open Cluster Messier 67.*
A. Van Maanen, Astrophysical Journal, **96**, 382 (1942)

109. *Investigation of Proper Motions in the Field of the Cluster M67.*
C. A. Murray, P. M. Corben, and M. R. Allchorn, Royal Observatory Bulletin No. 91 (1965)

110. *Spectral Types of Some of the Brighter Stars in the Cluster M67.*
D. M. Popper, Astronomical Journal, **59**, 445 (1954)

111. *Radial Velocities and Spectral Types of Some Bright Blue Stars in the Old Open Cluster M67.*
P. Pesch, Astrophysical Journal, **148**, 781 (1967)

112. *Praesepe: Magnitudes and Colors.*
H. L. Johnson, Astrophysical Journal, **116**, 640 (1952)

113. *On the Structure of the Hyades Cluster.*
H. G. Van Bueren, Bulletin of the Astronomical Institutes of the Netherlands, **11**, 385 (1952)

114. *The Hyades and Coma Berenices Star Clusters.*
H. L. Johnson, and C. F. Knuckles, Astrophysical Journal, **122**, 209 (1955)

115. *The Color-Magnitude Diagram of the Hyades Cluster.*
H. L. Johnson, R. I. Mitchell, and B. Iriarte, Astrophysical Journal, **136**, 75 (1962)

116. *Calibration of the Hyades-Praesepe Main Sequence by a New Treatment of the Stellar Motions.*
E. K. L. Upton, Astronomical Journal, **75**, 1097 (1970)

117. *Investigations on Proper Motion. XXI. Faint Members of the Pleiades Cluster.*
A. Van Maanen, Astrophysical Journal, **94**, 399 (1941)

118. *Catalogue de 3259 Étoiles dans les Pléiades.*
E. Hertzsprung, Annalen van de Sterrewacht te Leiden, **19**, 1A (1947)

119. *The Color-Magnitude Diagram of the Pleiades Cluster.*
H. L. Johnson, and R. I. Mitchell, Astrophysical Journal, **128**, 31 (1958)

120. *Photometry of the α Persei Cluster.*
R. I. Mitchell, Astrophysical Journal, **132**, 68 (1960)

121. *Studies of Stellar Rotation. IV. A Comparison of Rotational Velocities in the Alpha Persei Cluster and the Pleiades.*
R. P. Kraft, Astrophysical Journal, **148**, 129 (1967)

122. *Photometric and Spectroscopic Observations of the Double Cluster in Perseus.*
H. L. Johnson, and W. W. Morgan, Astrophysical Journal, **122**, 429 (1955)

123. *Observational Confirmation of a Theory of Stellar Evolution.*
H. L. Johnson, and W. A. Hiltner, Astrophysical Journal, **123**, 267 (1956)

124. *Ages and Structures of Stars in the h and χ Persei Association.*
R. Schild, Astrophysical Journal, **148**, 449 (1967)

125. *Absolute Magnitudes of Stars in the Scorpio-Centaurus Association.*
F. C. Bertiau, Astrophysical Journal, **128**, 533 (1958)

126. *The Scorpio-Centaurus Association. II. Spectral Types and Luminosities of 220 O, B, and A Stars.*
P. M. Morris, Monthly Notices of the Royal Astronomical Society, **122**, 325 (1961)

127. *The Luminosity Functions of Galactic Star Clusters.*
S. Van den Bergh, and D. Sher, Publications of the David Dunlap Observatory, Toronto, Canada, **2**, 203 (1960)

128. *Star Clusters.*
H. S. Hogg, Handbuch der Physik, **53**, 129 (1959)

129. *Globular Clusters in the Galaxy.*
H. C. Arp, Stars and Stellar Systems, **5**, 401, (1965)

130. *The Integrated Magnitudes and Colors of Globular Clusters.*
H. L. Johnson, Lowell Observatory Bulletin No. **99**, **4**, 117 (1959)

131. *Surface Photometry of the Globular Clusters 47 Tucanae and Omega Centauri.*
S. C. B. Gascoigne, and E. J. Burr, Monthly Notices of the Royal Astronomical Society, **116**, 570 (1956)

132. *A Photometric Study of the Globular Cluster 47 Tucanae.*
G. E. Kron, Publications of the Astronomical Society of the Pacific, **78**, 143 (1966)

133. *Photoelectric Photometry of Galactic and Extragalactic Star Clusters.*
G. E. Kron, and N. U. Mayall, Astronomical Journal, **65**, 581 (1960)

134. *Photométrie Photoélectrique d'Amas Globulaires.*
J. Rousseau, Annales d'Astrophysique, **27**, 681 (1964)

135. *Photoelectric Photometry of the E0 Galaxy NCC 3379.*
R. H. Miller, and K. H. Prendergast, Astrophysical Journal, **136**, 713 (1962)

136. *The Structure of Star Clusters. I. An Empirical Density Law.*
I. King, Astronomical Journal, **67**, 471 (1962)

137. *The Structure of Star Clusters. II. Steady-State Velocity Distributions.*
I. R. King, Astronomical Journal, **70**, 376 (1965)

138. *The Structure of Star Clusters. III. Some Simple Dynamical Models.*
I. R. King, Astronomical Journal, **71**, 64 (1966)

139. *The Structure of Star Clusters. IV. Photoelectric Surface Photometry in Nine Globular Clusters.*
I. R. King, Astronomical Journal, **71**, 276 (1966)

140. *The Structure of Star Clusters. V. Star Counts in 54 Globular Clusters.*
I. R. King, E. Hedemann, Jr., S. M. Hodge, and R. E. White, Astronomical Journal, **73**, 456 (1968)

141. *The Structure of Star Clusters. VI. Observed Radii and Structural Parameters in Globular Clusters.*
C. J. Peterson, and I. R. King, Astronomical Journal, **80**, 427 (1975)

142. *Studies of Globular Clusters. I. Star Counts in 23 Clusters.*
C. J. Peterson, Astronomical Journal, **81**, 617 (1976)

143. *The Masses of Globular Clusters. I. Surface Brightness Distributions and Star Counts.*
G. Illingworth, and W. Illingworth, Astrophysical Journal Supplement Series, **30**, 227 (1976)

144. *The Structure and Mass Function of the Globular Cluster M3.*
G. S. Da Costa, and K. C. Freeman, Astrophysical Journal, **206**, 128 (1976)

145. *The Surface-Brightness Distribution of the Globular Cluster M15.*
B. Newell, and E. J. O'Neil, Jr., Astrophysical Journal Supplement Series, **37**, 27 (1978)

146. *The Structure and Stellar Content of Globular Clusters. I. Surface-Brightness Profiles for Four Southern Clusters.*
G. S. Da Costa, Astronomical Journal, **84**, 505 (1979)

147. *Spectra of the Brighter Variables in Globular Clusters.*
A. H. Joy, Astrophysical Journal, **110**, 105 (1949)

148. *The Radial Velocities of Fifty Globular Clusters.*
N. U. Mayall, Astrophysical Journal, **104**, 290 (1946)

149. *Globular Clusters. I. The Radial Velocities of Southern Globular Clusters.*
T. D. Kinman, Monthly Notices of the Royal Astronomical Society, **119**, 157 (1959)

150. *The Galaxy and the Magellanic Clouds.*
F. J. Kerr, and A. W. Rodgers, Editors, International Astronomical Union Union Radio Scientifique Internationale Symposium No. 20. (Australian Academy of Science, Canberra, 1964)

151. *Radio Astronomy and the Galactic System.*
H. Van Woerden, Editor, International Astronomical Union Symposium No. 31, (Academic Press, New York, 1967)

152. *The Spiral Structure of Our Galaxy.*
W. Becker, and G. Contopoulos, Editors, International Astronomical Union Symposium No. 38. (Springer-Verlag, New York, 1970)

153. *A Model of the Distribution of Mass in the Galactic System.*
M. Schmidt, Bulletin of the Astronomical Institutes of the Netherlands, **13**, 15 (1956)

154. *Distribution and Systematic Motions of Neutral Hydrogen.*
P. O. Linblad, Radio Astronomy and the Galactic System, (Academic Press, New York, 1967) p. 143

155. *Interstellar Gas in the Central Region of the Galaxy.*
F. J. Kerr, Radio Astronomy and the Galactic System, (Academic Press, New York, 1967) p. 239

156. *Parkes Hydrogen-Line Survey of the Milky Way. II. The Section $l^{II} = 296°$ to 63°.*
F. J. Kerr, Australian Journal of Physics Astrophysical Supplement No. **9**, 1 (1970)

157. *Parkes Hydrogen-Line Survey of the Milky Way, III. A Synoptic View of the Galactic Equator, $l^{II} = 185°$ to 63°.*
F. J. Kerr, and J. V. Hindman, Australian Journal of Physics Astrophysical Supplement No. **18**, 1 (1970)

158. *Maryland-Green Bank Galactic 21-Cm Line Survey. Third Edition.*
G. Westerhout, (Astronomy Program, University of Maryland, College Park, Maryland, 1973)

159. *The Large-Scale Distribution of Hydrogen in the Galaxy.*
F. J. Kerr, Annual Review of Astronomy and Astrophysics, **7**, 39 (1969)

160. *Spiral Structure of Neutral Hydrogen in Our Galaxy.*
F. J. Kerr, International Astronomical Union Symposium No. **38**, 95 (1970)

161. *The Distribution of Mass in the Galactic Nucleus.*
R. H. Sanders, and T. Lowinger, Astronomical Journal, **77**, 292 (1972)

162. *Motions Near the Galactic Center and the "3-Kpc Arm".*
S. C. Simonson III, and G. L. Mader. Astronomy and Astrophysics, **27**, 337 (1973)

163. *A Density-Wave Map of the Galactic Spiral Structure.*
S. C. Simonson III, Astronomy and Astrophysics, **46**, 261 (1976)

164. *A Reexamination of the Rotation Curve for the Galaxy.*
R. P. Sinha, Astronomy and Astrophysics, **69**, 227 (1978)

165. *Studies of the Magellanic Clouds, III. Surface Brightness, Colors, and Integrated Magnitudes of the Clouds.*
G. de Vaucouleurs, Astronomical Journal, **62**, 69 (1957)

166. *Rotation and Mass of the Large Magellanic Cloud.*
G. de Vaucouleurs, Astrophysical Journal, **131**, 265 (1960)

167. *Photoelectric Photometry of the Andromeda Nebula in the U, B, V System.*
G. de Vaucouleurs, Astrophysical Journal, **128**, 465 (1958)

168. *Positions of Emission Nebulae in M31.*
W. Baade, and H. Arp, Astrophysical Journal, **139**, 1027 (1964)

169. *Spiral Structure in M31.*
H. Arp, Astrophysical Journal, **139**, 1045 (1964)

170. *A Spectrometer Survey of Atomic Hydrogen in the Andromeda Nebula.*
E. Argyle, Astrophysical Journal, **141**, 750 (1965)

171. *A High-Resolution 21-Cm Hydrogen-Line Survey of the Andromeda Nebula.*
M. S. Roberts, Astrophysical Journal, **144**, 639 (1966)

172. *The Hydrogen Distribution in Galaxies.*
M. S. Roberts, Radio Astronomy and the Galactic System. (Academic Press, New York, 1967) p. 189.

173. *Rotation of the Andromeda Nebula from a Spectroscopic Survey of Emission Regions.*
V. C. Rubin, and W. K. Ford, Jr., Astrophysical Journal, **159**, 379 (1970)

174. *Radial Velocities and Line Strengths of Emission Lines Across the Nuclear Disk of M31.*
V. C. Rubin, and W. K. Ford, Jr., Astrophysical Journal, **170**, 25 (1971)

# APPENDIX A

# MANY-PARTICLE SYSTEMS

## MANY–PARTICLE SYSTEMS

### Pressure

Let $N_i$ be the number per unit volume of particles with mass $m_i$ and velocity $\mathbf{v}_i$. The volume of particles per unit time which passes through a unit surface with unit normal $\mathbf{n}$ is the absolute value of $\mathbf{n} \cdot \mathbf{v}_i$. The momentum per unit volume is $N_i m_i \mathbf{v}_i$. The pressure is the absolute value of the normal component of the rate of transfer of momentum. The pressure $p$ is given by the equation

$$p = \sum N_i m_i \mathbf{n} \cdot \mathbf{v}_i \mathbf{v}_i \cdot \mathbf{n} \tag{1}$$

where summation with respect to $i$ is for all $\mathbf{v}_i$ from both sides of the surface. Insofar as the distribution of velocity is isotropic, the average value of each diagonal component of the tensor $\mathbf{v}_i \mathbf{v}_i$ is one third of the average value of the trace of the tensor $\mathbf{v}_i \mathbf{v}_i$. The pressure for an isotropic distribution of velocity is given by the equation

$$p = \tfrac{1}{3} \sum N_i m_i v_i^2 \tag{2}$$

In a perfect gas, the pressure $p$ and the density $\rho$ are related to the temperature $T$ by the equation

$$\frac{p}{\rho} = RT = \frac{\tfrac{1}{3} \sum N_i m_i v_i^2}{\sum N_i m_i} \tag{3}$$

where $R$ is the gas constant per unit mass. Thus the mean thermal energy per unit mass may be identified with $\frac{3}{2}RT$. The heat capacity per unit mass may be identified with $\frac{3}{2}R$.

### Virial

Let the particles in a system of particles exert gravitational forces upon each other. Let $\mathbf{r}_i$ be the position and let $m_i$ be the mass of the $i$th particle. The force $\mathbf{f}_i$ on the $i$th particle is given by Newton's law

$$\mathbf{f}_i = m_i \frac{d^2 \mathbf{r}_i}{dt^2} \tag{4}$$

Half of the trace of the tensor of inertia of the system is given by the sum

$$\sum m_i \mathbf{r}_i^2 \tag{5}$$

Differentiation twice with respect to time gives the equation

$$\tfrac{1}{2} \frac{d^2}{dt^2} \sum m_i \mathbf{r}_i^2 = \sum m_i \left( \frac{d\mathbf{r}_i}{dt} \right)^2 + \sum m_i \mathbf{r}_i \cdot \frac{d^2 \mathbf{r}_i}{dt^2} \tag{6}$$

The kinetic energy $T$ is given by the equation

$$T = \tfrac{1}{2} \sum m_i \left( \frac{d\mathbf{r}_i}{dt} \right)^2 \tag{7}$$

and the virial $Q$ is given by the equation

$$Q = -\tfrac{1}{2} \sum \mathbf{r}_i \cdot \mathbf{f}_i \tag{8}$$

The gravitational interaction between the $i$th and $j$th particles is expressed by the forces

$$\mathbf{f}_i = -Gm_i m_j \frac{(\mathbf{r}_i - \mathbf{r}_j)}{|\mathbf{r}_i - \mathbf{r}_j|^3} = -\mathbf{f}_j \tag{9}$$

The interaction makes the contribution

$$\mathbf{r}_i \cdot \mathbf{f}_i + \mathbf{r}_j \cdot \mathbf{f}_j = -\frac{Gm_i m_j}{|\mathbf{r}_i - \mathbf{r}_j|} \tag{10}$$

to the summation. Thus the virial $Q$ is related to the potential energy $V$ by the equation

$$Q = -\tfrac{1}{2} V \tag{11}$$

Insofar as the system is in a steady state, integration of the derivatives of the tensor of inertia remain bounded. The averages with respect to time of the kinetic energy and the potential energy satisfy the virial theorem

$$2\langle T \rangle + \langle V \rangle = 0 \tag{12}$$

where $\langle T \rangle$ is the average kinetic energy and $\langle V \rangle$ is the average potential energy.

In the case of two particles which are in Keplerian orbit, the virial theorem is satisfied when averages with respect to time are taken over one period.

**Transport**

If the system of particles is undisturbed, the particles tend to acquire a Maxwellian distribution of velocity. Their properties are described by kinetic theory. Let v be the mean velocity as defined by the equation

$$\mathbf{v} = \frac{\sum m_i \mathbf{v}_i}{\sum m_i} \tag{13}$$

and let $s$ be the root mean square random velocity as defined by the equation

$$s^2 = \frac{\sum m_i (\mathbf{v}_i - \mathbf{v})^2}{\sum m_i} \tag{14}$$

Then the velocity of sound $c$ is given by the equation

$$c = \sqrt{\frac{dp}{d\rho}} = \tfrac{1}{3}\sqrt{5}\, s \tag{15}$$

The integrations for transport of momentum or energy converge over an unlimited space when the particles interact with short-range forces. The integrations do not converge over an unlimited space when the particles interact with the inverse square law which is a long-range force. It is assumed that each particle occupies a cell of average radius $R$ such that

$$\tfrac{4}{3}\pi R^3 = \frac{1}{N} \tag{16}$$

where $N$ is the number of particles per unit volume. If it is assumed further that the particles obey the virial theorem, then the integration can be completed within the

sphere of radius $R$. The kinematic viscosity is given by the equation

$$\frac{\mu}{\rho} = 0.573315\, Rs \tag{17}$$

The thermal conductivity is given by the equation

$$K = \tfrac{5}{2} c_v \mu \tag{18}$$

where $c_v$ is the increase in random energy per unit mass per unit temperature.

It is possible for a finite disk to become isothermal, but it is impossible for a finite sphere to become isothermal. Conduction in the sphere continues to transport random energy from the interior to the surface where energy is carried off by the evaporation of particles.

# APPENDIX B

# PLANCK RADIATION FUNCTIONS

## PLANCK RADIATION FUNCTIONS

*Definitions*

Through any surface in a black body at equilibrium there is a flux of photons and a flux of energy. The rates of flow are expressed by the following variables.

$N_\lambda$ = number of photons per unit time, per unit area, per unit wave length, at wave length $\lambda$ and temperature $T$.

$M_\lambda$ = number of photons per unit time, per unit area, for all wave lengths from 0 to $\lambda$ at temperature $T$.

$R_\lambda$ = energy per unit time, per unit area, per unit wave length, at wave length $\lambda$ and temperature $T$.

$S_\lambda$ = energy per unit time, per unit area, for all wave lengths from 0 to $\lambda$ at temperature $T$.

Planck radiation functions are defined and tabulated in *Miscellaneous Physical Tables* by the Work Projects Administration and the National Bureau of Standards[58]. Modern values for the physical constants are tabulated in *Reviews of Modern Physics* by Taylor, Parker, and Langenberg[59].

The velocity of light is given by the equation

$$c = 299792.5 \frac{(\text{km})}{(\text{sec})} \tag{1}$$

Let the radiation constants $c_1, c_2$ be defined in terms of the Planck constant $h$, the Boltzmann constant $k$, and the velocity of light $c$ by the equations

$$c_1 = 2\pi hc^2 = 3.741844 \times 10^{-5} \frac{(\text{erg})(\text{cm})^2}{(\text{sec})} \tag{2}$$

$$c_2 = \frac{hc}{k} = 1.438833\,(\text{cm})(^\circ K) \tag{3}$$

Let the dimensionless variable $x$ be defined by the equation

$$x = \frac{c_2}{\lambda T} \tag{4}$$

Then the flux $N_\lambda$ is given by the equation

$$N_\lambda = \frac{2\pi c}{c_2^4} T^4 N(x) \tag{5}$$

where the function $N(x)$ is defined by the equation

$$N(x) = \frac{x^4}{e^x - 1} \tag{6}$$

and the ratio between constants is given by the equation

$$\frac{2\pi c}{c_2^4} = 4.395002 \times 10^{10} \frac{1}{(\text{cm})^3(\text{sec})(^\circ K)^4} \tag{7}$$

The flux $M_\lambda$ is given by the equation

$$M_\lambda = \int_0^\lambda N_\lambda \, d\lambda = \frac{2\pi c}{c_2^3} T^3 M(x) \tag{8}$$

where the function $M(x)$ is defined by the equation

$$M(x) = \int_x^\infty \frac{x^2}{e^x - 1} \, dx \tag{9}$$

and the ratio between constants is given by the equation

$$\frac{2\pi c}{c_2^3} = 6.323674 \times 10^{10} \frac{1}{(\text{cm})^2(\text{sec})(^\circ K)} \tag{10}$$

The flux $R_\lambda$ is given by the equation

$$R_\lambda = \frac{c_1}{c_2^5} T^5 R(x) \tag{11}$$

where the function $R(x)$ is defined by the equation

$$R(x) = \frac{x^5}{e^x - 1} \tag{12}$$

and the ratio between constants is given by the equation

$$\frac{c_1}{c_2^5} = 6.067835 \times 10^{-6} \frac{(\text{erg})}{(\text{cm})^3(\text{sec})(^\circ K)^5} \tag{13}$$

The flux $S_\lambda$ is given by the equation

$$S_\lambda = \int_0^\lambda R_\lambda \, d\lambda = \frac{c_1}{c_2^4} T^4 S(x) \tag{14}$$

where the function $S(x)$ is defined by the equation

$$S(x) = \int_x^\infty \frac{x^3}{e^x - 1} \, dx \tag{15}$$

and the ratio between constants is given by the equation

$$\frac{c_1}{c_2^4} = 8.730601 \times 10^{-6} \frac{(\text{erg})}{(\text{cm})^2(\text{sec})(^\circ K)^4} \tag{16}$$

The functions of $x$ are evaluated with the aid of series expansions.

*Analysis*

The functions may be expressed with the aid of the expansion

$$\frac{x}{e^x - 1} = \sum_{n=0}^{\infty} B_n \frac{x^n}{n!} \tag{17}$$

where $B_n$ is the $n$th Bernoulli number. The first few numbers are given by the equations

$$B_0 = 1, \quad B_1 = -\tfrac{1}{2}, \quad B_2 = \tfrac{1}{6}, \quad B_3 = 0, \quad B_4 = -\tfrac{1}{30}, \quad B_5 = 0, \quad B_6 = \tfrac{1}{42}, \quad \cdots \tag{18}$$

Thus if $x \leq 2$ then the functions are computed with the aid of the formulae

$$\frac{x^4}{e^x - 1} = \sum_{n=0}^{\infty} B_n \frac{x^{n+3}}{n!} \tag{19}$$

$$\int_0^x \frac{x^2}{e^x - 1}\, dx = \sum_{n=0}^{\infty} B_n \frac{x^{n+2}}{(n+2)n!} \tag{20}$$

$$\frac{x^5}{e^x - 1} = \sum_{n=0}^{\infty} B_n \frac{x^{n+4}}{n!} \tag{21}$$

$$\int_0^x \frac{x^3}{e^x - 1}\, dx = \sum_{n=0}^{\infty} B_n \frac{x^{n+3}}{(n+3)n!} \tag{22}$$

An expansion of the denominator with the aid of the binomial theorem leads to the series expansion

$$\frac{1}{e^x - 1} = \sum_{k=1}^{\infty} e^{-kx} \tag{23}$$

Thus if $x > 2$ then the functions are computed with the aid of the formulae

$$\int_x^{\infty} \frac{x^2}{e^x - 1}\, dx = \sum_{k=1}^{\infty} e^{-kx} \left( \frac{2}{k^3} + \frac{2x}{k^2} + \frac{x^2}{k} \right) \tag{24}$$

$$\int_x^{\infty} \frac{x^3}{e^x - 1}\, dx = \sum_{k=1}^{\infty} e^{-kx} \left( \frac{6}{k^4} + \frac{6x}{k^3} + \frac{3x^2}{k^2} + \frac{x^3}{k} \right) \tag{25}$$

Although these series are absolutely convergent for positive $x$ they do not converge rapidly for small $x$. The integration when $x = 0$ is expressed in terms of the Riemann zeta function. In the first case $\zeta(3)$ is given by the equation

$$\zeta(3) = \sum_{k=1}^{\infty} \frac{1}{k^3} = 1.2020569031595943 \tag{26}$$

The value of $\zeta(3)$ has been computed to 70 decimal digits by A. H. Morris, Jr. In the second case $\zeta(4)$ is given by the equation

$$\zeta(4) = \sum_{k=1}^{\infty} \frac{1}{k^4} = \frac{\pi^4}{90} \tag{27}$$

The zeta functions are used in the evaluation of the functions as series of Bernoulli numbers.

*Programming*

The flux of radiation is obtained by reference to either of the following two subroutines.

SUBROUTINE PLNKPF (AX, FN, FM)

**********

FORTRAN SUBROUTINE FOR PLANCK PHOTON FLUX FUNCTIONS

**********

The argument $x$ is given in the argument AX. The flux of photons is computed with series expansions. The functions $N(x), M(x)$ are stored in the functions FN, FM.

SUBROUTINE PLNKEF (AX, FR, FS)

**********

FORTRAN SUBROUTINE FOR PLANCK ENERGY FLUX FUNCTIONS

**********

The argument $x$ is given in the argument AX. The flux of energy is computed with series expansions. The functions $R(x), S(x)$ are stored in the functions FR, FS.

# APPENDIX C

# MAPS

# UNITED STATES

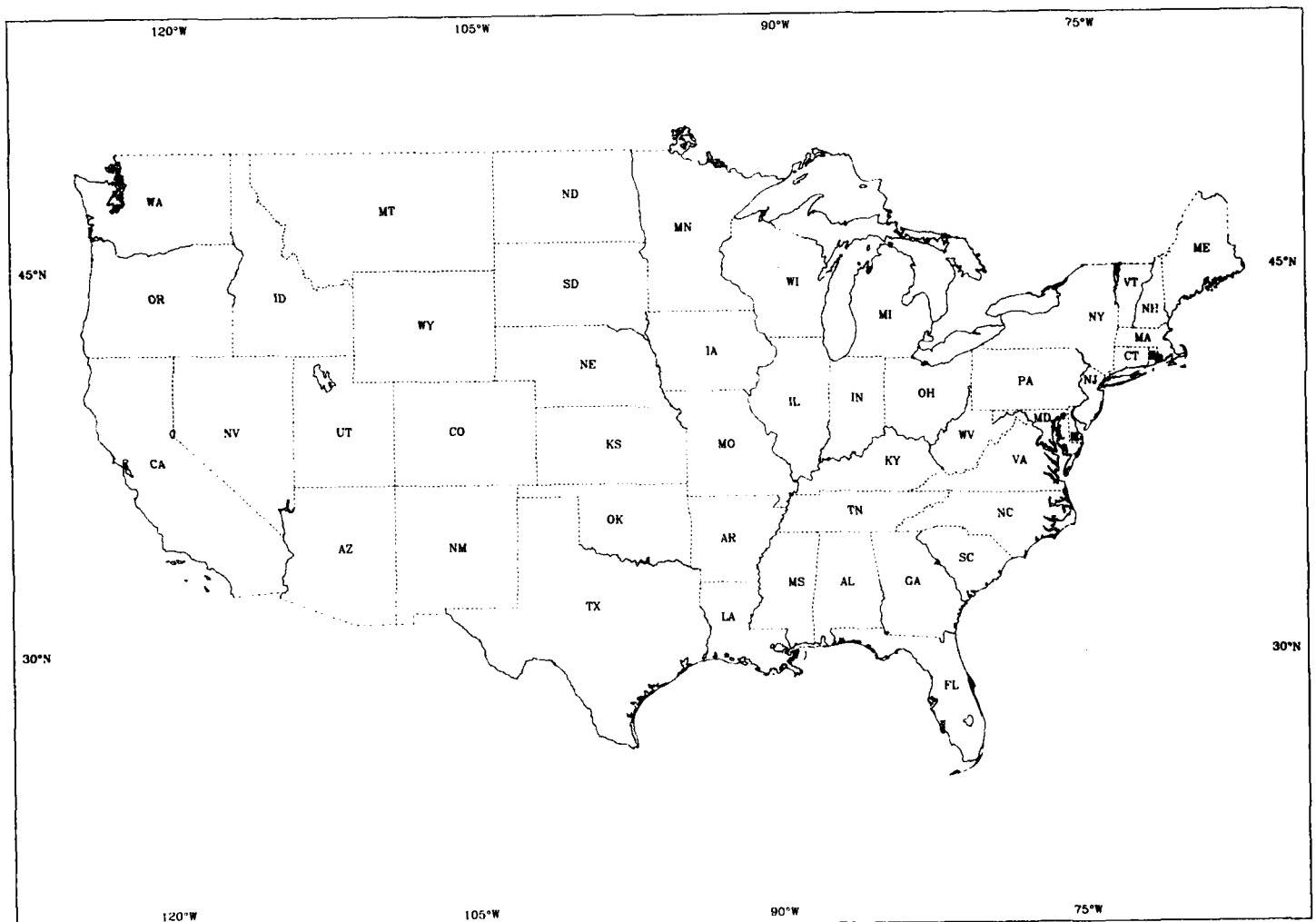


Digitization at Naval Surface Weapons Center, Dahlgren, Virginia 22448
Year 1982

USA DATA BANK
*MERCATOR PROJECTION*

Typography at Naval Surface Weapons Center, Dahlgren, Virginia 22448
Scale 1/35000000

# UNITED STATES

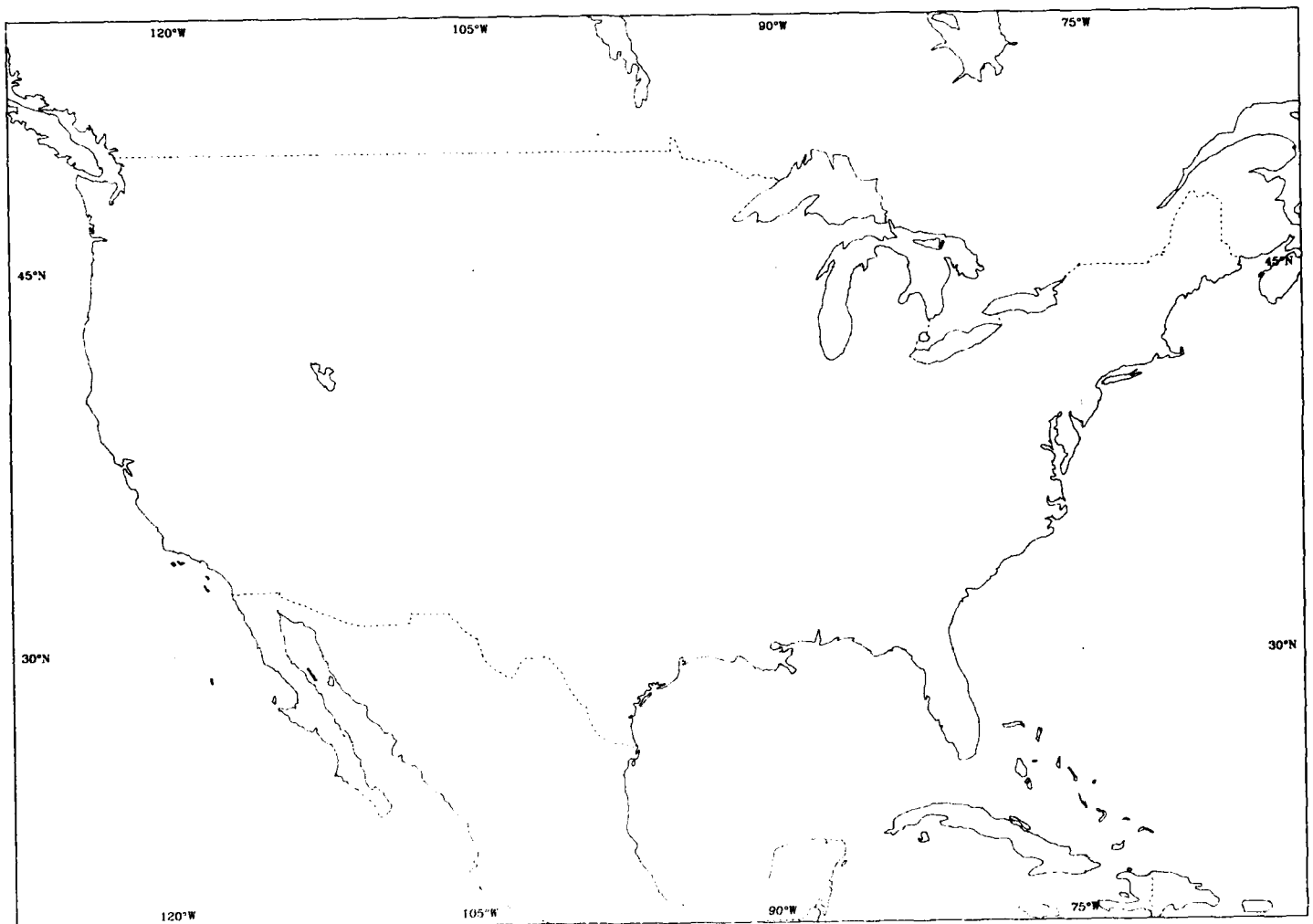


Digitization at Central Intelligence Agency, Washington D. C. 20505
Year 1972

WORLD DATA BANK I
*MERCATOR PROJECTION*

Typography at Naval Surface Weapons Center, Dahlgren, Virginia 22448
Scale 1:35000000

# UNITED STATES

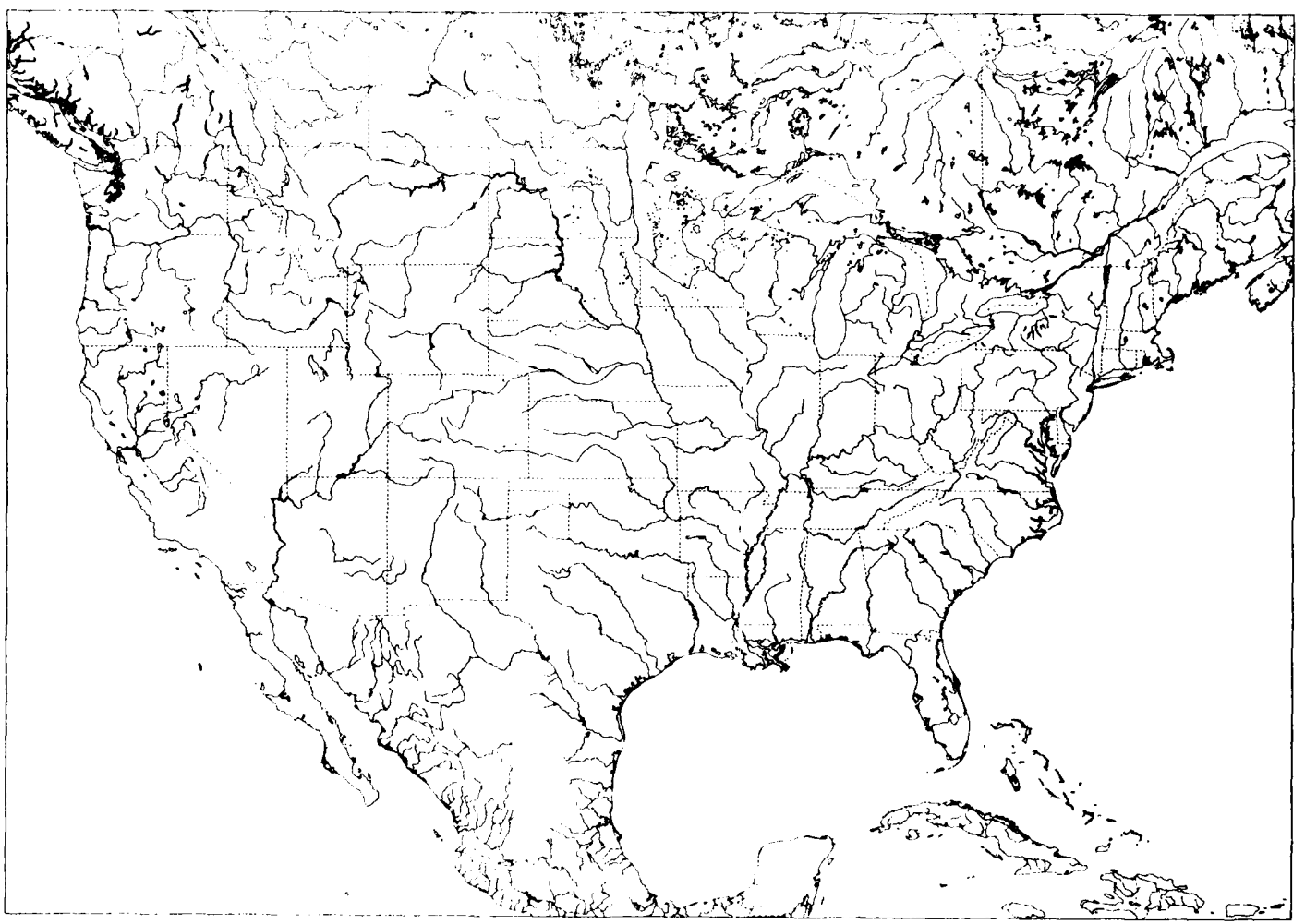

Digitization at Central Intelligence Agency, Washington, D. C. 20505
Year 1976

WORLD DATA BANK I
*MERCATOR PROJECTION*

Typography at Naval Surface Weapons Center, Dahlgren, Virginia 22448
Scale 1/35000000

# MOON MARIA

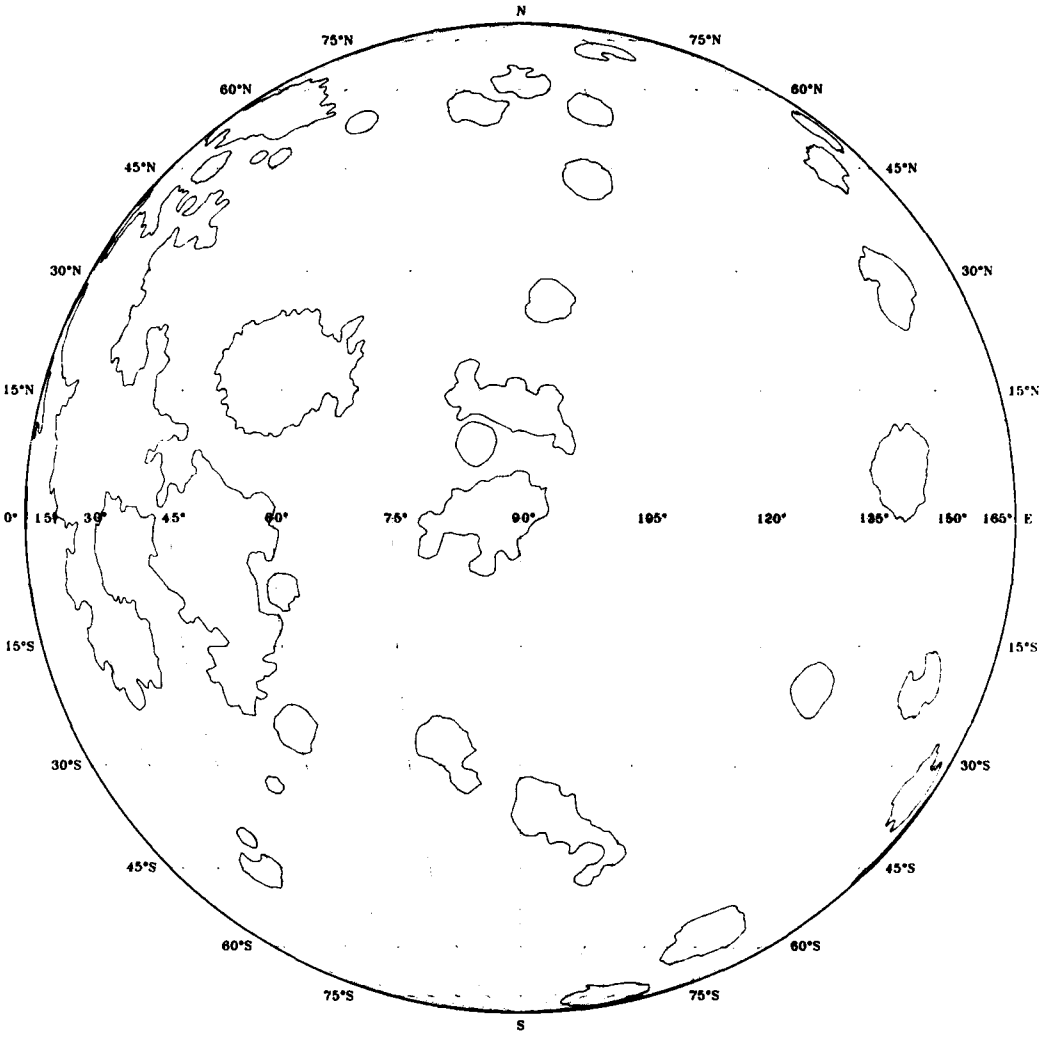


**EAST SIDE**

***ORTHOGRAPHIC PROJECTION***

Digitization from ACIC Lunar Charts dated 1970

# MOON MARIA

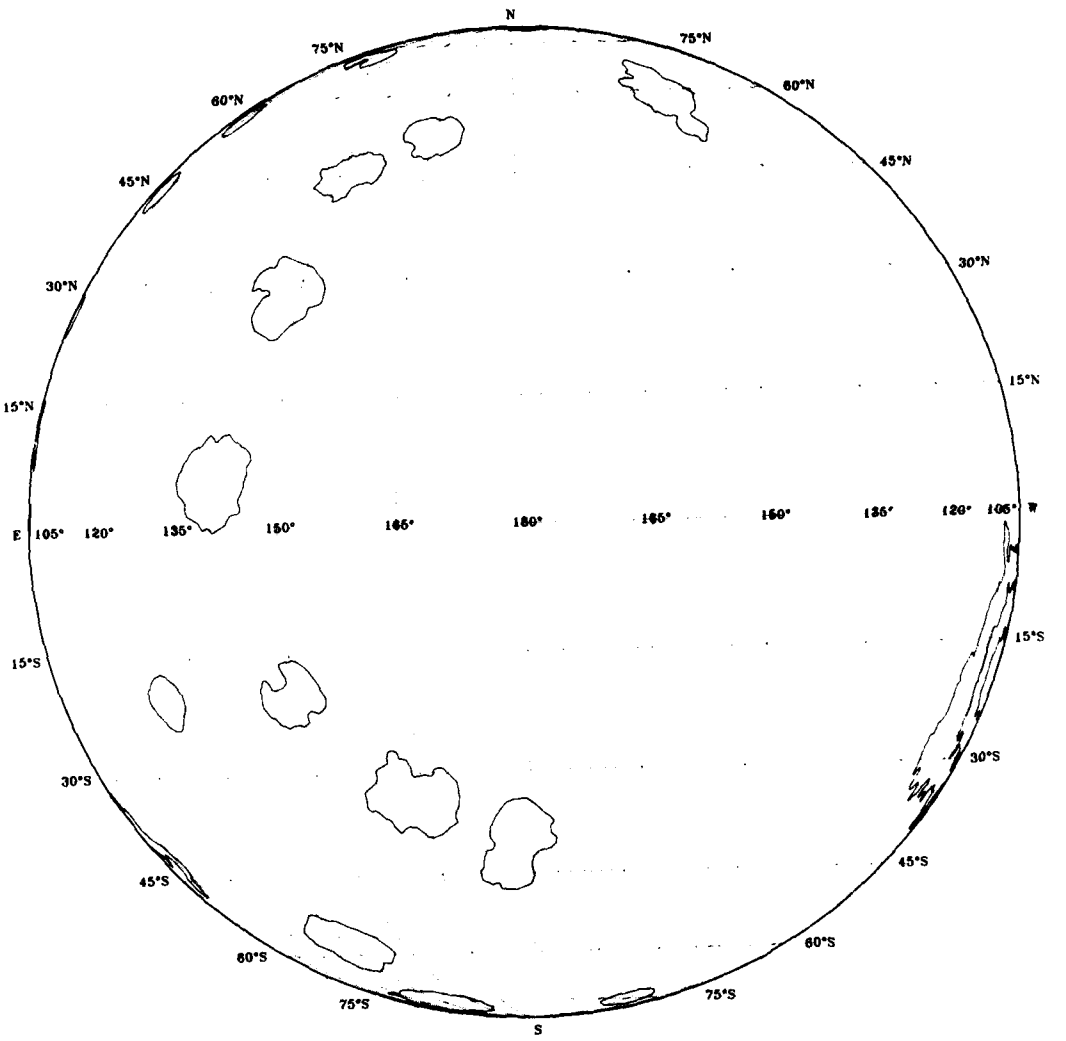


FAR SIDE

*ORTHOGRAPHIC PROJECTION*

Digitization from ACIC Lunar Charts dated 1970

# MOON MARIA

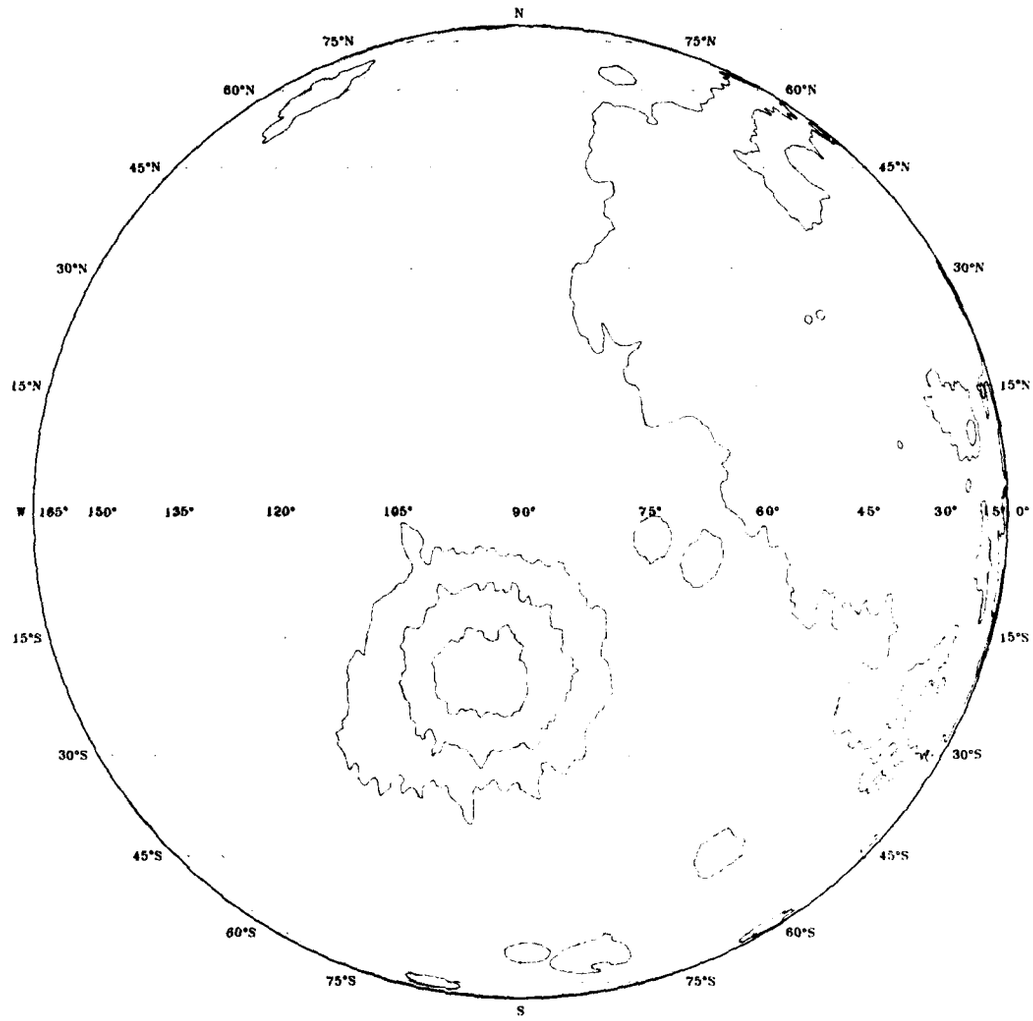


WEST SIDE

*ORTHOGRAPHIC PROJECTION*

Digitization from ACIC Lunar Charts dated 1970

# MOON MARIA

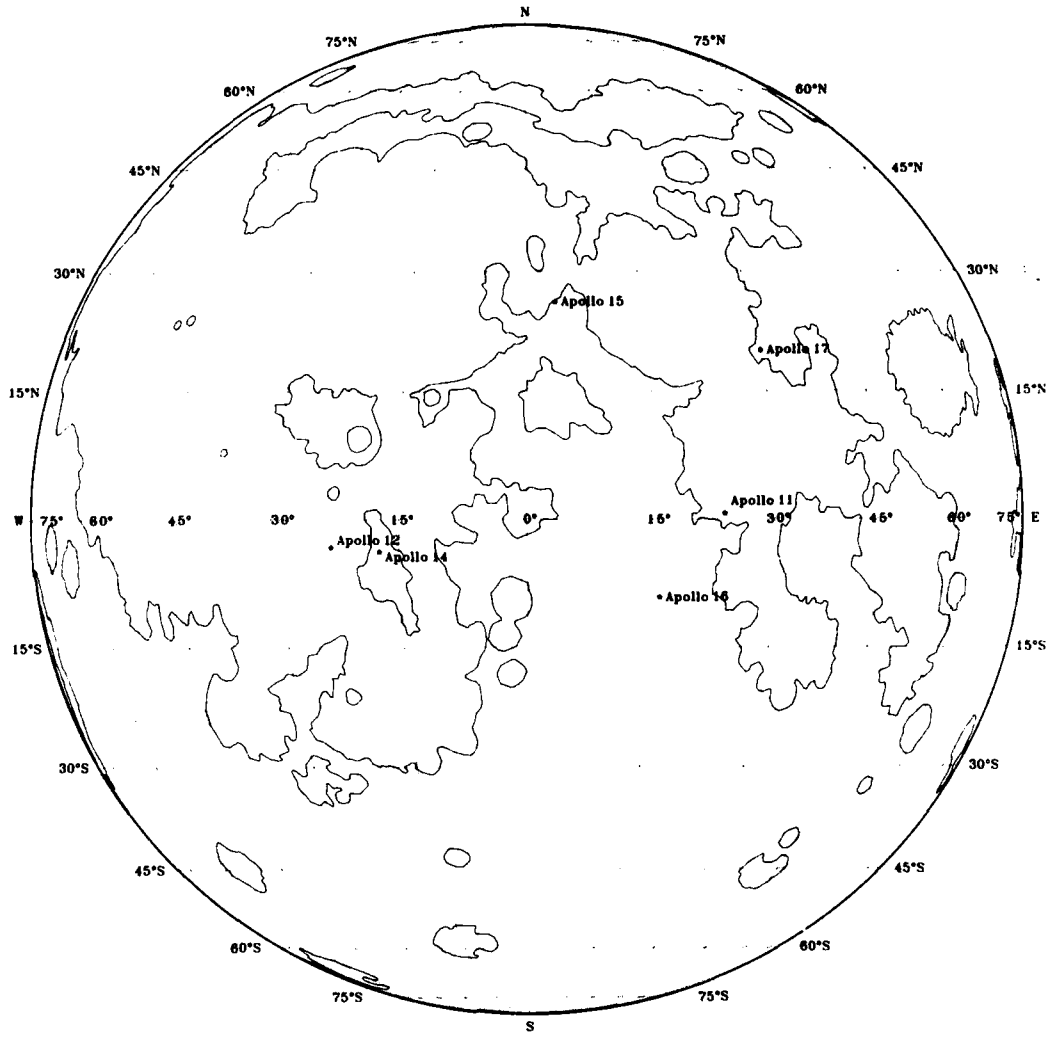


NEAR SIDE

*ORTHOGRAPHIC PROJECTION*

Digitization from ACIC Lunar Charts dated 1970

# CONSTELLATIONS

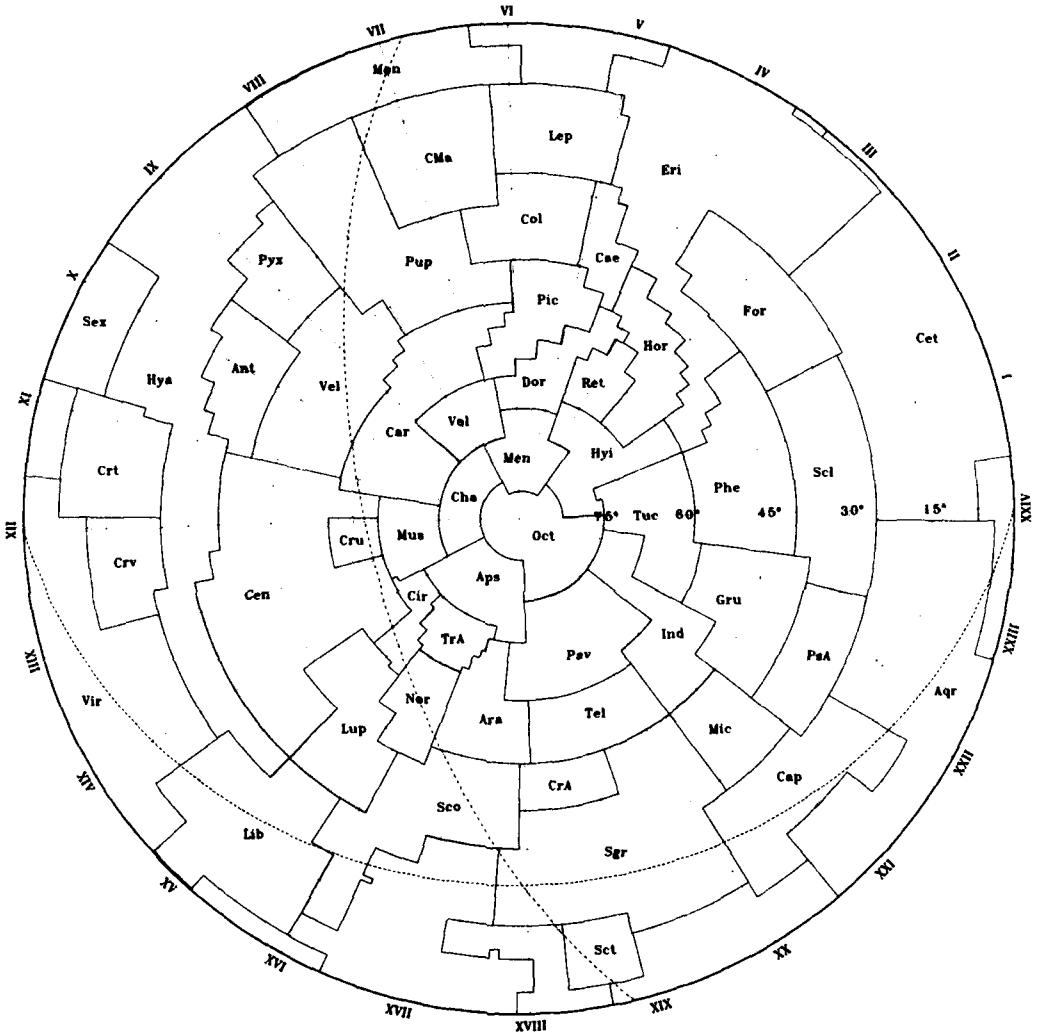


SOUTHERN HEMISPHERE

*POLAR EQUIDISTANT PROJECTION*

EPOCH 1950.0

---, ECLIPTIC

– – –, GALACTIC EQUATOR

# CONSTELLATIONS

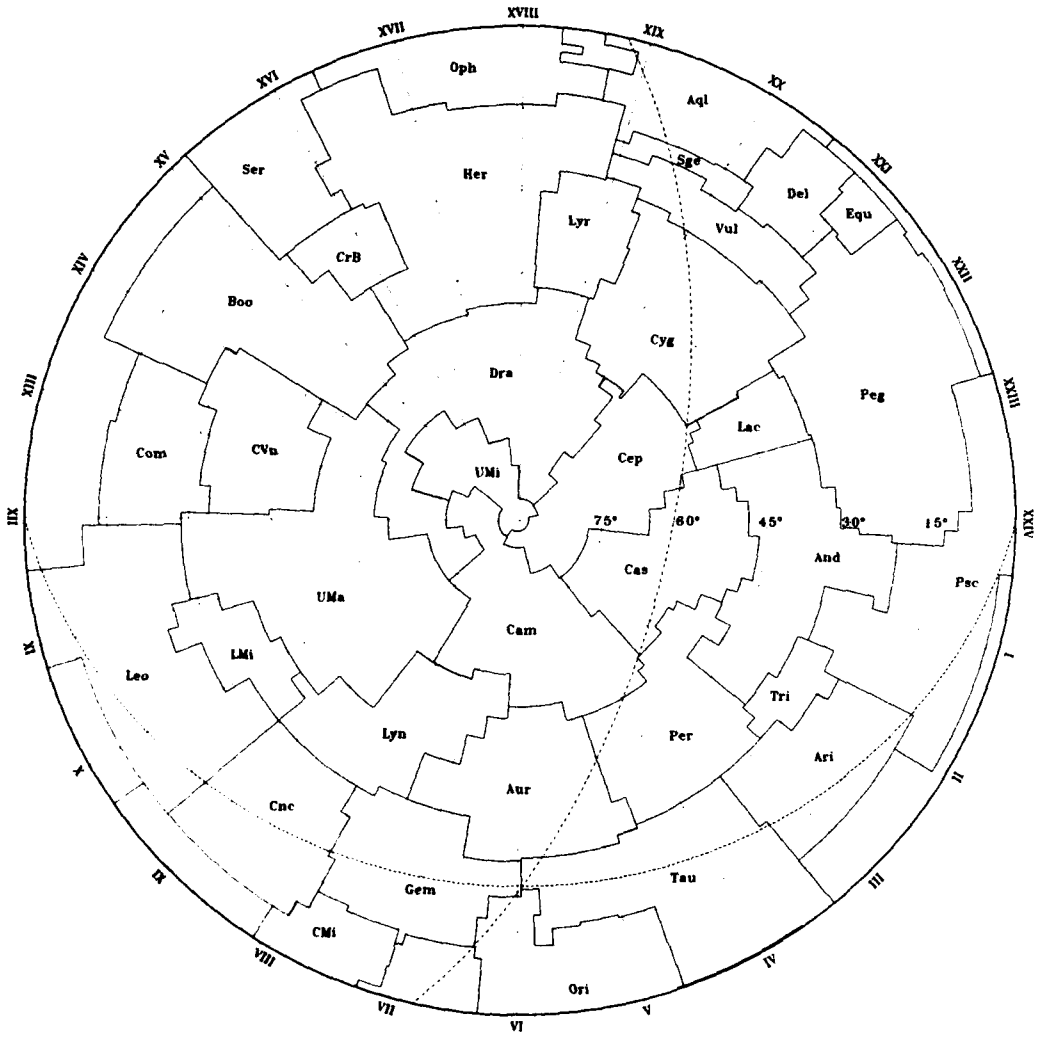


NORTHERN HEMISPHERE

*POLAR EQUIDISTANT PROJECTION*

EPOCH 1950.0

---. ECLIPTIC

– –. GALACTIC EQUATOR

# MILKY WAY

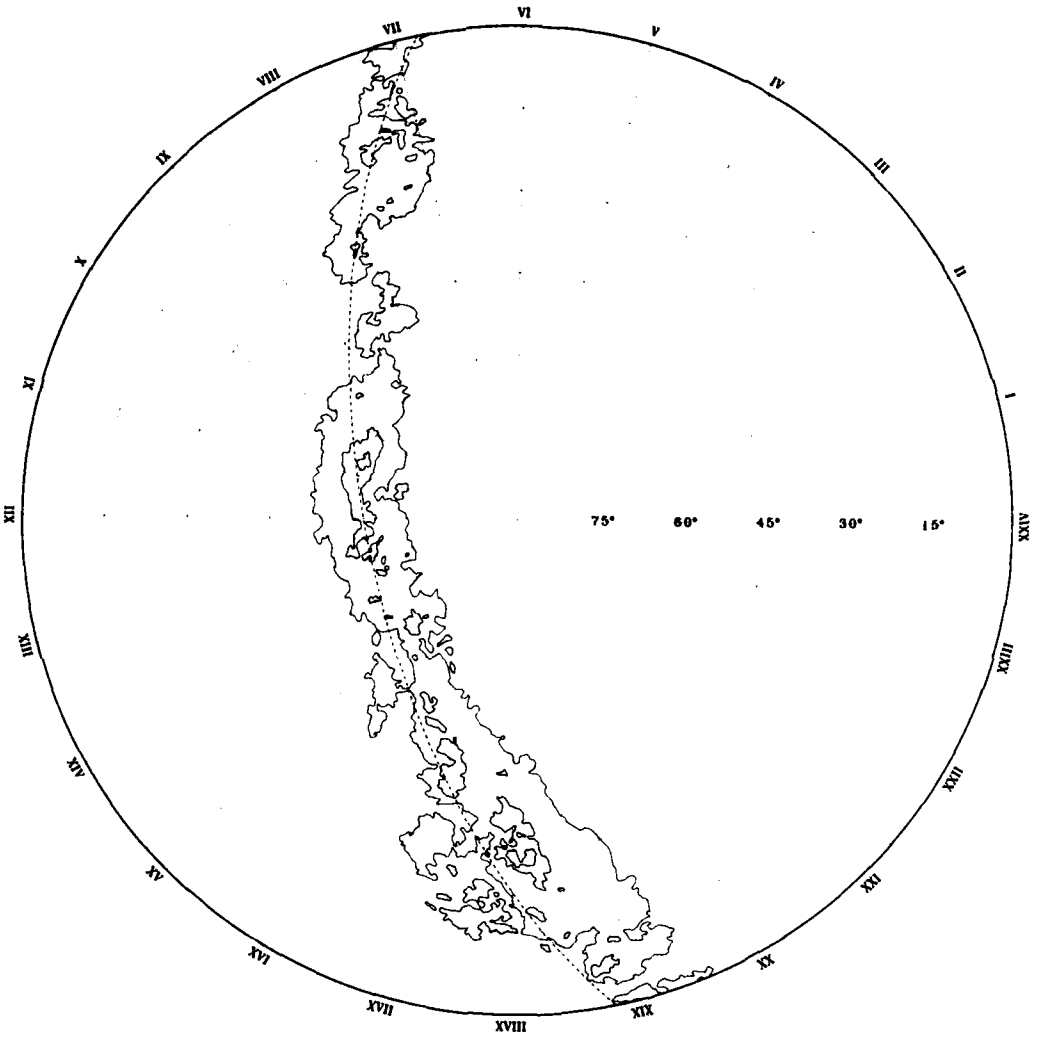


SOUTHERN HEMISPHERE

*POLAR EQUIDISTANT PROJECTION*

EPOCH 1950.0

*. GALACTIC CENTER

– –. GALACTIC EQUATOR

# MILKY WAY

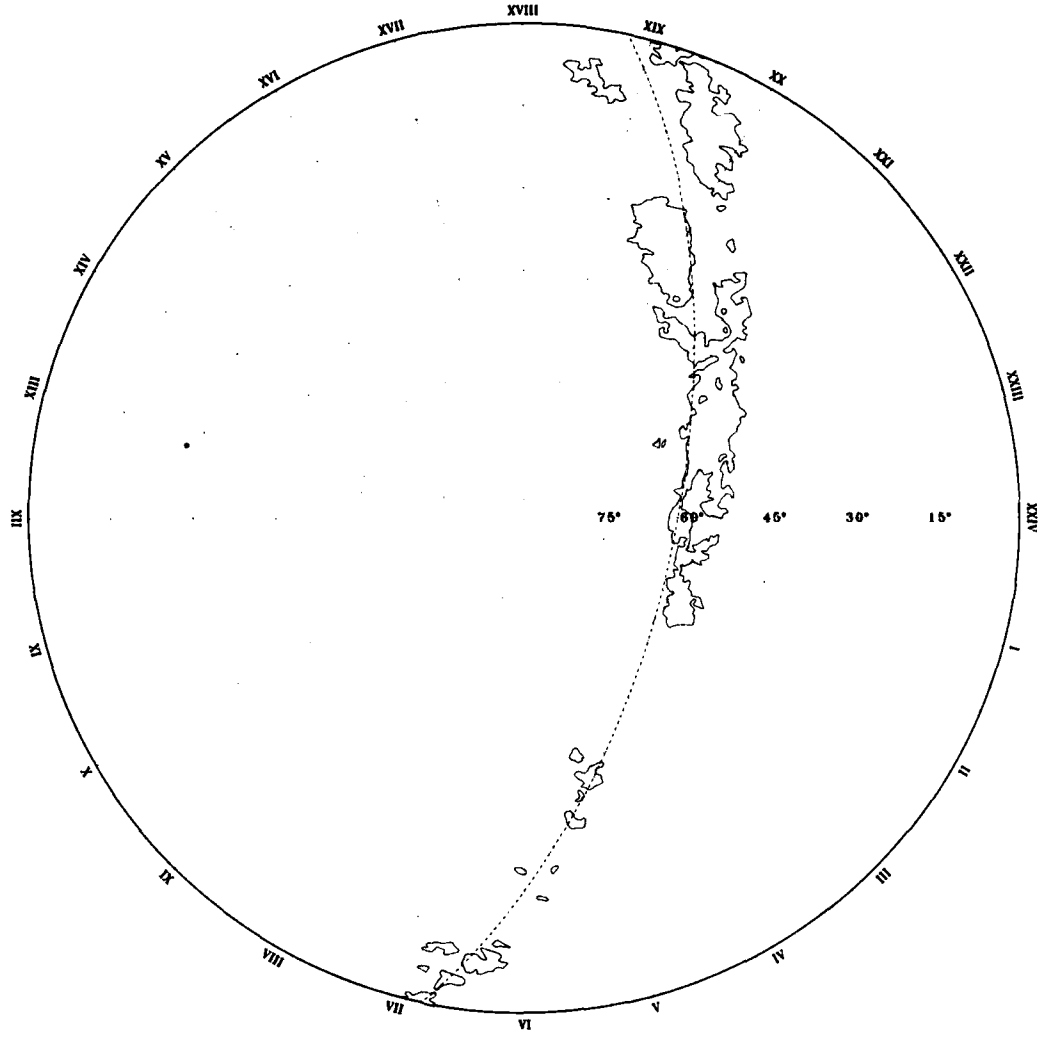


NORTHERN HEMISPHERE

*POLAR EQUIDISTANT PROJECTION*

EPOCH 1950.0

*. GALACTIC POLE

– –. GALACTIC EQUATOR

# CELESTIUM

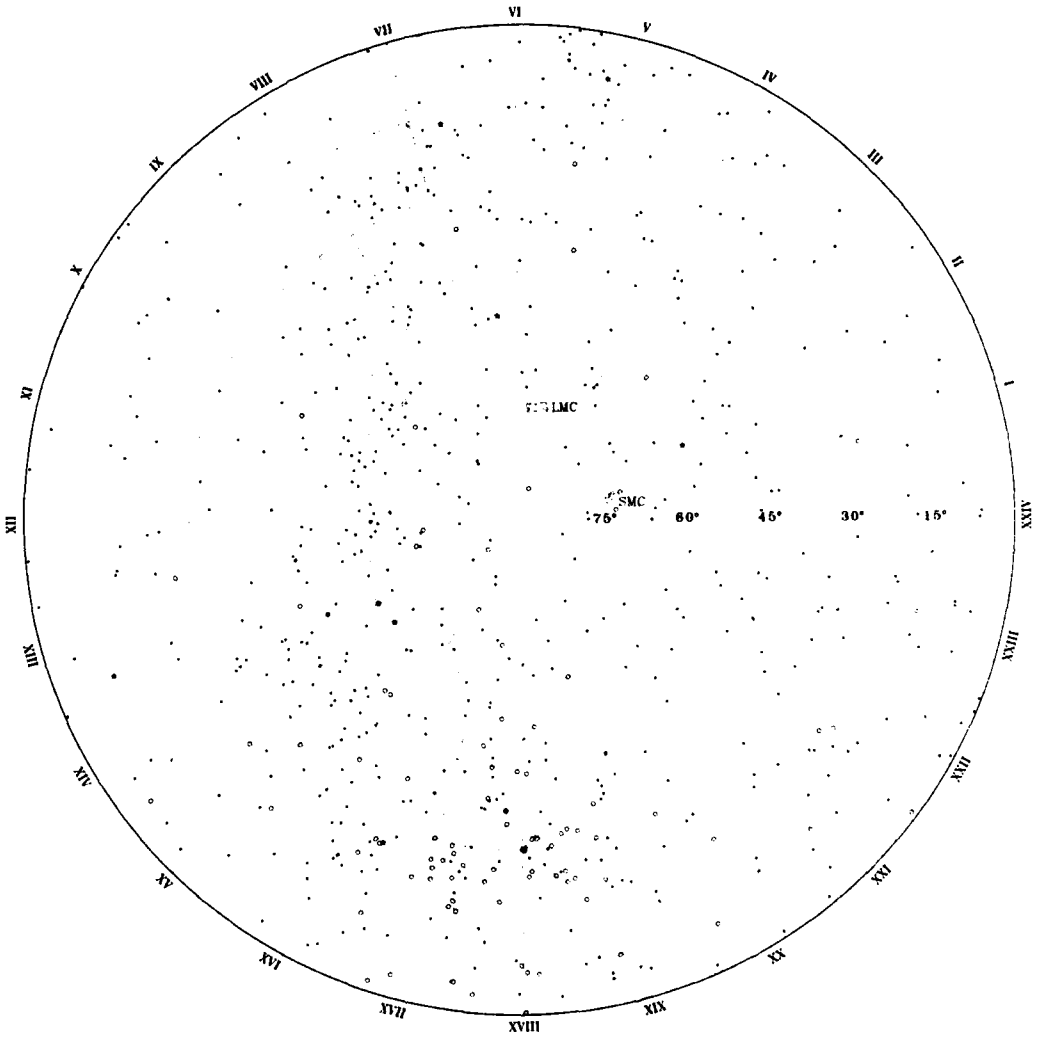


**SOUTHERN HEMISPHERE**

***POLAR EQUIDISTANT PROJECTION***

***EPOCH 1950.0***

•, Stars ($V \geq 1.0$)  ○, Globular Clusters  •, Stars ($V < 1.0$)

# CELESTIUM

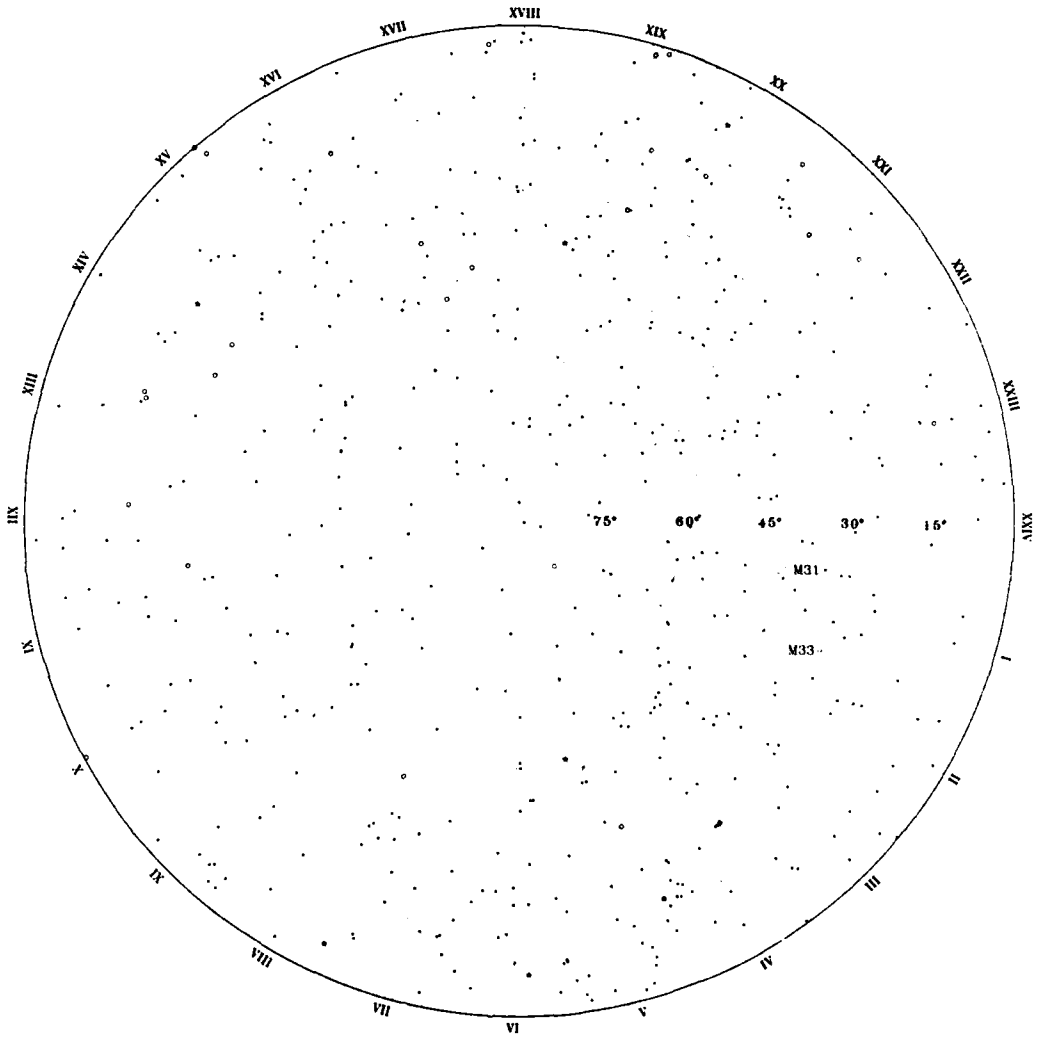


NORTHERN HEMISPHERE

*POLAR EQUIDISTANT PROJECTION*

EPOCH 1950.0

•. Stars ($V \leq 1.0$)  ○. Globular Clusters  •. Stars ($V > 1.0$)

# APPENDIX D

## SPECTRA

## SOLAR SPECTRUM

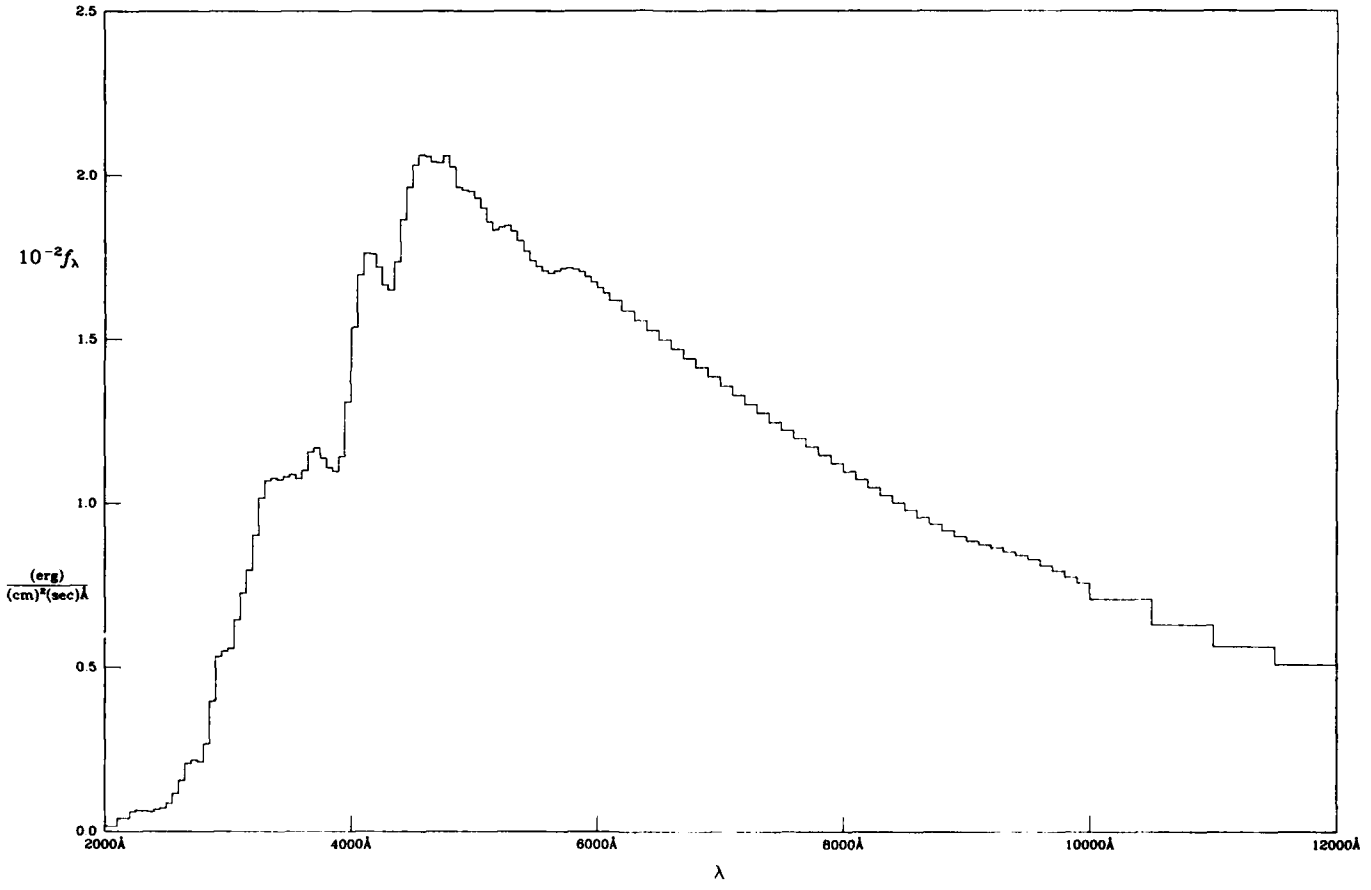


High Altitude Observations by Thekaekara.

## STELLAR SPECTRUM

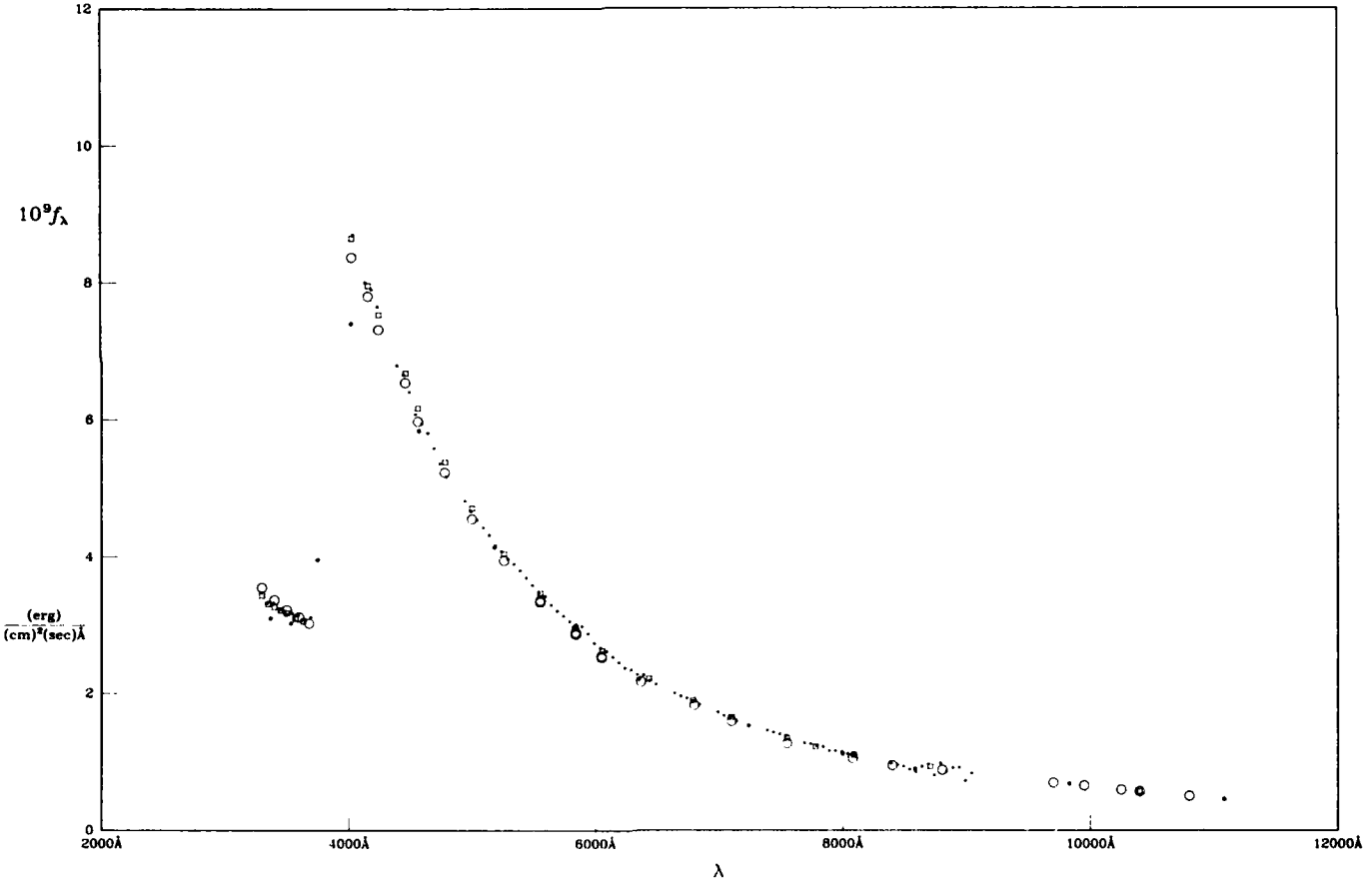


Observations of Vega

○, calibration by Oke and Schild. □, calibration by Hayes and Latham. ·, calibration by Tug, White, and Lockwood. •, 13-color photometry by Johnson and Mitchell

## STELLAR SPECTRUM

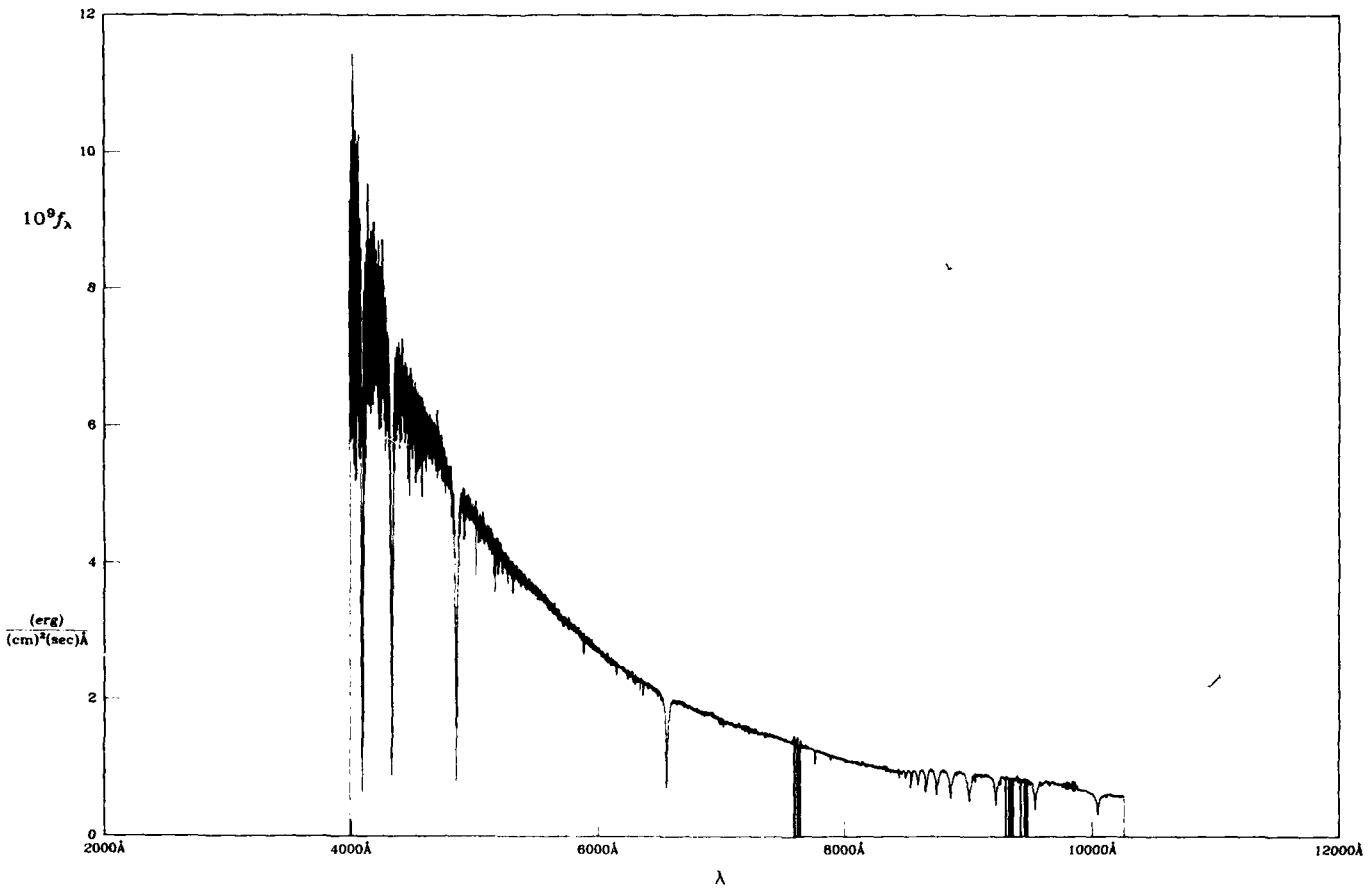


Observations of Vega

-, 6192 color interferometry by Johnson

# APPENDIX E

# DISTRIBUTION

## DISTRIBUTION

Defense Documentation Center
Cameron Station
Alexandria, VA 22314 (12)

Defense Printing Service
Washington Navy Yard
Washington, DC 20374

Library of Congress
Washington, DC 20540
Attn: Gift and Exchange Division (4)

C
D
E
F
G
K
K05H
K05S
K05D
K10
K20
K30
K40
K50
K60
K70
K80
R
U
V
X21 (2)
X220 (6)

UNCLASSIFIED

SECURITY CLASSIFICATION OF THIS PAGE (When Data Entered)

| REPORT DOCUMENTATION PAGE | | READ INSTRUCTIONS BEFORE COMPLETING FORM |
|---|---|---|
| 1. REPORT NUMBER<br>NSWC/DL TR-3789 | 2. GOVT ACCESSION NO. | 3. RECIPIENT'S CATALOG NUMBER |
| 4. TITLE (and Subtitle)<br>TERRESTRIAL AND CELESTIAL CARTOGRAPHY | | 5. TYPE OF REPORT & PERIOD COVERED |
| | | 6. PERFORMING ORG. REPORT NUMBER |
| 7. AUTHOR(s)<br>A. V. Hershey | | 8. CONTRACT OR GRANT NUMBER(s) |
| 9. PERFORMING ORGANIZATION NAME AND ADDRESS<br>Naval Surface Weapons Center (K05)<br>Dahlgren, Virginia 22448 | | 10. PROGRAM ELEMENT, PROJECT, TASK AREA & WORK UNIT NUMBERS<br>NIF |
| 11. CONTROLLING OFFICE NAME AND ADDRESS | | 12. REPORT DATE<br>May 1979 |
| | | 13. NUMBER OF PAGES<br>85 |
| 14. MONITORING AGENCY NAME & ADDRESS(if different from Controlling Office) | | 15. SECURITY CLASS. (of this report)<br>UNCLASSIFIED |
| | | 15a. DECLASSIFICATION/DOWNGRADING SCHEDULE |

16. DISTRIBUTION STATEMENT (of this Report)

Approved for public release; distribution unlimited.

17. DISTRIBUTION STATEMENT (of the abstract entered in Block 20, if different from Report)

18. SUPPLEMENTARY NOTES

19. KEY WORDS (Continue on reverse side if necessary and identify by block number)

| | | |
|---|---|---|
| maps | distance | computation |
| domains | velocity | |
| sunlight | data banks | |
| starlight | catalogs | |

20. ABSTRACT (Continue on reverse side if necessary and identify by block number)

World Data Bank I has been reordered in such a way that the latitudes where coastlines cross meridians are sorted in order of latitude for each minute of longitude. Whether a satellite position is over sea or over land is determined by the parity of the next lower crossing. Stellar data on distance and velocity as well as direction are given in a small catalog. Boundary data for moon maria, constellations, and the Milky Way are given in a set of files.

DD FORM 1 JAN 73 1473 EDITION OF 1 NOV 65 IS OBSOLETE
S/N 0102-LF-014-6601

UNCLASSIFIED

SECURITY CLASSIFICATION OF THIS PAGE (When Data Entered)